Investigation of the activation mechanism of the volume-regulated anion channel VRAC and its role in cell proliferation and migration

Inaugural-Dissertation

to obtain the academic degree

Doctor rerum naturalium (Dr. rer. nat.)

submitted to the Department of Biology, Chemistry, Pharmacy

of Freie Universität Berlin

by

Tianbao Liu

from Shandong, China

Berlin 2021

This work was prepared under the supervision of Prof. Dr. Tobias Stauber at the Freie Universität Berlin from September 2016 until December 2020.

1st Reviewer: **Prof. Dr. Tobias Stauber**

Institute of Chemistry and Biochemistry

Department of Biology, Chemistry, Pharmacy

Freie Universität Berlin

2nd Reviewer: **Prof. Dr. Helge Ewers**

Institute of Chemistry and Biochemistry

Department of Biology, Chemistry, Pharmacy

Freie Universität Berlin

Date of defense: April 08, 2021

PREFACE

Part of this work has been published in the following peer-reviewed journal article:

Liu T and Stauber T (2019) The Volume-Regulated Anion Channel LRRC8/VRAC Is Dispensable for Cell Proliferation and Migration. *Int J Mol Sci*, 20: E2663. https://doi.org/10.3390/ijms20112663

Parts of the experiments in this thesis were performed by others, as depicted in the results part.

STATUTORY DECLARATION

I confirm that I have prepared this dissertation entitled "*Investigation of the activation mechanism of the volume-regulated anion channel VRAC and its role in cell proliferation and migration*" autonomously and without impermissible help. All external sources and resources have been specified and properly cited or acknowledged. This thesis has not been submitted, accepted, rated as insufficient or rejected in any other doctorate procedure.

Berlin, 2021

Tianbao Liu

ACKNOWLEDGMENTS

I would like to express my deeply gratitude to Prof. Dr. Tobias Stauber for granting me the privilege of working in his excellently equipped laboratory and for always having an open door when I needed advice. His unconditional support and constant interest in my work have been of great help.

I would like to thank Prof. Dr. Helge Ewers for reviewing my PhD thesis.

I would also like to thank Benjamin König for sharing his abundant knowledge about microscopes and computer programs.

I would also like to acknowledge Antje Buttgereit for helping me when I encountered difficulties in the experiments.

My thanks go to Dr. Lisa von Kleist, who took me familiar with the entire laboratory and the use of all instruments.

I would express my special gratitude to Lingye Chen, for the motivating discussion and valuable suggestions on my project.

My thanks go as well to AG Ewers, AG Stricker, AG Freund and AG Knaus, all Freie Universität Berlin, and AG Relógio, Charité, for sharing their laboratory devices and equipment.

I am deeply grateful to the all present and former members of the Stauber lab for the inspiring discussions, the great working environment, the continuous support, and for all the fun we had during my doctoral study.

Finally, I would like to thank my wife Yin Li and my parents for all the support.

TABLE OF CONTENTS

LIST OF FIGURES ..... **XIV**

LIST OF TABLES ..... **XVI**

LIST OF ABBREVIATIONS ..... **XVII**

ABSTRACT ..... **XX**

ZUSAMMENFASSUNG ..... **XXI**

1 INTRODUCTION **1**

1.1 The volume-regulated anion channel VRAC **1**

1.1.1 The structure of LRRC8/VRAC channel 2

1.2 Physiological and pathophysiological roles of VRAC **6**

1.2.1 VRAC in regulatory volume decrease (RVD) 6

1.2.2 VRAC in cell proliferation and migration 8

1.2.3 Specific roles of the different LRRC8 subunits 10

1.2.4 VRAC roles in other (patho-)physiological processes 12

1.3 Mechanisms of VRAC activation and regulation **15**

1.3.1 Ionic strength 16

1.3.2 Protein phosphorylation 17

1.3.3 G-proteins and G-protein-coupled receptors 18

2 AIM OF THE WORK **19**

3 RESULTS **20**

3.1 Roles of VRAC in cell proliferation and migration **20**

3.1.1 Knockout of LRRC8A does not impinge on C2C12 proliferation or migration 20

3.1.2 LRRC8/VRAC is not required for the proliferation of HEK-293 cells 22

3.1.3 VRAC blockers and disruption of LRRC8s do not suppress HCT116 proliferation and migration 23

3.1.4 LRRC8A/VRAC is dispensable for proliferation and migration of glioblastoma cells 25

3.1.5 VRAC inhibition by DCPIB or LRRC8A downregulation has no effect on PI3K/Akt signaling in GBM cells 30

3.2 Mechanisms of activation and regulation of VRAC **34**

3.2.1 FRET changes reflect C terminus movement during VRAC gating 34

3.2.2 Effect of PKD pharmacological inhibition on swelling-induced VRAC activation 36
3.2.3 Downregulation of PKD1 or PKD2 inhibits VRAC activity 40
3.2.4 PMA induces VRAC activation and recruits C1 domain-containing proteins to the plasma membrane 41
3.2.5 Hypotonic stress does not recruit DAG biosensors to the plasma membrane, possibly DAG is rapidly converted to PA 42
3.2.6 Phosphorylation of PKCs or PKDs in response to hypotonicity 44

4 DISCUSSION 46

4.1 LRRC8A/VRAC is dispensable for cell proliferation and migration 46
4.2 Mechanisms of VRAC activation and regulation 49
4.2.1 FRET approach in study the activity of VRAC channel 49
4.2.2 PKD regulates the activation of VRAC 50
4.2.3 Hypotonicity induces influx of PKD inhibitor via LRRC8/VRAC 53
4.2.4 Conclusion & Outlook 55

5 MATERIALS AND METHODS 56

5.1 Materials 56
5.1.1 Chemicals 56
5.1.2 Drugs 56
5.1.3 Cell lines 57
5.1.4 Antibodies 58
5.1.5 siRNAs 58
5.1.6 Plasmids 59
5.1.7 Cell culture medium components 59
5.1.8 Imaging buffers 60
5.2 Methods 61
5.2.1 Cell culture 61
5.2.2 Bacterial transformation 61
5.2.3 Generation of C2C12 LRRC8A knockout cell lines 61
5.2.4 Transfection of mammalian cells 62
5.2.5 Drug treatment 63
5.2.6 Cell proliferation assays 63
5.2.7 Cell migration assays 63
5.2.8 Cell counting kit-8 (CCK8) cell proliferation assay 64
5.2.9 Western blotting 64

5.2.10 Expression constructs 65
5.2.11 FRET measurements 65
5.2.12 Qualitative and quantitative microscopy 66
5.2.13 Statistical analysis 66
6 REFERENCES 67
7 PUBLICATIONS 92

LIST OF FIGURES

Figure 1. Structure of LRRC8/VRAC channel 4
Figure 2. Mechanism of regulatory volume decrease 7
Figure 3. Schematic presentation of cell volume regulation during cell migration ... 9
Figure 4. Schematic presentation of mechanisms underlying VRAC physiological functions 13
Figure 5. LRRC8A depletion has no effect on C2C12 cell proliferation 21
Figure 6. LRRC8A depletion does not impair C2C12 cell migration 22
Figure 7. LRRC8 subunit depletion does not affect HEK-293 proliferative ability . 23
Figure 8. Effect of LRRC8 subunit knockout or carbenoxolone (CBX) treatment on cell proliferation and migration of HCT116 cells 24
Figure 9. Volume-regulated anion channel (VRAC) blockers do not impair proliferation of GBM cells 26
Figure 10. VRAC blockers have no effect on GBM cell movement 27
Figure 11. Gene-specific siRNA reduces LRRC8A expression in GBM cells 28
Figure 12. Downregulation of LRRC8A protein is dispensable for GBM proliferation and migration 29
Figure 13. Treatment with DCPIB has no effect on PI3K/Akt signaling 31
Figure 14. siRNA-mediated knockdown of LRRC8A has no effect on PI3K/Akt signaling 33
Figure 15. cFRET changes reflect activation of VRAC in response to hypotonic swelling 35
Figure 16. Effect of PKD inhibitors on hypotonicity-induced VRAC activation 37
Figure 17. Activation of VRAC facilitates PKD inhibitor uptake 38
Figure 18. A lower concentration of PKD inhibitor CRT0066101 does not impair swelling-induced VRAC activation 39
Figure 19. siRNA-mediated knockdown of PKD1/2 suppresses hypotonic-induced cFRET drop 40
Figure 20. The DAG analog PMA induces VRAC activation 41
Figure 21. Application of PMA induces recruitment of DAG biosensors to the plasma membrane 42
Figure 22. Effect of hypotonic cell swelling on DAG and PA translocation 43

Figure 23. Effect of PMA and hypotonic on PKD phosphorylation 44
Figure 24. Hypotonic stress does not induce phosphorylation of PKCs..... 45

LIST OF TABLES

Table 1 | Drugs 56
Table 2 | Cell lines 57
Table 3 | Primary antibodies 58
Table 4 | Secondary antibodies 58
Table 5 | Used siRNAs and their sequence 58
Table 6 | Plasmids 59
Table 7 | Cell culture medium components 59

LIST OF ABBREVIATIONS

AVD	apoptotic volume decrease
C2	two-fold rotational symmetry
C3	three-fold rotational symmetry
C6	six-fold rotational symmetry
CBX	carbenoxolone
CCC	cation-Cl transporter
CCK8	cell counting kit-8
CFP	cyan-fluorescent protein
cFRET	corrected FRET
CFTR	cystic fibrosis transmembrane conductance regulator
cGAMP	2′3′cGMP-AMP
DAG	diacylglycerol
DCPIB	4-[(2-Butyl-6,7-dichloro-2-cyclopentyl-2,3-dihydro-1-oxo-1*H*-inden-5-yl)oxy]butanoic acid
DGK	diacylglycerol kinase
DOG	dioctanoylglycol
ECD	extracellular domain
EL	extracellular loop
ER	endoplasmic reticulum
FRET	Förster-resonance energy transfer
GFP	green-fluorescent protein
GPCR	G-protein coupled receptor
HSV-1	herpes simplex virus 1
I^{AA}	intensity measured with acceptor excitation and acceptor emission, acceptor channel
$I_{Cl,vol}$	volume-activated chloride current
$I_{Cl,swell}$	swelling-induced chloride conductance
I^{DA}	intensity measured with donor excitation and acceptor emission, FRET channel
I^{DD}	intensity measured with donor excitation and donor emission, donor channel

ICD	intracellular domain
IFN	interferon
IL	intracellular loop
IP_3	inositol trisphosphate
K2P	two pore-domain potassium channel
K_{Ca}	Ca^{2+}-activated K^+ channel
KCC	K-Cl cotransporter
KO	knockout
LRR	leucine-rich repeat
LRRC8	leucine-rich repeat-containing protein family 8
LRRCT	leucine-rich repeat C terminus
LRRD	leucine-rich repeat domain
LRRNT	leucine-rich repeat N terminus
LUT	look-up table
MTT	3-(4,5-dimethylthiazol-2-yl)-2,5-diphenyltetrazolium bromide
NKCC	Na-K-Cl cotransporter
NPPB	5-nitro-2-(3-phenylpropyl-amino)benzoic acid
NTC	N-terminal coil
OSR1	oxidative stress-responsive 1 protein
PA	phosphatic acid
PDBu	phorbol 12,13-dibutyrate
PI3K	phosphatidyl-inositol 3-Kinase
PIP_2	phosphatidylinositol-4,5-bisphosphate
PIP_3	phosphatidylinositol-3,4,5-triphosphate
PKA	cAMP-dependent kinase
PKC	protein kinase C
PKD	protein kinase D
PKG	cGMP-dependent kinase
PLC	phospholipase C
PM	plasma membrane
PMA	phorbol-12-myristate-13-acetate
PTK	protein tyrosine kinase
PTP	protein tyrosine phosphatases

ROI	region of interest
RVD	regulatory volume decrease
RVI	regulatory volume increase
SD	standard deviation
S1P	sphingosine-1-phosphate
S1PR	sphingosine-1-phosphate receptor
seFRET	sensitized-emission FRET
siRNA	small interfering RNA
SPAK	SPS1-related proline/alanine-rich kinase
STING	stimulator of interferon genes
TMD	transmembrane domain
TMH	transmembrane helix
TTYH	tweety homologue
VRAC	volume-regulated anion channel
VSOAC	volume-sensitive organic osmolyte/anion channel
VSOR	volume-sensitive outwardly rectifying anion channel
WST-8	[2-(2-methoxy-4-nitrophenyl)-3-(4-nitrophenyl)-5-(2,4-disulfophenyl)-2H-tetrazolium, monosodium salt]
YFP	yellow-fluorescent protein

SI units and SI prefixes are used according to the International System of Units. Nomenclature and symbolism for amino acids and peptides follows the guidelines of the IUPAC-IUB Joint Commission on Biochemical Nomenclature (JCBN): “Nomenclature and symbolism for amino acids and peptides. Recommendations 1983.”

ABSTRACT

The volume-regulated anion channel (VRAC) is a key player in regulatory volume decrease (RVD) and has been proposed to play pivotal roles in many physiological processes. Although VRAC's potential physiological functions and activation mechanism were studied extensively, conflicting results were obtained regarding the role of VRAC in cell proliferation and migration, as well as its activation mechanism. The lack of specific pharmacological VRAC inhibitors and the unknown molecular entity of VRAC hampered further progress aiming to elucidate its activation mechanism and proposed physiological roles. The discovery of LRRC8 heteromers as an essential component of VRAC enabled the investigation of its physiological roles and activation mechanism of VRAC using molecular biological tools.

Here, I systematically examined the role of VRAC during cell growth and motility for various cell types, including C2C12 myoblasts, HCT116 cells, HEK-293 cells and U251 and U87 glioblastoma cells. Surprisingly, neither pharmacological inhibition of VRAC by carbenoxolone, 4-[(2-Butyl-6,7-dichloro-2-cyclopentyl-2,3-dihydro-1-oxo-1*H*-inden-5-yl)oxy]butanoic acid (DCPIB) or 5-nitro-2-(3-phenylpropyl-amino)benzoic acid (NPPB), nor siRNA-mediated knockdown or disruption of the essential VRAC subunit LRRC8A affected cell proliferation and migration in any of the investigated cell lines. I also found that inhibition of VRAC with DCPIB or siRNA against *LRRC8A* has no effect on PI3K/Akt signaling in glioblastoma cells. These results indicate that, contrasting the prevailing assumption in the literature, VRAC is dispensable for cell proliferation and migration.

Furthermore, by using a Förster-resonance energy transfer (FRET)-based approach, I investigated the potential activation mechanism of VRAC involving protein kinase D (PKD). This revealed that both pharmacological inhibition and siRNA-mediated knockdown of PKDs impaired hypotonicity-induced VRAC activation. Hypotonicity treatment induced the formation of phosphatidic acid (PA) at the plasma membrane. These results corroborate the notion that hypotonicity-induced VRAC activation involves diacylglycerol (DAG) and PA signaling.

ZUSAMMENFASSUNG

Der volumenregulierte Anionenkanal (VRAC) spielt eine Schlüsselrolle bei der des regulatorischen Verringerung des Zellvolumens (RVD) und soll dadurch eine Rolle bei vielen physiologischen Prozessen spielen. Obwohl die potenziellen physiologischen Funktionen und der Aktivierungsmechanismus von VRAC ausführlich untersucht wurden, wurden widersprüchliche Ergebnisse hinsichtlich der Rolle von VRAC bei der Zellproliferation und -migration sowie seines Aktivierungsmechanismus erzielt. Das Fehlen spezifischer pharmakologischer VRAC-Inhibitoren und die unbekannte molekulare Identität von VRAC behinderten weitere Fortschritte, um den Aktivierungsmechanismus und die vorgeschlagenen physiologischen Rollen aufzuklären. Die Entdeckung von LRRC8-Heteromeren als wesentlicher Bestandteil von VRAC ermöglichten, die physiologischen Rollen und den Aktivierungsmechanismus von VRAC zu untersuchen.

Hier untersuchte ich systematisch die Rolle von VRAC während der Zellproliferation und der Motilität für verschiedene Zelltypen, einschließlich C2C12-Myoblasten, HCT116-Zellen, HEK-293-Zellen und U251- und U87-Glioblastomzellen. Überraschenderweise beeinflusste weder die pharmakologische Hemmung von VRAC durch Carbenoxolon, 4-[(2-Butyl-6,7-dichloro-2-cyclopentyl-2,3-dihydro-1-oxo-1*H*-inden-5-yl)oxy]butanoic acid (DCPIB) oder 5-nitro-2-(3-phenylpropyl-amino)benzoic acid (NPPB), noch der siRNA-vermittelte Abbau oder die Gendeletion der essentiellen VRAC-Untereinheit LRRC8A die Zellproliferation und -migration in einer der untersuchten Zelllinien. Ich fand auch, dass die Hemmung von VRAC mit DCPIB oder siRNA gegen *LRRC8A* keinen Einfluss auf die PI3K/Akt-Signalübertragung in Glioblastomzellen hat. Diese Ergebnisse zeigen, dass VRAC entgegen der vorherrschenden Annahme in der Literatur für die Zellproliferation und -migration entbehrlich ist.

Des Weiteren habe ich unter Verwendung eines FRET-Ansatzes den Aktivierungsmechanismus des VRAC untersucht. Sowohl die pharmakologische Hemmung als auch der siRNA-vermittelte Abbau von Proteinkinasen des Typs D beeinträchtigten die durch Hypotonie induzierte VRAC-Aktivierung. Extrazelluläre Hypotonie induzierte die Bildung von Phosphatidsäure an der Plasmamembran.

Diese Ergebnisse legen nahe, dass Hypotonie-induzierte VRAC-Aktivierung Diacylglycerin und Phosphatidsäure involviert.

1 INTRODUCTION

1.1 The volume-regulated anion channel VRAC

The volume-regulated anion channel (VRAC), alternatively named the volume-sensitive outwardly rectifying (VSOR) anion channel (Okada, 1997) or the volume-sensitive osmolyte/anion (VSOAC) channel (Strange et al., 1996), is a key constituent of the cellular response to osmotic swelling (Jentsch, 2016) and ubiquitously expressed in almost all vertebrate cells (Chen et al., 2019b; Jentsch, 2016; Pedersen et al., 2016).

Regulatory volume decrease (RVD) is a tightly regulated process depends on a swelling activated Cl^- conductance of the plasma membrane. This conductance was first described in the late 1970s and early 1980s using microelectrodes and radioactive flux measurements (Grinstein et al., 1982; Hoffmann, 1978). More than three decades ago, large VRAC currents were first identified in T lymphocytes (Cahalan and Lewis, 1988) and human intestinal epithelial cells (Hazama and Okada, 1988) using whole-cell patch clamp electrophysiology. Subsequently, they have been observed in almost all vertebrate cell types investigated (Nilius et al., 1997; Okada, 1997; Strange et al., 1996). As determined from shifts in the reversal potential of volume-activated chloride current ($I_{Cl,\ vol}$) upon anion substitution, the permeability sequence among anions is as follows: $I^- > NO3^- > Br^- > Cl^- > F^-$ (Akita and Okada, 2014; Nilius and Droogmans, 2003; Nilius et al., 1997). Thus, VRAC prefers larger halides over smaller ones. Additionally, VRAC conducts large osmolytes such as myoinositol and taurine (Jackson and Strange, 1993; Kirk et al., 1992; Qiu et al., 2014; Voss et al., 2014).

Although the functional properties of VRAC have been extensively studied over the last 30 years, the molecular identity of the underlying protein entity was discovered much later. In 2014, two groups independently identified leucine-rich repeat containing 8A (LRRC8A) as an indispensable component in constituting VRAC by using high-throughput fluorescence assays (YFP quenching) and genome-wide RNA silencing methods (Qiu et al., 2014; Voss et al., 2014). Both groups revealed that siRNA-mediated LRRC8A knockdown diminished the YFP quenching caused by swelling-induced iodide influx through VRAC. Swelling-induced chloride

conductance ($I_{Cl,swell}$) was reduced by knockdown of LRRC8A (Qiu et al., 2014; Voss et al., 2014) or completely abolished by genomic disruption (Voss et al., 2014) in patch-clamp recordings, but could be rescued by LRRC8A transfection (Voss et al., 2014).

LRRC8 is a protein family comprising of five members, LRRC8A-LRRC8E, which was first described in a girl with agammaglobulinemia (Sawada et al., 2003). VRAC is heteromeric complex consisting of the essential subunit LRRC8A and at least one of the other LRRC8 protein (LRRC8B to LRRC8E) (Qiu et al., 2014; Syeda et al., 2016; Voss et al., 2014).

1.1.1 The structure of LRRC8/VRAC channel

LRRC8 proteins share a common ancestor with pannexins, and were proposed to form hexameric channels (Abascal and Zardoya, 2012), a notion supported by experimental data (Gaitan-Penas et al., 2016; Lutter et al., 2017; Syeda et al., 2016). Recently, an important breakthrough in the field of VRAC is that the structures of LRRC8/VRAC channels was revealed by cryo-EM (Deneka et al., 2018; Kasuya et al., 2018; Kefauver et al., 2018; Kern et al., 2019; Nakamura et al., 2020). High-resolution cryo-EM confirmed that LRRC8A homomers (Deneka et al., 2018; Kasuya et al., 2018; Kefauver et al., 2018; Kern et al., 2019) and LRRC8D homomers (Nakamura et al., 2020) VRAC channels are hexamers. Further down, a low-resolution cryo-EM structure of LRRC8A/C channels suggests a similar hexameric structure for LRRC8 heteromers (Deneka et al., 2018).

The secondary structural elements verified in the cryo-EM structures of mouse and human LRRC8A are shown in Figure 1A and 1B. LRRC8A comprises four regions defined as intracellular domain (ICD), transmembrane domain (TMD), extracellular domain (ECD), and leucine-rich repeat domain (LRRD). When functioning as a VRAC subunit, the N and C termini of LRRC8A are located in the cytoplasmic side of the plasma membrane. The N terminus is 23 amino acids long and is largely unresolved in all structures (Deneka et al., 2018; Kasuya et al., 2018; Kefauver et al., 2018) except for a short N-terminal coil (NTC) that projects into the pore domain of the channel (Kefauver et al., 2018).

The membrane domain comprises four transmembrane helices (TMH1-4). TMH1-2 and TMH3-4, which are connected by two extracellular loops, EL1 and EL2, and one intracellular loop (IL1) (Figure 1A). EL1 consists of one α helix (EL1H) and one β strand (EL1β). The region between EL1H and EL1β is disordered and comprises a proline-rich domain. EL2 possesses two β strands, EL2β1 and EL2β2. The intracellular loop (IL1), which connects TMH2 and TMH3, contains three α-helices with an undetermined stretch between the second and third helices that harbors several putative phosphorylation sites (Abascal and Zardoya, 2012). A second intracellular loop (IL2) is links TMH4 and the LRR region and contains four α-helices (ILH1-4) (Figure 1A). A threonine (T44) of LRRC8A located on the extracellular side of TMH1 (Figure 1D) was reported to play an important role in ion permeation (Qiu et al., 2014; Syeda et al., 2016). Replacement of T44 to cysteine markedly increases I^- permeability. In contrast, arginine substitution at T44 diminishes permeability to I^-. Syeda and colleagues reported that mutating T44 to cysteine in LRRC8C, LRRC8D, or LRRC8E subunits increased I^- permeability identically as the T44C mutation of LRRC8A (Syeda et al., 2016). Cryo-EM structures confirmed that TM1 constitutes part of the VRAC pore and that T44 projects into the pore on the extracellular side of the cell membrane (Deneka et al., 2018; Kasuya et al., 2018; Kefauver et al., 2018).

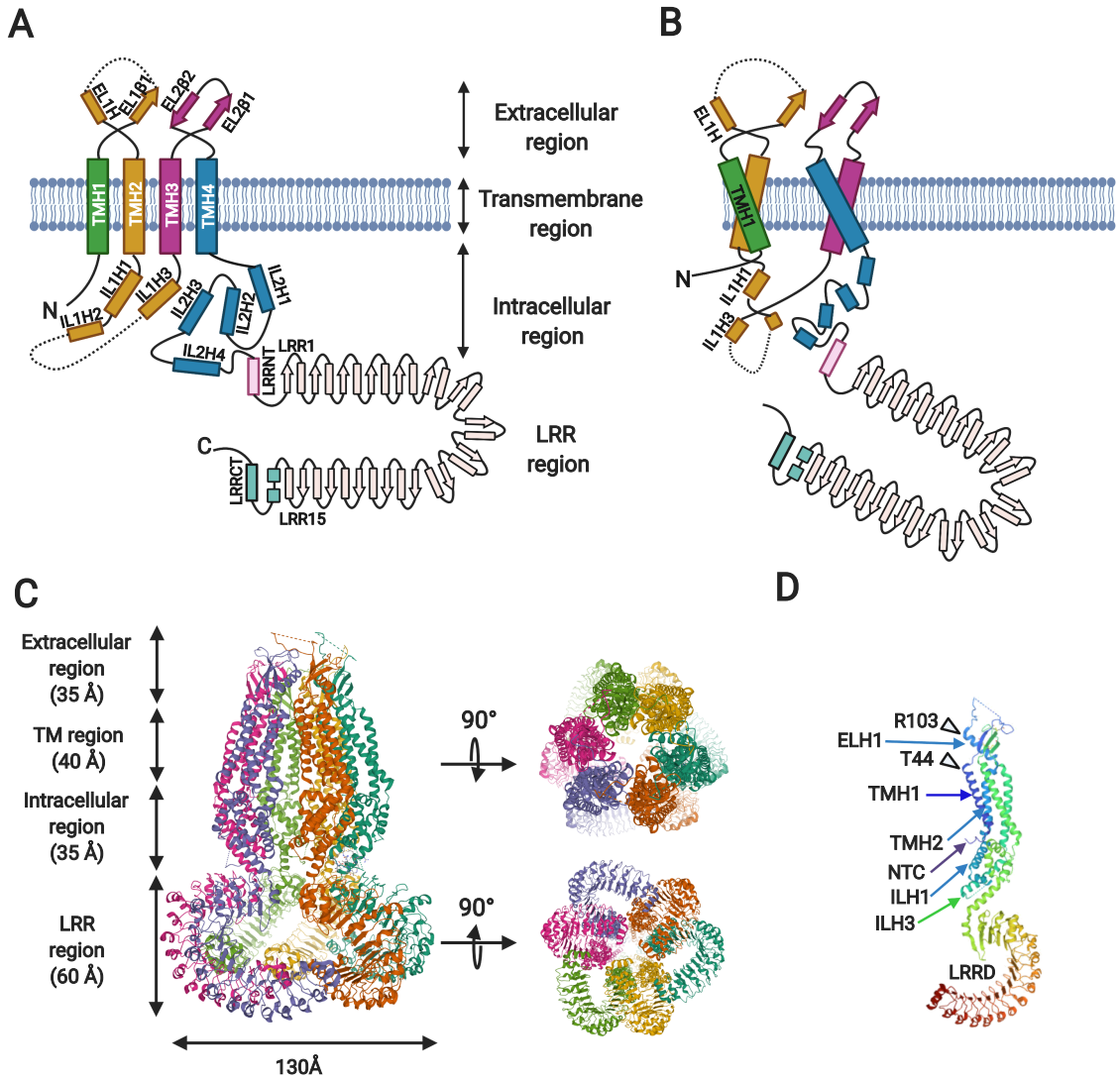

Figure 1. Structure of LRRC8/VRAC channel

(**A**) Schematic representation of a single LRRC8A protein topology. LRRC8A is composed of four regions, extracellular, transmembrane, intracellular, and LRR regions. EL, extracellular loop; H, α-helix; IL, intracellular loop; β, β strand; LRRCT, LRR region C terminus; LRRNT, LRR region N terminus; TMH, transmembrane helix. Dashed lines represent protein regions that were not resolved in cryo-EM structures. (**B**) Schematic representation of single LRRC8A subunit within a hexamer. The channel pore mainly consists of ELH1, TMH1, N terminus, ILH1 and ILH3. Figure modified from (Kasuya et al., 2018). (**C**) Overall structure of the Human LRRC8A hexamer viewed from within membrane (left) and from the extracellular (right, upper) and intracellular (right, lower) sides. TM, transmembrane. LRR, leucine-rich repeat. Adapted from (Kasuya et al., 2018). (**D**) Ribbon representation of an LRRC8A subunit. EL, extracellular loop; H, α-helix; IL, intracellular loop; LRRD leucine-rich repeat domain; TMH, transmembrane helix. Adapted from (König and Stauber, 2019).

The LRR region contains a N-terminal helix (LRRNT), C-terminal helices (LRRCT) and 15 leucine-rich repeats (LRR1-15), each repeat containing a β-strand and an α-helix. The 15 LRRs in each LRRC8 subunit form a typical horseshoe-shaped structure (Figure 1A, B). LRRC8 are homologous to pannexins and connexins (Abascal and Zardoya, 2012). The big structural difference between pannexins or connexins and the LRRC8 proteins depends on the C-terminus, which is extremely long in the LRRC8 proteins. Both constricted and expanded conformations of the C-terminus were found in the LRRC8A hexamer (Kasuya et al., 2018; Kern et al., 2019). Moreover, all cryo-EM structures revealed that the LRRDs are highly flexible and display various orientations (Deneka et al., 2018; Kasuya et al., 2018; Kefauver et al., 2018; Kern et al., 2019; Nakamura et al., 2020), suggesting a possible conformational rearrangement of LRRDs during channel gating. Since the LRRDs are unique to VRAC channels compared to gap junction proteins (Maeda et al., 2009; Oshima et al., 2016), LRRDs are of particular interest for the structure-function relationship of LRRC8/VRAC. A number of studies associated several types of protein kinases with activation or regulation of VRAC (Bryan-Sisneros et al., 2000; Eggermont et al., 2001; Hermoso et al., 2004; König et al., 2019; Sadoshima et al., 1996; Senju et al., 2015; Sorota, 1995; Tilly et al., 1993; Voets et al., 1998). In the LRRDs, there are several predicted phosphorylation sites such as protein kinase C (PKC), and cAMP-/cGMP-dependent kinases (PKA/PKG) (Mongin, 2016). Perhaps phosphorylation changes the charge of LRRDs and subsequent lead to the conformation rearrangements, resulting in VRAC channel gating.

The VRAC pore is primarily composed of the EL1H helix in the extracellular region, the TMH1 helix in the transmembrane region, IL1H1 and IL1H3 helices in the intracellular region, as well as the N terminus (Figure 1B). The channel pore is lined with hydrophilic and positively charged amino acids. EL1H constitutes part of the extracellular constriction of the channel pore, the constriction is formed by a ring of arginines, R103. This arginine ring was reported to determine the inactivation kinetics (Ullrich et al., 2016; Yamada and Strange, 2018) and cation permeability (Deneka et al., 2018; Kefauver et al., 2018). In addition, R103 was found to be crucial for voltage-dependent block by extracellular ATP (Kefauver et al., 2018). Kern and colleagues revealed the structure of LRRC8A, in conjunction with its inhibitor, DCPIB, and found that R103 arginine lines are involved here as well (Kern

et al., 2019). The negatively charged butanoic acid group of DCPIB plugs the channel like a cork in a bottle-binding in the extracellular selectivity filter, preventing ion conduction (Kern et al., 2019).

LRRC8A structure shows a hexameric protein that is 165-180 Å long and 110-130 Å wide (Figure 1C). The six subunits are arranged around an axis of symmetry that determine the ion conduction path, with both the N- and C termini residing on the cytoplasmic side and facing the pore lumen. Most structures concluded a six-fold rotational (C6 symmetry) arrangement of the transmembrane domain, including the intracellular, transmembrane, and extracellular regions (Deneka et al., 2018; Kefauver et al., 2018; Kern et al., 2019). Whereas the LRR region displayed three-fold rotational (C3) symmetry and formed a trimer of dimers structure. In contrast, Kasuya and colleagues reported the entire channel exhibited C3 symmetry (Kasuya et al., 2018). More recently, Nakamura et al. reported the overall HsLRRC8D structure exhibited a two-fold symmetric (C2 symmetry) “dimer of trimers” arrangement (Nakamura et al., 2020).

1.2 Physiological and pathophysiological roles of VRAC

The most extensively studied physiological function of VRAC is its role in regulatory volume decrease (RVD). Besides its role in regulation of cell volume, VRAC was linked to a wide range of physiological and pathophysiological processes. However, a note of caution is warranted because the studies that assigned these physiological and pathological roles to VRAC predominantly relied on rather unspecific pharmacological blockers (Bowens et al., 2013; Fujii et al., 2015; Jentsch et al., 2016). The breakthrough discovery of LRRC8 heteromers as VRAC provides enormous opportunities to assess previously proposed physiological and pathophysiological roles and to explore novel function of VRAC.

1.2.1 VRAC in regulatory volume decrease (RVD)

Cell volume regulation is an extremely important homeostatic function since it is not only involved in cell shape, but also a variety of physiological and pathological processes, such as cell growth, cell migration and cell death (Hoffmann et al., 2009; Jentsch, 2016; Lang et al., 1998). In vertebrates, the osmolarity of intracellular fluid

may alter during physiological processes, for instance, accumulation of metabolic products and transepithelial transport (Miley et al., 1997). The osmolarity of the extracellular fluid is tightly controlled on a systemic level and usually kept constant (Pedersen et al., 2011), however, some animal cells are regularly exposed to changes in extracellular osmolarity under normal physiological conditions, such as the gastrointestinal tract cells and distal kidney tubule cells. Moreover, a variety of pathophysiological conditions such as ischemia, hypoxia, hyponatremia and systemic disturbances in ion and pH homeostasis may trigger cell swelling or shrinking (Hoffmann et al., 2009).

Since plasma membranes are permeable to water, reduction in extracellular osmolality or increase in intracellular osmolality induces a rapid net influx of water across the cell membrane, resulting in cell swelling. To counteract osmotic alterations, cells regulate their volume decrease by releasing K^+ and Cl^- and organic osmolytes followed by water. After the initial swelling, cells gradually restore their original volume, even in the continued presence of low osmolarity (Figure 2).

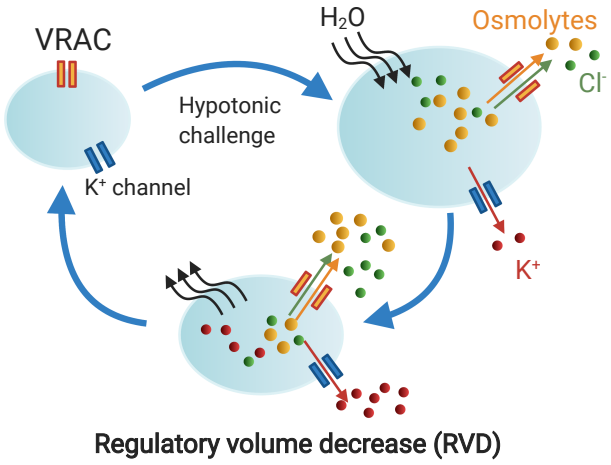

Figure 2. Mechanism of regulatory volume decrease
Hypotonic challenge osmotically leads to swelling by driving water into the cell and subsequent activation of VRAC and K^+ channels, which mediate efflux of K^+, Cl^- and organic osmolytes, followed by H_2O, to facilitate the regulatory volume decrease (RVD). Modified from (Stauber, 2015).

Several volume-sensitive K^+ channels have been characterized in regulatory volume decrease (RVD) for a variety of cell types (Wehner, 2006). Whereas, due to almost all cell types exhibit much larger basal conductance for K^+ than for Cl^-, RVD mainly depends on a swelling-induced increase in Cl^- conductance (Hoffmann et al., 2009; Nilius et al., 1997; Okada et al., 2009). Such an increase in anion permeability mediates by a major key player of the RVD response termed volume-regulated

anion channel (VRAC), a ubiquitously expressed Cl^- channel which is activated by hypotonicity-induced cell swelling (Pedersen et al., 2016).

Extensive studies showed that knockout and knockdown of VRAC-forming LRRC8 proteins led to severely impaired RVD in many cell types from various organisms (Formaggio et al., 2019; Kang et al., 2018; Lück et al., 2018; Qiu et al., 2014; Voss et al., 2014; Yamada et al., 2016), demonstrating that VRAC is major player in RVD. Besides Cl^-, VRAC mediates the release of various organic osmolytes such as taurine and glutamate during RVD in vertebrate cells (Jentsch, 2016; Pedersen et al., 2016; Stauber, 2015; Strange et al., 2019).

1.2.2 VRAC in cell proliferation and migration

Proliferation and migration are fundamental cell physiological processes that involve cell volume regulation (Hoffmann et al., 2009; Lang et al., 1998). Due to its critical role in regulatory volume decrease (RVD), VRAC has been implicated in cell volume changes during cell proliferation and migration (Hoffmann et al., 2009; Schwab et al., 2012). Maximal VRAC currents were reported to alter during cell cycle progression in human cervical cancer cells (Shen et al., 2000). During cell cycle progression, the transient activation of Cl^- channels led to a decrease in cell volume after an initial volume increase (Habela and Sontheimer, 2007; Klausen et al., 2010; Lang et al., 2006).

Over the past years, several (rather unspecific) VRAC inhibitors were reported to impair proliferation of various cell types (He et al., 2012; Klausen et al., 2007; Liang et al., 2014; Maertens et al., 2001; Rouzaire-Dubois et al., 2000; Wondergem et al., 2001; Wong et al., 2018). Nonetheless, so far, no proliferation defect has been reported for diverse LRRC8A deletion cell lines published during the last six years. Consistently, siRNA-mediated knockdown of LRRC8A has no impact on HeLa cell cycle progression (Sirianant et al., 2016). Recently, a novel VRAC blocker, the flavonoid Dh-morin, was found to effectively suppress endogenous VRAC currents in endothelial cells, without impairing the proliferation of human umbilical vein endothelial (HUVEC) cells (Xue et al., 2018), excluding a prominent role for VRAC in the cell cycle progression of this cell line. In addition, the anti-proliferative effect of cardiac glycosides was also linked, albeit not necessarily directly, to an increase

in VRAC activity in HT-29 cells and could be inhibited by the VRAC blocker DCPIB (Fujii et al., 2018).

Cell migration is primarily regulated by cytoskeletal rearrangements and directed membrane transport. Osmotic water flux by the differential activity of ion channels and transporters mediating local changes in cell volume was reported to contribute to cell motility (Jaeger et al., 1999; Schwab et al., 1995). Cell migration can be described as a repetitive cycle of protrusion at the leading edge that is followed by retraction at the trailing end (Schwab et al., 2012). The uptake of inorganic ions and H_2O (a regulatory volume increase, RVI) at the cell front by locally active Na^+-K^+-$2Cl^-$ cotransport, Na^+/H^+ exchange or nonselective cation channels, and a volume decrease at the rear part by releasing K^+ and Cl^- through activated K^+ and Cl^- channels followed by water efflux (RVD) will cause a net translocation of the cell (Figure 3).

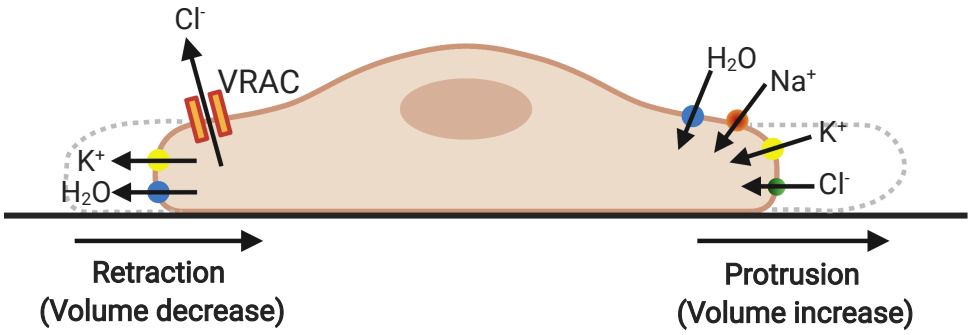

Figure 3. Schematic presentation of cell volume regulation during cell migration
The uptake of inorganic ions and H_2O contributes to volume increase at the leading edge, whereas net KCl efflux followed by H_2O leads to volume loss at the trailing end, including that of chloride by VRAC, may contribute to cell movement. Figure adabted from (Chen et al., 2019b).

Several ion channels and transporters involving in cell volume regulation have been reported to be components of the cellular migration machinery. For instance, the Na^+-K^+-$2Cl^-$ cotransporter NKCC1 (Haas and Sontheimer, 2010; Reid et al., 2005), Ca^{2+}-activated K^+ channel K_{Ca} 3.1 (Cruse et al., 2006; Schilling et al., 2004; Sciaccaluga et al., 2010), as well as VRAC (Mao et al., 2007; Schneider et al., 2008). Glycine-induced cell swelling was associated with the motility of murine microglial cells (Kittl et al., 2018); and indeed, cell displacement was shown to be solely driven by directed cellular osmotic water transport in an artificial confined environment

when actin polymerization was suppressed (Stroka et al., 2014). The VRAC blocker DCPIB was found to reduce the motility of glioblastoma cell lines (Wong et al., 2018) and siRNA-mediated knockdown of LRRC8A was found to impair the migration of human colon cancer HCT116 cells (Zhang et al., 2018).

In summary, there are controversial data in respect of the involvement of VRAC in cell cycle progression and migration. Accordingly, systematic studies combining pharmacological and molecular biological tools and comparison of different cell types are required to draw a comprehensive picture of a potential role of VRAC in these processes.

1.2.3 Specific roles of the different LRRC8 subunits

The *Lrrc8* gene family comprises five members termed *LRRC8A, LRRC8B, LRRC8C, LRRC8D, and LRRC8E* (Abascal and Zardoya, 2012; Voss et al., 2014). LRRC8A is an essential subunit of VRAC (Qiu et al., 2014; Voss et al., 2014), which traffics to the cell membrane when expressed alone in cells (Syeda et al., 2016), whereas LRRC8B, LRRC8C, LRRC8D, and LRRC8E are retained in the endoplasmic reticulum when expressed alone (Voss et al., 2014). For physiological function and normal volume sensitivity, LRRC8A must be coexpressed with at least one other LRRC8 family member (B-E) (Gaitan-Penas et al., 2016; Syeda et al., 2016; Voss et al., 2014; Yamada and Strange, 2018). VRAC was proposed to be formed by heteromers of LRRC8 proteins, which has recently been confirmed by cryo-EM structures of LRRC8A homomers, LRRC8D homomers and LRRC8A/C heteromers (see section 1.1.1). Most cryo-EM structures revealed that VRAC exhibits a hexameric assembly with a trimer of dimers. Several fundamental biophysical properties like single channel conductance, inactivation kinetics, substrate specificity and the extent of rectification are determined by the variable LRRC8 subunit combination (Syeda et al., 2016; Ullrich et al., 2016; Voss et al., 2014; Yamada and Strange, 2018).

LRRC8A is ubiquitously expressed in vertebrate cells and has been detected in all tissues analyzed so far. *Lrrc8a*$^{-/-}$ mice displayed high postnatal lethality (Kumar et al., 2014), and several studies confirmed the physiological importance of LRRC8A by utilizing gene disruption or knockdown in a cell type-specific manner or in cell

culture (Chen et al., 2019a; Kang et al., 2018; Lück et al., 2018; Stuhlmann et al., 2018; Yang et al., 2019; Zhang et al., 2017). Interestingly, LRRC8A expressed alone gave no detectable whole-cell currents (Qiu et al., 2014; Voss et al., 2014), whereas its overexpression suppressed endogenous VRAC activity (Qiu et al., 2014; Syeda et al., 2016; Voss et al., 2014). Recently, the Stauber lab found that the essential LRRC8A subunit was relatively low abundant in C2C12 myoblasts, 3T3 fibroblasts and various organs, which suggested the presence of only one or two LRRC8A per hexameric VRAC (Pervaiz et al., 2019). This may explain the larger currents when LRRC8A was diluted in LRRC8A/C co-expression (Yamada et al., 2016) and the suppression of endogenous VRAC currents by LRRC8A overexpression (Qiu et al., 2014; Syeda et al., 2016; Voss et al., 2014).

Only low VRAC currents were observed in *LRRC8(C,D,E)*$^{-/-}$ HCT116 cells (Voss et al., 2014) and VRAC currents were abolished in HEK cells when the same subunits were knocked out (Lutter et al., 2017). Hence, LRRC8A/B heteromers give rise to VRAC activity that may be cell type-specific. Ghosh et al. found that both overexpression and knockdown of human LRRC8B in HEK293 cells altered the Ca^{2+} level in the endoplasmic reticulum (ER), they deduced that LRRC8B participated in intracellular Ca^{2+} homeostasis by acting as a leak channel in the ER (Ghosh et al., 2018). However, this proposal should be viewed cautiously. Overexpression and knockdown of LRRC8B perhaps affect ER functions in an indirect way. More detailed studies are needed before additional channel functions are ascribed to LRRC8 proteins.

LRRC8C was identified as an accelerating factor for adipogenesis, *fad*158, prior to it was recognized as a VRAC subunit (Tominaga et al., 2004). Knockdown of LRRC8C expression prevented adipocyte differentiation of 3T3-L1 cells. In addition, Overexpression of LRRC8C facilitated adipogenesis of NIH-3T3 cells (Tominaga et al., 2004). Consistent with the involvement in adipogenesis, LRRC8C-deficient mice exhibited reduced body weight and fat mass when fed a high-fat diet (Hayashi et al., 2011). In adipocyte-specific LRRC8A depletion mice, lower weight was also observed, this was assigned to an impact on insulin signaling (Zhang et al., 2017).

LRRC8D-mediated VRAC increases the permeability of VRAC to cellular osmolyte taurine, lysine and platinum-based anticancer drugs (Lutter et al., 2017; Planells-

Cases et al., 2015; Qiu et al., 2014; Voss et al., 2014). Furthermore, LRRC8D is a mammalian protein required for the import of the protein synthesis inhibitor blasticidin S (Lee et al., 2014). Compared to LRRC8C and LRRC8E, LRRC8D-containing VRAC exhibited larger outward rectification and lesser permeability preference of I^- over Cl^- (Syeda et al., 2016), although this anion-conducting selectivity was comparatively small and was not detected in another study (Voss et al., 2014). Moreover, LRRC8C, LRRC8D and LRRC8E coexpression with LRRC8A conduct aspartate and glutamate (Lutter et al., 2017; Schober et al., 2017). However, coexpression of LRRC8D and LRRC8A was recently shown to inhibit 2′3′cGMP-AMP (cGAMP) transport (Lahey et al., 2020).

LRRC8E, which shows the largest difference in expression levels between tissues, increases the permeability to negatively charged osmolytes such as ATP glutamate and aspartate and which can function as signaling molecules (Gaitán-Peñas et al., 2016; Lutter et al., 2017; Schober et al., 2017). In 2020, two groups found that LRRC8A/LRRC8E-containing VRAC channels could transport cGAMP (Lahey et al., 2020; Zhou et al., 2020a). So like LRRC8D, LRRC8E may play a role in cell-cell communication by VRAC.

1.2.4 VRAC roles in other (patho-)physiological processes

In addition to the roles described above, VRAC has been found to play a role in other physiological and pathological processes (Figure 4). For example, the spontaneous house mouse mutant *ébouriffé* (*ebo*) (Lalouette et al., 1996), which expresses a truncated LRRC8A mutant that markedly lacks VRAC channel activity (Platt et al., 2017), having intact T-cell development and function while retaining some of the phenotypic features of *Lrrc8a*$^{-/-}$ mice, including abnormal hair, infertility, kidney abnormalities and reduced survival (Kumar et al., 2014; Platt et al., 2017). Furthermore, germ cell-specific *Lrrc8a*$^{-/-}$ was reported to result in abnormal sperm and male infertility (Bao et al., 2018; Lück et al., 2018). Developing sperm lacking LRRC8A displayed a swollen cytoplasm and later exhibited severe disorganization of mitochondrial sheaths in the midpiece region, as well as angulation or flagellar coiling. The severe malformation of spermatids can be explained by impaired cell volume regulation that leads to swelling of the cytoplasm that hampers the elimination of excess cytoplasm during further development (Lück et al., 2018).

Bao and colleagues reported a heterozygous R545H missense mutation in *LRRC8A* in a patient with a male sterility disorder termed Sertoli cell-only syndrome (Bao et al., 2018). They proposed that the R545H mutation may lead to sterility (Bao et al., 2018). However, such a conclusion should be viewed with caution because the R545H mutant only mildly reduced VRAC currents by 25~30% when LRRC8A was coexpressed with LRRC8C or LRRC8D subunit in *Xenopus oocytes* (Bao et al., 2018). In addition, the patient investigated is heterozygous R545H mutant. However, heterozygous mice display normal fertility (Kumar et al., 2014).

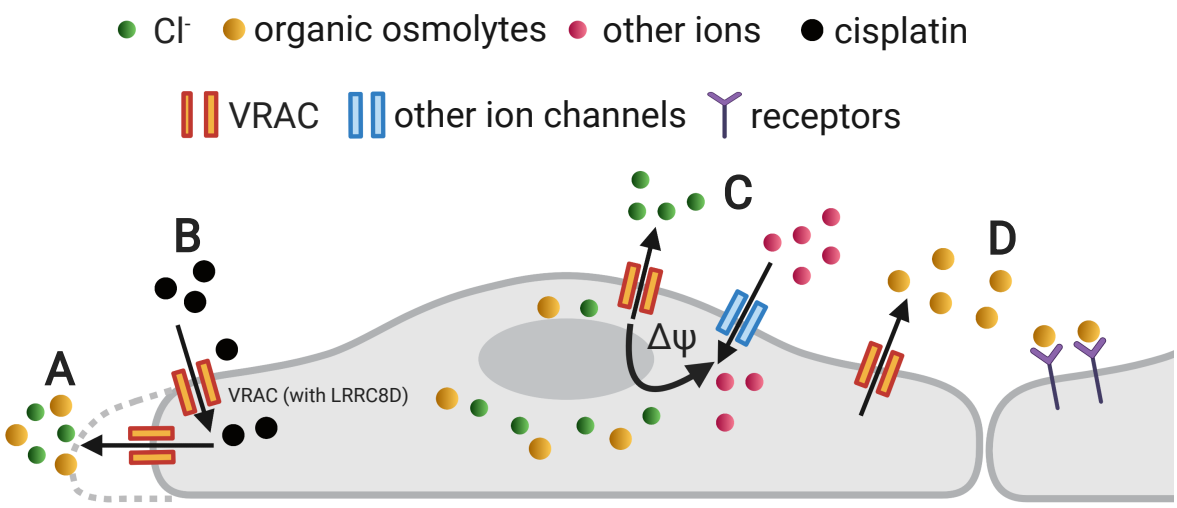

Figure 4. Schematic presentation of mechanisms underlying VRAC physiological functions

(**A**) The release of Cl^- and organic osmolytes leads to osmotic efflux of water resulting in a volume decrease. (**B**) Cisplatin enters the cell through LRRC8D-containing VRAC. Activation of VRAC leads to apoptotic volume decrease (AVD), which facilitate apoptosis. (**C**) VRAC opening alters the membrane potential towards the equilibrium potential of Cl^-, influencing the transport of other ions. (**D**) VRAC-conducting organic osmolytes act as signaling molecules. Figure modified from (Chen et al., 2019b).

Pharmacological studies suggested a role for VRAC in glucose sensing and insulin secretion of pancreatic β-cells. Glucose uptake and metabolism lead to cell swelling (Miley et al., 1997), and it was proposed that VRAC activation induced efflux of Cl^- would contribute to the depolarization of plasma membrane (Best et al., 2010). In 2018, two studies independently found that in pancreatic β-cells, glucose- or

hypotonicity-induced cell swelling evoked VRAC currents and this contributed to membrane depolarization, which caused electrical excitation to some extent (Kang et al., 2018; Stuhlmann et al., 2018). Besides, the Stauber lab has recently shown that VRAC facilitates C2C12 myoblast differentiation by promoting membrane hyperpolarization via a yet unknown mechanism (Chen et al., 2019a).

Several laboratories have implicated that microglia and astrocytes release excitatory amino acids (EAAs) like glutamate via VRAC in response to bradykinin, hypotonicity or purinergic signaling through ATP (Akita et al., 2011; Benfenati et al., 2009; Harrigan et al., 2008; Kimelberg et al., 1990; Liu et al., 2009; Liu et al., 2006; Mongin and Kimelberg, 2002; Roy, 1995). In astrocytes, EAA release is considered to contribute to physiological astrocyte-neuron communication (Akita and Okada, 2014; Elorza-Vidal et al., 2019; Mongin, 2016). Increase in extracellular glutamate and subsequent overactivation of glutamate receptors, a process called excitotoxicity, has emerged as a crucial mechanism of neuronal cell damage in brain diseases (Lai et al., 2014). VRAC has also been proposed to mediate EAA release and excitotoxicity under conditions like stroke, trauma, hyponatremia, and epilepsy (Mongin, 2016). Several studies reported that pharmacological inhibition of VRAC diminished ischemic brain damage (Feustel et al., 2004; Inoue et al., 2007; Vakili et al., 2009). Downregulation of LRRC8A/VRAC was found to reduce swelling-activated release of the EAAs in astrocytes (Hyzinski-García et al., 2014; Schober et al., 2017). Furthermore, *Lrrc8a*$^{-/-}$ mice displayed impaired glutamatergic transmission and provided neuroprotection from ischemic stroke (Yang et al., 2019; Zhou et al., 2020b).

Extracellular 2′3′-cyclic-GMP-AMP (cGAMP) is characterized as a second messenger that is secreted by infected or malignant cells (Sun et al., 2013) and imported into host cells to activate the innate immune stimulator of interferon genes (STING) pathway (Ishikawa and Barber, 2008; Sun et al., 2009; Zhong et al., 2008). Recently, two groups independently identified that LRRC8/VRAC functions as a conduit for the transport of cGAMP (Lahey et al., 2020; Zhou et al., 2020a). Expression of LRRC8A and LRRCE (Lahey et al., 2020; Zhou et al., 2020a) or LRRC8C (Lahey et al., 2020) was shown to promote cGAMP transport. In contrast, LRRC8D hindered the transmission of cGAMP (Lahey et al., 2020). Zhou and

colleagues reported that VRAC inhibition led to increased viral propagation in response to herpes simplex virus 1 (HSV-1) infection (Zhou et al., 2020a). In addition, *Lrrc8e*$^{-/-}$ mice displayed impaired interferon (IFN) responses and compromised immunity to HSV-1 (Zhou et al., 2020a).

Apoptosis, a form of programmed cell death, is mostly accompanied by a decrease in cellular volume, which denominated apoptotic volume decrease (AVD) (Bortner and Cidlowski, 1998; Lang and Hoffmann, 2012; Orlov et al., 2013). In analogy to RVD, VRAC was proposed to play a role in AVD (Kunzelmann, 2016; Lang and Hoffmann, 2012). Such an implication was found for VRAC in butyrate-triggered apoptosis of colonic epithelial cells (Shimizu et al., 2015), during chondrocyte loss (Kumagai et al., 2016) and during myocardial ischemia/reperfusion injury (Xia et al., 2016). Apoptosis inducers such as cisplatin, Fas ligand and staurosporine were reported to activate VRAC independent of cell swelling under isotonic conditions (Gradogna et al., 2017; Okada et al., 2006; Planells-Cases et al., 2015; Shimizu et al., 2004). Pharmacological inhibition of VRAC reduced apoptosis induced by several compounds, including the anti-cancer drug cisplatin (Cai et al., 2015; Hasegawa et al., 2012; Ise et al., 2005; Poulsen et al., 2010; Shimizu et al., 2015). Induction of apoptosis with staurosporine and cisplatin was blocked by LRRC8A knockout in HCT116 cells (Planells-Cases et al., 2015), although knockdown of LRRC8A in HeLa cells reportedly did not eliminate AVD upon application of staurosporine (Sirianant et al., 2016).

1.3 Mechanisms of VRAC activation and regulation

The mechanism responsible for VRAC activation upon hypotonic swelling is largely unclear. Many studies suggested that the activation of VRAC could be affected or induced by a variety of stimuli, intracellular molecules, second messengers and signaling pathways, the most prominent of which I will discuss below. However, none of them has proved critical enough to obtain a general stand of different cell types. Moreover, most of the work regarding VRAC's activation was performed without knowing the molecular identity of VRAC. Collectively, a clear comprehensive illustration of VRAC activation is still lacking. The identification of VRAC's molecular nature and especially the general structure of VRAC (see section 1.1), provide

strong support to investigate the underlying activation and regulation mechanisms of VRAC activity.

1.3.1 Ionic strength

VRAC is not sensitive to cell volume per se, as cell volume is an extensive thermodynamic parameter, which cannot be sensed by the cell directly. However, cell swelling is associated with changes of diverse parameters that can be sensed by the cell, such as mechanical and chemical changes in the lipid bilayer of the plasma membrane, interaction of the plasma membrane with the cytoskeleton, or changes of intracellular ionic strength and macromolecule concentration (Jentsch, 2016). One of the most important questions is whether VRAC depends on an extrinsic sensor that could be coupled to the channel either directly or via a signal transduction pathway.

Major changes in extracellular osmolarity are rare under normal physiological conditions in vertebrates. Isovolumetric stimuli, such as reduction of intracellular ionic strength or during metabolic changes, may be more physiologically relevant for VRAC activation (Pedersen et al., 2015). Several studies suggested that VRAC activation is triggered directly by reduced ionic strength in endothelial cells (Sabirov et al., 2000; Voets et al., 1999). Notably, lowering ionic strength was shown to activate VRAC both after in vitro reconstitution and in whole-cell recording (Syeda et al., 2016). However, it should be noted that VRAC could also be activated in an isosmotic swelling with constant ionic strength or isovolumic conditions (Best and Brown, 2009; Cannon et al., 1998; Nilius and Droogmans, 2003; Zhang and Lieberman, 1996). Recently, by using a newly developed optical sensor for VRAC activity, our lab could show that VRAC cannot be directly activate by reduced ionic strength in living cells (König et al., 2019). On the one hand, reduced ionic strength did not activate ER- and Golgi-localized VRAC channels, they were only activated when they reach the plasma membrane. On the other hand, lowering ionic strength was dispensable to maintain plasma membrane-localized VRAC active. VRAC persisted active in isotonic solution after activation by hypotonic swelling when applying the diacylglycerol kinase (DGK) inhibitor dioctanoylglycol (DOG), even though ionic strength restored to normal levels (König et al., 2019).

1.3.2 Protein phosphorylation

Several reports stated that tyrosine phosphorylation might be essential in modulation of VRAC activity, either directly or in a permissive fashion (Bryan-Sisneros et al., 2000; Eggermont et al., 2001; Sadoshima et al., 1996; Sorota, 1995; Tilly et al., 1993; Voets et al., 1998). Pharmacological inhibitors of protein tyrosine kinase (PTK) including genistein, tyrphostin B46 and tyrphostin A25 restrained VRAC activation (Bryan-Sisneros et al., 2000; Sorota, 1995; Tilly et al., 1993; Voets et al., 1998). In addition, hypoosmotic swelling triggered protein tyrosine phosphorylation in cardiac myocytes, which was only prevented by tyrosine kinase inhibitors (Sadoshima et al., 1996). While it is not yet clear which tyrosine kinase is specifically responsible for the swelling-induced phosphorylation, evidence has pointed to the importance of Src family (Lepple-Wienhues et al., 1998). It is also worthwhile to note that inhibition of protein tyrosine phosphatases (PTP) suppressed VRAC activation in bovine chromaffin cells and mouse fibroblasts (Doroshenko, 1998; Thoroed et al., 1999).

Phospholipase C (PLC) activity has been implicated to play a role in $I_{Cl,swell}$ activation (Catacuzzeno et al., 2014; Zholos et al., 2005). Pharmacological Inhibition of PLC by a specific inhibitor led to reduced current upon hypotonic swelling (Catacuzzeno et al., 2014; Zholos et al., 2005). In addition, several studies suggested that cell swelling led to the activation of PLC via an undetermined mechanism (Fujii et al., 1999; Moore et al., 2002; Ruwhof et al., 2001). The literature on the role of protein kinase C (PKC) family, which is activated through PLC signaling pathway, in activating and regulating VRAC is confusing. Conventional PKC isoform α and βI were found to contribute to ATP-induced activation of VRAC (Rudkouskaya et al., 2008). Moreover, PKCα was reported to play a regulatory role in cell volume in response to hypotonicity (Hermoso et al., 2004; Senju et al., 2015). Recently, PKCμ, also known as protein kinase D (PKD), was shown to be of importance in the activation of VRAC (König et al., 2019). However, PKC activity did not affect the activation of VRAC by hypotonic swelling in human glioblastoma (GBM) cells (Catacuzzeno et al., 2014). Chelerythrine chloride (CC), a specific inhibitor of PKC, activated a current similar to the hypotonic-induced current of VRAC under isotonic conditions (Dick et al., 1998). In rat brain endothelial cells, application of PKC

activator phorbol 12,13-dibutyrate (PDBu) inhibited the increase in current normally observed following hypotonic swelling (von Weikersthal et al., 1999). Additionally, a study pointed out that PKC is unessential in $I_{Cl,\ swell}$ generation or regulation in HaCaT cells (Zholos et al., 2005).

1.3.3 G-proteins and G-protein-coupled receptors

There are two general classes of G-proteins: heterotrimeric and monomeric G-proteins. GTP-binding proteins appear to be modulators of VRAC activity. Activation of G-proteins leads to an increase in the sensitivity to cell swelling (Voets et al., 1998). This is consistent with the finding that Rho GTPases regulate VRAC currents in bovine endothelial cells (Nilius et al., 1999) and NIH3T3 mouse fibroblasts (Pedersen et al., 2002).

G-protein-coupled receptors (GPCRs) comprise one of the largest families of cell surface receptors with over 900 members, which transduce extracellular signals into intracellular effector pathways through the activation of heterotrimeric G-proteins (Lappano and Maggiolini, 2011). GPCRs have been shown to regulate calcium, potassium, and sodium voltage-gated ion channel activity in neurons and other excitable cells (Abbracchio et al., 2006). Some studies reported that stimulation of purinergic G-protein-coupled receptors (P2YRs) in astrocytes leads to a limited isovolumic activation of VRAC (Akita et al., 2011; Darby et al., 2003; Mongin and Kimelberg, 2005; Takano et al., 2005). Moreover, signaling through several other G-protein-coupled receptors has been shown to similarly activate astrocytic VRAC (Fisher et al., 2008; Fisher et al., 2010; Franco et al., 2008). VRAC has also been found to be activated isovolumically by S1P, which can activate sphingosine-1-phosphate receptors (S1PR), known as a family of plasma membrane GPCRs (Burow et al., 2015). Although they have been extensively studied, the activation mechanism(s) of VRAC seem complex and are far from being understood.

2 AIM OF THE WORK

The volume-regulated anion channel (VRAC) has been implicated in many physiological processes, such as cellular osmolyte release, differentiation, insulin secretion, apoptosis and anti-cancer drug uptake. Likely due to its crucial role in regulatory volume decrease (RVD), VRAC was shown to be involved in cell volume changes during cell proliferation and migration as well. Besides aiming to clarify its physiological roles, many studies have focused on revealing the activation mechanism of VRAC. However, most of the studies were heavily relying on unspecific pharmacological manipulations and performed without known molecular identity of VRAC. The discovery of LRRC8 proteins as the pore-forming VRAC components and the cryo-EM structure of VRAC encouraged me to investigate putative physiological roles and the mechanism underling VRAC gating.

In this thesis, I initially aim to systematically assess the potential role of VRAC in cell growth and motility for several cell lines, including cancer and non-cancer cell lines, by using not only pharmacological manipulations, but also siRNA against *LRRC8A* and genomic VRAC subunit knockout. Secondly, I aimed at characterizing the ambiguous activation and regulatory mechanisms of VRAC in response to hypotonic swelling in living cells using much less invasive optical approaches, including a new FRET-based sensor established by the Stauber group and high-efficiency DAG and PA optical biosensors. The new FRET optical tool cannot only detect the real-time activity of VRAC channels, but also explore the functional roles of different LRRC8 subunit compositions. DAG and PA optical biosensors can follow signaling in real time, and may offer insights of a kinetic optical signal. With these optical tools, I attempt to reveal the signaling pathway underlying VRAC activation.

3 RESULTS

3.1 Roles of VRAC in cell proliferation and migration

3.1.1 Knockout of LRRC8A does not impinge on C2C12 proliferation or migration

LRRC8A has been identified as an essential component of the VRAC (Qiu et al., 2014; Voss et al., 2014). To identify the functional significance of VRAC in the proliferation and migration, I first examined the effect of VRAC subunit LRRC8A depletion on proliferation and migration of C2C12 mouse myoblast cells. A variety of clonal genome-edited cell lines (generated by Anja Kopp in the Stauber lab) deficient for the essential VRAC subunit LRRC8A (clones 27, 13 and 14) and a line (clone 4) with only heterozygous LRRC8A deletion that had experienced the same transfection and selection process as the knockout clones were used. I initially tested the expression levels of LRRC8A in C2C12 cells, loss of LRRC8A in the knockout clones and decreased levels in clone 4 in comparison to wild-type C2C12 cells was confirmed by Western blotting (Figure 5A).

Next, I assessed the effects of LRRC8A depletion on C2C12 growth by monitoring the confluence of the cells on long-term live-cell experiments. I found no significant differences in the proliferative properties among the knockout clones (clone 27, 13 and 14), wild-type cells and the heterozygous clone (clone 4) (Figure 5B), indicating that VRAC is non-essential for C2C12 cell proliferation.

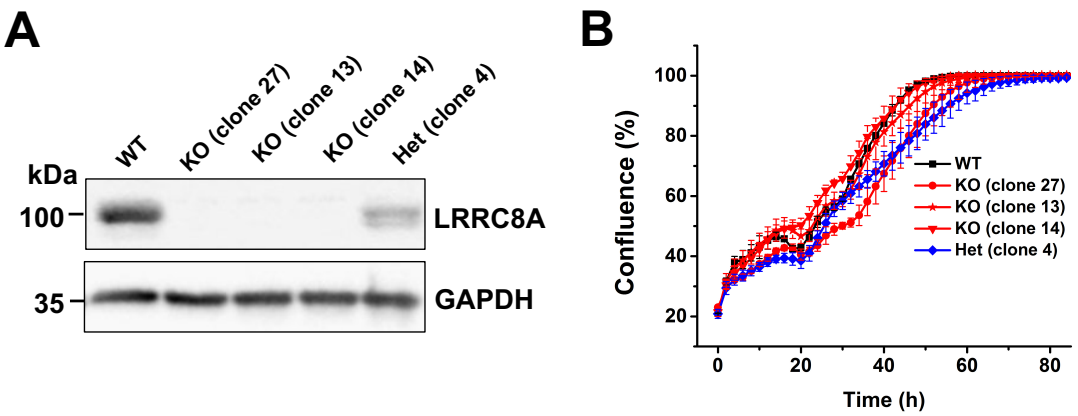

Figure 5. LRRC8A depletion has no effect on C2C12 cell proliferation

(**A**) Expression Levels of LRRC8A in wild-type (WT), LRRC8A-knockout (KO) and heterozygous (Het) C2C12 cells were determined by western blotting. GAPDH on the same blot was used as an internal control. A representative blot of three independent experiments is shown. (**B**) Growth curve of WT, KO and Het C2C12 cells. Results are expressed as mean ± SD from four experiments.

Next, I determined the effects of LRRC8A subunit depletion on C2C12 cell migration using an *in vitro* wound healing migration assay with time-lapse live-cell imaging. After 24 hours culture, I observed that the migration speed of LRRC8A knockout (clone 27, 26.22 ± 2.15 µm/h; clone 13, 23.91 ± 2.36 µm/h; clone 14, 27.79 ± 4.77 µm/h) was similar to that of wild-type C2C12 cells (26.49 ± 2.70 µm/h) and heterozygous cells (clone 4, 26.98 ± 3.33 µm/h) (Figure 6B). These results indicate that VRAC plays no crucial role in C2C12 migration in the wound healing assay. Taken together, LRRC8A, and hence VRAC activity, is dispensable for C2C12 proliferation and migration.

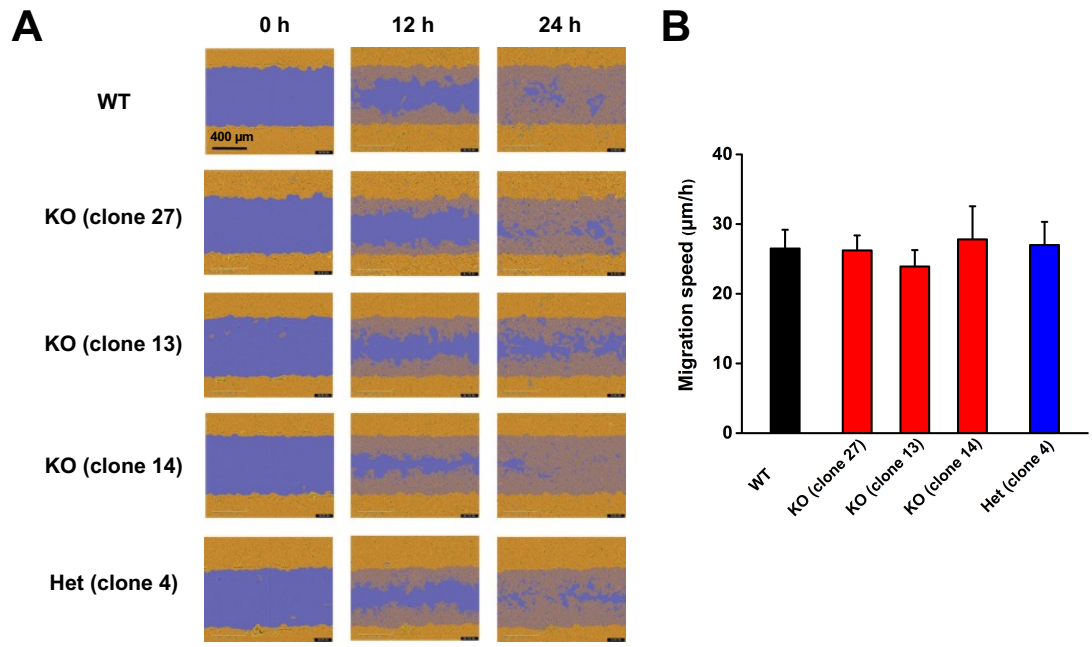

Figure 6. LRRC8A depletion does not impair C2C12 cell migration

(**A**) Representative images from a time-lapse measurement of a wound healing assay with C2C12 cells (either wild-type (WT) or monoclonal lines of LRRC8A KO and one heterozygous, as indicated) at 0, 12 and 24 h. The initial wound mark illustrated in blue, cells in orange on blue overlay represents migrated cells. Scale bar, 400 µm. (**B**) Quantification of migration speed of C2C12 cells in time-lapse measurements as shown in (**A**) determined 14 h after wounding. Results are expressed as mean ± SD from n = 14 experiments.

3.1.2 LRRC8/VRAC is not required for the proliferation of HEK-293 cells

Although the cell proliferation assay performed as above reflects relative cell numbers, I tried another approach to assess the cell proliferation and cell viability. To investigate the functional significance of VRAC in HEK-293 cell proliferation, I examined the effect of LRRC8 subunit depletion on the proliferative ability of HEK-293 using Cell Counting Kit-8 (CCK8) proliferation assays. I observed that the combined knockout of all five LRRC8 subunits did not significantly suppress HEK-293 cell proliferation. Surprisingly, depletion of LRRC8A alone inhibited the proliferative ability of HEK-293 cells (Figure 7). It is well known that LRRC8A is an essential component of VRAC, compared with the knockout of all five subunits, knocking out only LRRC8A subunit impaired the proliferation of HEK-293 cells, which is more likely to affect cell viability during the knockout process.

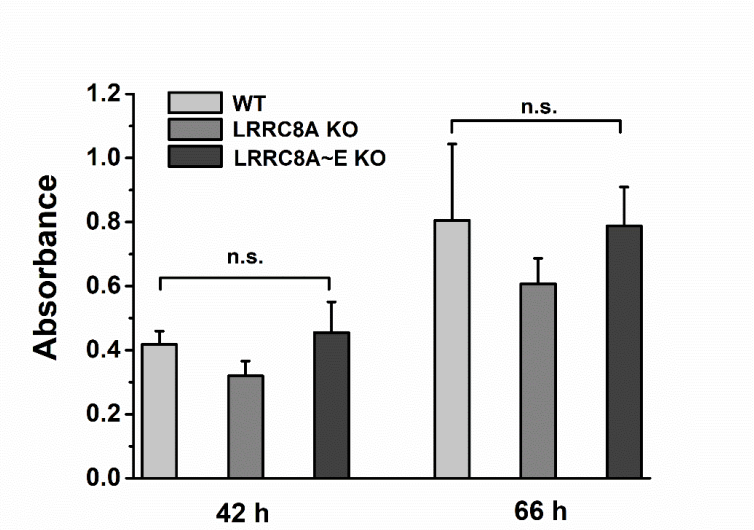

Figure 7. LRRC8 subunit depletion does not affect HEK-293 proliferative ability
Effects of LRRC8A-knockout and all five LRRC8 subunits knockout (LRRC8A~E KO) on HEK-293 cell proliferation were determined by CCK8 cell proliferation assay at indicated time points. Results are expressed as mean ± SD from four experiments. Statistics: n.s., not significant, Student's *t*-test.

3.1.3 VRAC blockers and disruption of LRRC8s do not suppress HCT116 proliferation and migration

Ion channels are increasingly being associated with cancer progression through the regulation of cell growth and migration (Arcangeli and Becchetti, 2015; Fraser and Pardo, 2008; Prevarskaya et al., 2018; Sirianant et al., 2016). As the data suggest a role for VRAC in regulation of cancer cell volume, I aimed at testing its implications for fundamental physiological processes of cell proliferation and migration that require cell volume regulation. To this end, I first examined the effects of genomic VRAC knockout on HCT116 proliferation. Although the proliferation of genomic VRAC knockout clones seemed slightly decreased when compared with wild-type cells during the first 48 h, the proliferation of a clonal cell line lacking the essential LRRC8A subunit of VRAC was virtually equal to that of wild-type cells over the whole time course. Another clonal cell line, lacking all five LRRC8 members, even displayed an increase in proliferation (Figure 8A). These results demonstrate that VRAC is not critically involved in HCT116 proliferation. Next, I examined the effect of the genomic VRAC deletion and of the VRAC inhibitor carbenoxolone (CBX) on HCT116 cell motility in the wound healing assay. Neither pharmacological inhibition

of VRAC with up to 50 µM CBX, nor gene knockout of VRAC affected motility of HCT116 cells (Figure 8B). In a word, these data pointing to the likely unimportance of VRAC for human colon cancer proliferation and migration.

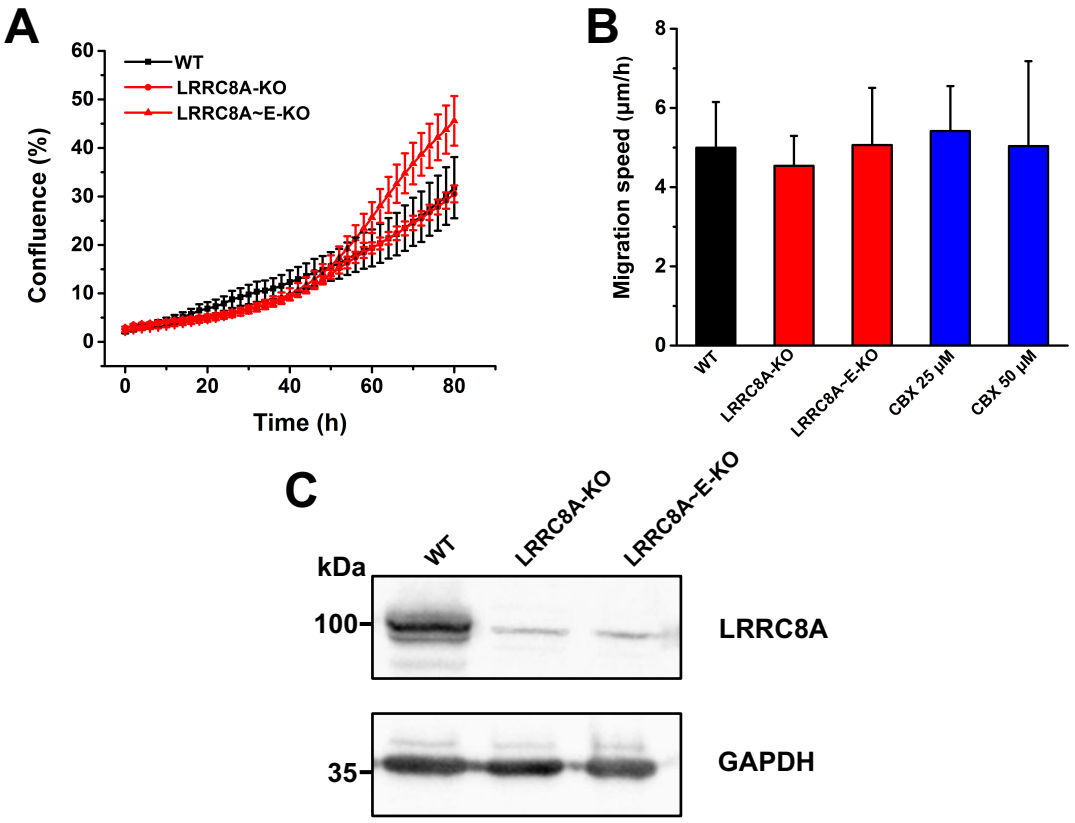

Figure 8. Effect of LRRC8 subunit knockout or carbenoxolone (CBX) treatment on cell proliferation and migration of HCT116 cells

(**A**) Proliferation curve of wild-type (WT), LRRC8A-knockout (KO), and LRRC8A~E-knockout (KO) HCT116 cells. The results shown are representative of 6-9 experiments. (**B**) Effects of LRRC8 subunits knockout or treatment with CBX on HCT116 cell migration. Cell migration speed was determined 24 h after wounding. The results shown are representative of seven experiments. (**C**) Knockout of the LRRC8A subunit was confirmed by Western blotting. GAPDH on the same blot was used as an internal control. A representative blot of three independent experiments is shown. The weak band of LRRC8A-KO, and LRRC8A~E-KO HCT116 cells has previously been shown to be unspecific (Voss et al., 2014).

3.1.4 LRRC8A/VRAC is dispensable for proliferation and migration of glioblastoma cells

While VRAC plays an unessential role in HCT116 cell proliferation and migration, the contribution of VRAC to cell proliferation and migration may vary between cell types. Glioblastoma multiforme (GBM), a common and rapidly growing malignant brain tumor, robustly relies on the characteristics of intensive cell invasion and death evasion, which make surgery and concomitant therapies greatly limited (Louis et al., 2007; Preusser et al., 2011). Various ion channels that regulate GBM cell membrane potential and cell volume play an important role in maintaining these processes. The swelling-induced chloride current ($I_{Cl,swell}$) was reported to be highly expressed in GBM cells (Catacuzzeno et al., 2014). The volume-regulated anion channel (VRAC), which mediates $I_{Cl,swell}$ and can be activated by hypoxia and thus contribute cell volume regulation, arguably plays a role (Caramia et al., 2019; Sforna et al., 2017). Furthermore, VRAC was reported to be involved in the proliferation and migration of GBM cells (Wong et al., 2018).

To evaluate the potential contribution of VRAC to GBM cell proliferation and migration, I initially assessed the effects of pharmacological inhibitors CBX and DCPIB on the established glioblastoma cell lines U251 and U87 (Figure 9). U251 or 87 cell proliferation rates of CBX treatment at the concentration of 20, 50 or 100 µM were not significantly different compared with the control group (Figure 9A, B). Consistently, proliferation was neither affected by VRAC inhibition with up to 100 µM DCPIB (Figure 9C, D).

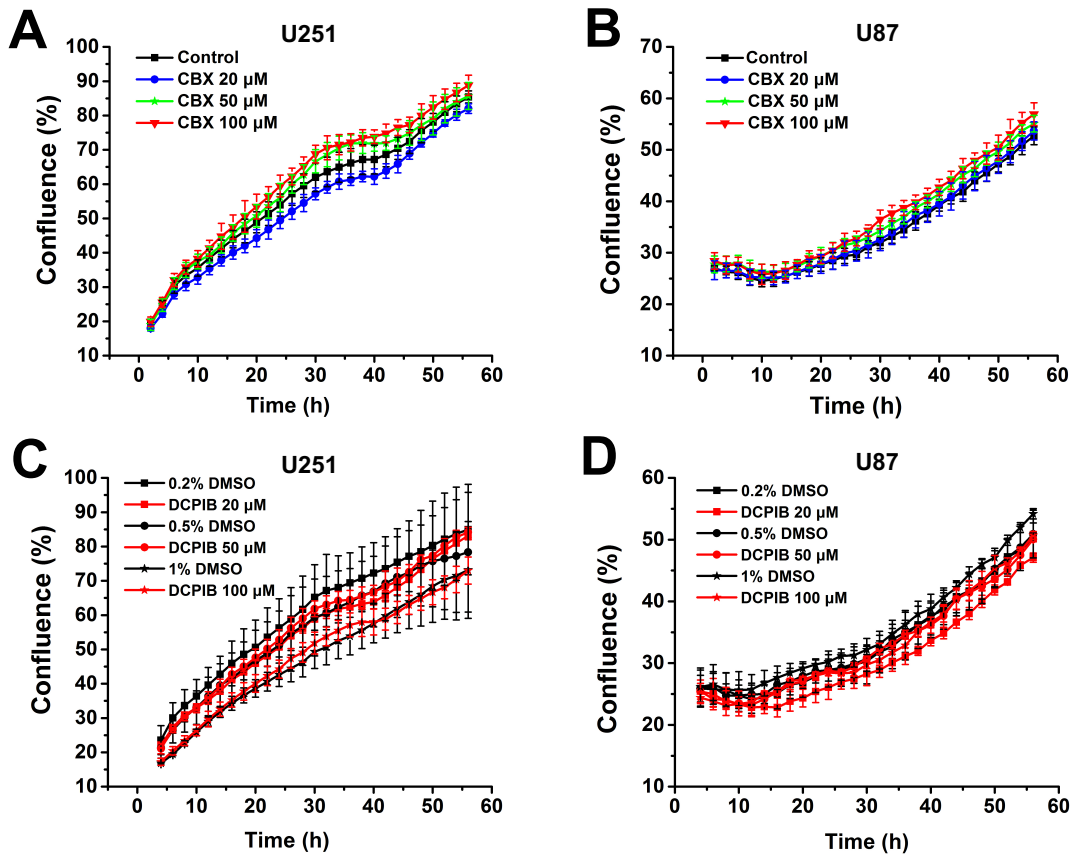

Figure 9. Volume-regulated anion channel (VRAC) blockers do not impair proliferation of GBM cells

Growth curve of U251 (**A, C**) and U87 (**B, D**) after treatment with indicated concentrations of CBX (**A, B**) or DCPIB (**C, D**). Data are presentative as mean ± SD of 3-7 independent experiments.

Next, I evaluated the effect of the VRAC inhibitors on GBM cell migration in the wound healing assay. Although the migration speed of U251 cells decrease with the increase of inhibitor concentration, the cell migration speed of the inhibitor-treated was not significantly different from that of the control groups (Figure 10A). Likewise, I observed no significant differences in migration speed between inhibitor-treated and control U87 cells (Figure 10B). Collectively, these results demonstrate that VRAC activity is not required for GBM cell proliferation and 2D migration.

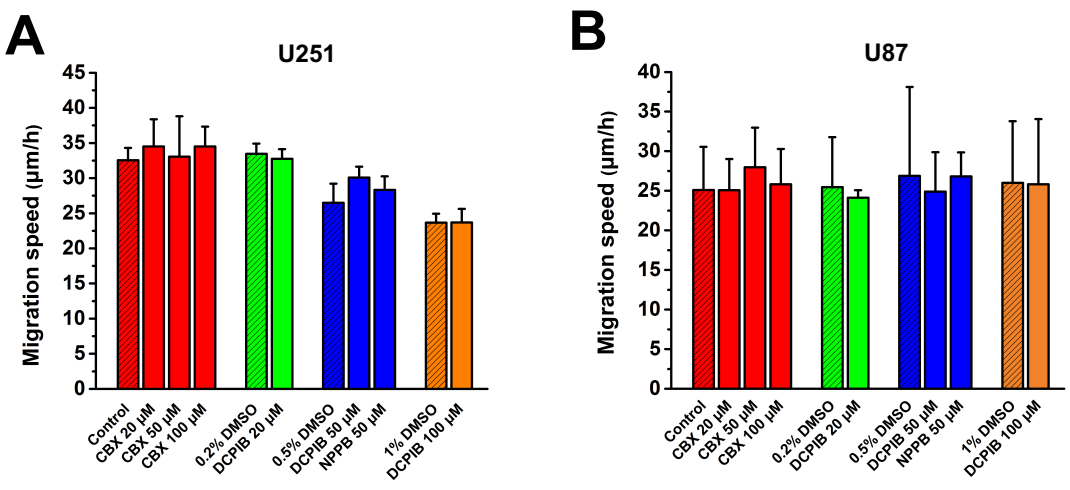

Figure 10. VRAC blockers have no effect on GBM cell movement

Analysis of the cell migration rate of U251 (**A**) and U87 (**B**) after treatment with indicated concentrations of CBX, NPPB or DCPIB. Cells were allowed to migrate into the scrape area for 24 h. The diagonal lines represent controls. Results are expressed as mean ± SD of n = 4-10 experiments.

Since these data apparently conflict with a previously reported effect of DCPIB on GBM migration (Wong et al., 2018), I additionally approached the role of VRAC by silencing the expression of the essential VRAC subunit LRRC8A with siRNA. I tested two individual siRNAs for their ability to knockdown LRRC8A expression in C2C12 cells. Western blotting confirmed a robust knockdown of LRRC8A protein, siRNA2 being more efficient than siRNA1 after two days of transfection (data not shown). The more efficient siRNA2 was used in all subsequent assays. Western blotting confirmed a robust reduction of LRRC8A protein amount after transfection with siRNA2 against *LRRC8A* for 48 h or 72 h in U251 and U87 cells at two days (by roughly 40% and 30%, respectively) and three days (by roughly 70%) after transfection with siRNA2 against *LRRC8A* (Figure 11).

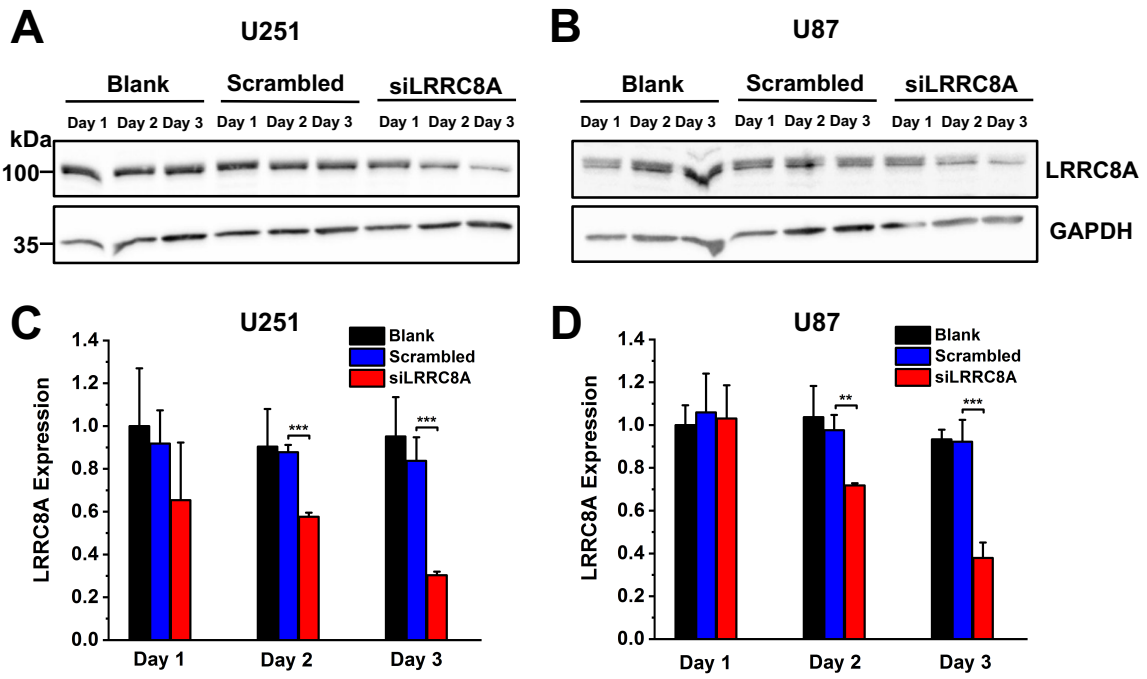

Figure 11. Gene-specific siRNA reduces LRRC8A expression in GBM cells

Representative images of three independent experiments for U251 (**A**) and U87 (**B**) were shown. GAPDH used as loading control. Expression of LRRC8A protein significantly reduced after U251 (**C**) and U87 (**D**) cells transfected with siRNA against *LRRC8A* for two days and three days. Quantification of western blotting was determined by densitometry analysis and normalized to GAPDH. Data are graphically represents as mean ± SD. Statistics: ** $P < 0.01$, *** $P < 0.001$ vs. scrambled. Student's *t*-test.

Next, I examined whether gene-specific knockdown of the essential LRRC8A affect GBM cell proliferation and migration. I observed that proliferation of both cell lines, assessed from 48 h after siRNA or control transfection onwards, was not affected by the LRRC8A knockdown (Figure 12A, B). In the wound healing assay, also started 48 h after transfection, I observed no significant differences in the migration speed between non-transfected cell, cells transfected with control siRNA and cells transfected with siRNA against *LRRC8A* at various time points after transfection (Figure 12C, D).

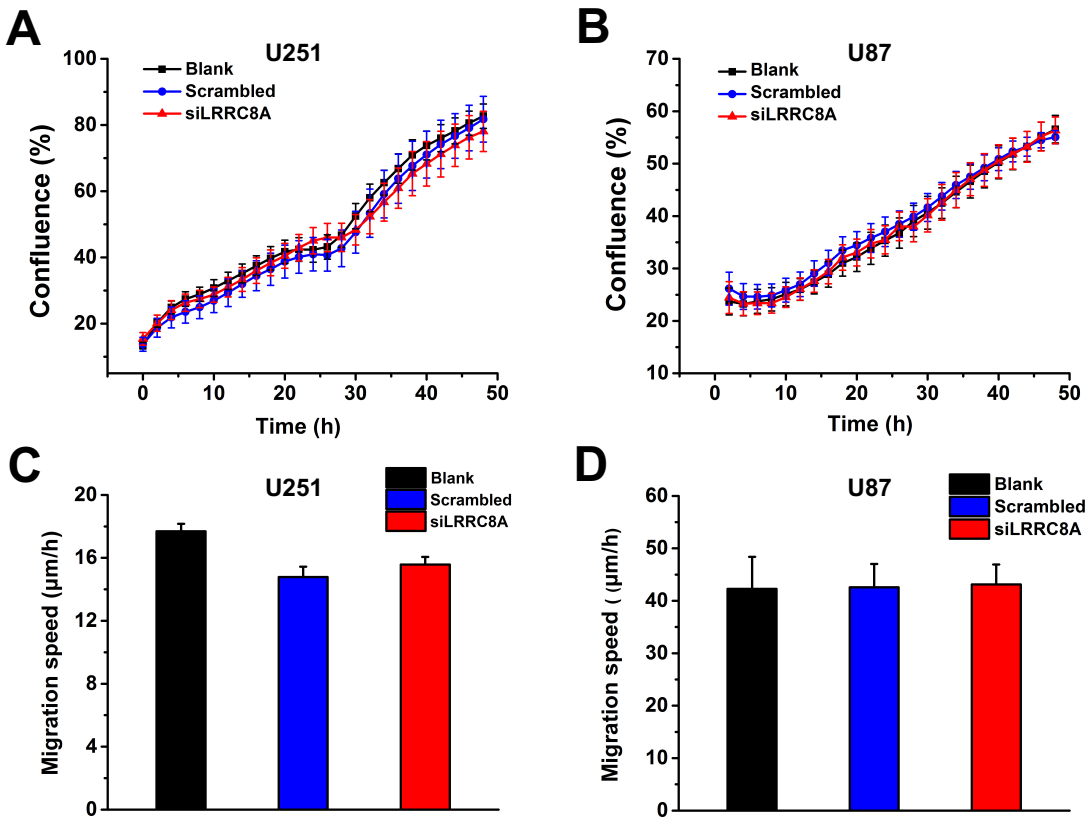

Figure 12. Downregulation of LRRC8A protein is dispensable for GBM proliferation and migration

Proliferation of U251 (**A**) and U87 (**B**) started 48 h after transfection with gene-specific *LRRC8A* siRNA. The data are the mean ± SD of n = 8 experiments. (**C**) U251 cell migration started after 48 h transfection with siRNA against *LRRC8A*. Cell migration speed were determined 24 h post-wounding. The reported values are the mean ± SD of n = 5 experiments. (**D**) U87 cell migration started after 48 h transfection with siRNA against *LRRC8A*. Note the high values due to absence of Mitomycin in the wound healing assay in this case. The data were calculated after cell migrated for 14 h. The reported values are the mean ± SD of n = 7 experiments.

Together, these results from pharmacological inhibition of VRAC and downregulation of LRRC8A indicate that VRAC is dispensable for glioblastoma cell proliferation and migration in the wound healing assay.

3.1.5 VRAC inhibition by DCPIB or LRRC8A downregulation has no effect on PI3K/Akt signaling in GBM cells

Since the activation of mTOR signaling by the phosphatidyl-inositol 3-kinase/protein kinase B (PI3K/Akt) pathway has been reported to be involved in the regulation of GBM cell proliferation and migration (Djuzenova et al., 2019; Mecca et al., 2018; Memmel et al., 2017), I examined whether VRAC is involved in PI3K/Akt/mTOR signaling. To this end, I assessed the phosphorylation status of Akt and the mTOR substrate ULK by Western blotting (Figure 13). DCPIB (100 µM) treatment of U251 or U87 GBM cells for one or two days did not alter the ratio of phosphorylated Akt of all Akt (p-Akt/t-AKt), as well as ratio of p-ULK/t-ULK (Figure 13B-E).

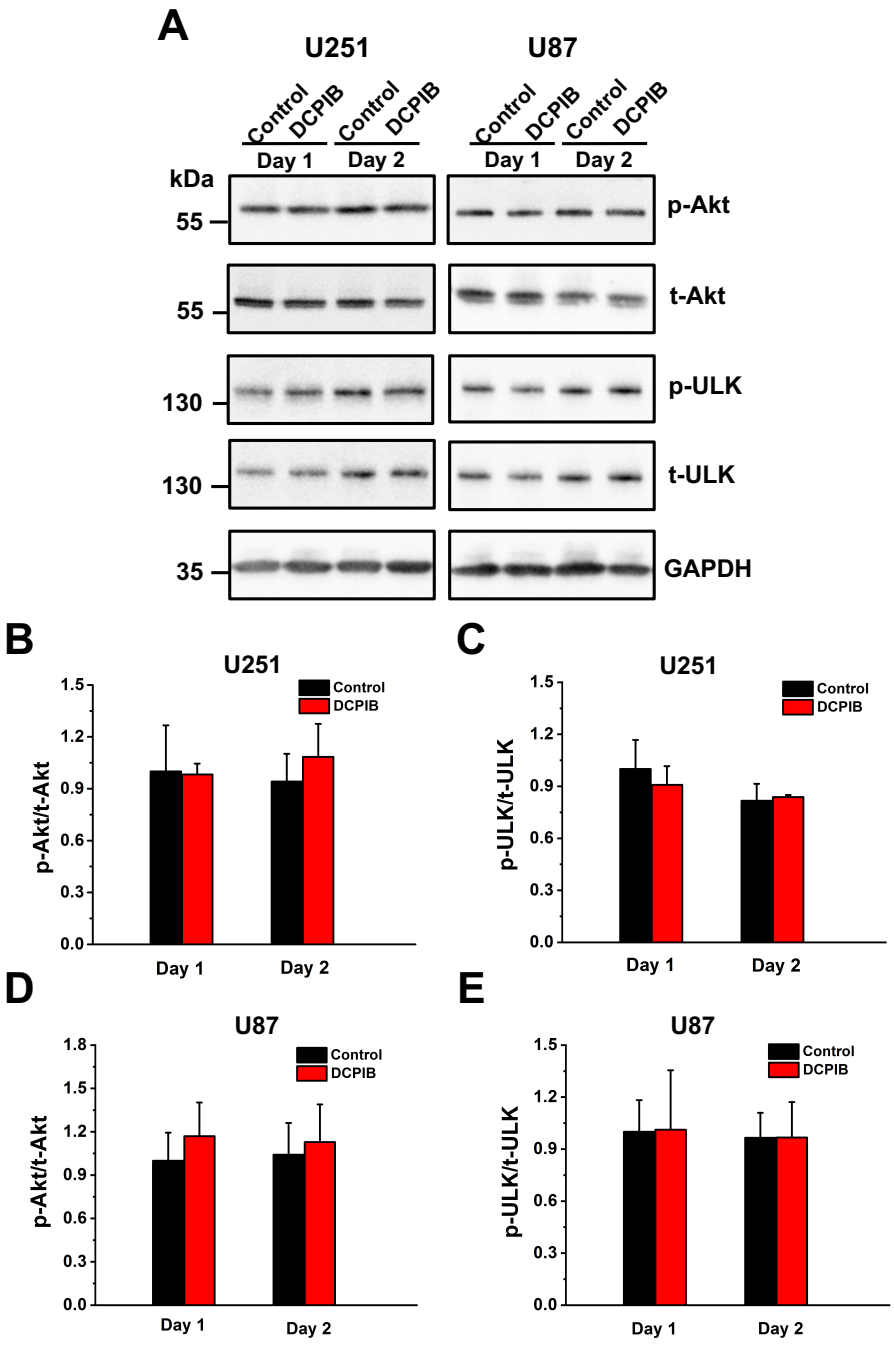

Figure 13. Treatment with DCPIB has no effect on PI3K/Akt signaling

(**A**) Western blotting of GBM cells treatment with DCPIB (100 µM) at day one or day two for total amount and phosphorylated forms of Akt and ULK. GAPDH was used as loading control. A representative blot of three independent experiments is shown. (**B-E**) Analysis of the p-Akt/t-Akt (**B, D**) and p-ULK/t-ULK (**C, E**) ratio for U251 (**B, C**) and U87 (**D, E**) cells. All results are expressed as mean ± SD of n = 3 experiments.

Although DCPIB is the best-in-class VRAC blocker, few reports have been shown that DCPIB suffers from off-target activity toward various channels and transporters. DCPIB were found to inhibit inward rectifying K^+ (Kir) channels (Deng et al., 2016), H/K-ATPase (Fujii et al., 2015), two pore-domain potassium (K2P) channels (Lv et al., 2019) and connexin hemichannels (Cx43) (Bowens et al., 2013). For these reasons, I investigated the potential involvement of VRAC in PI3K/Akt signaling pathway using a gene-specific siRNA knockdown. Similar to DCPIB, the phosphorylation of AKt and ULK was not changed three days after *LRRC8A* siRNA transfection in U251 and U87 cells, when LRRC8A protein levels were significantly decreased (Figure 14). Taken together, the results demonstrate that neither pharmacological VRAC inhibition nor siRNA-mediated downregulation of LRRC8A affected PI3K/Akt signaling.

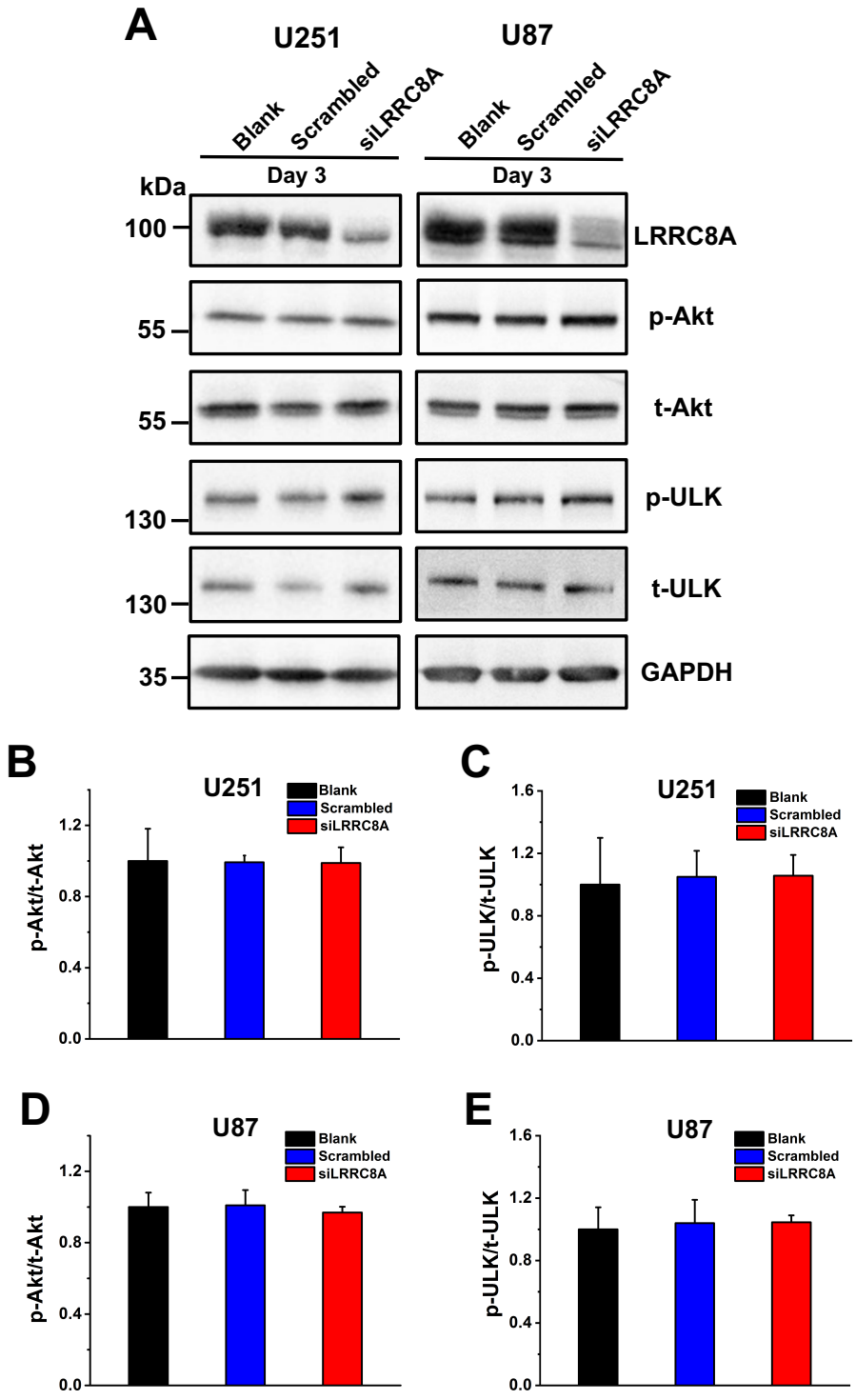

Figure 14. siRNA-mediated knockdown of LRRC8A has no effect on PI3K/Akt signaling
(**A**) Western blotting of GBM cells for total amount and phosphorylated forms of Akt and ULK 72 h after siRNA transfection. For LRRC8A, the same samples were used as in Figure 11A and 11B. GAPDH used as loading control. A representative blot of three independent experiments is shown. (**B-E**) Analysis of the p-Akt/t-Akt (**B, D**) and p-ULK/t-ULK (**C, E**) ratio for U251 (**B, C**) and U87 (**D, E**) cells. All data are presented as mean ± SD of n = 3 independent experiments.

3.2 Mechanisms of activation and regulation of VRAC

The volume-regulated anion channel (VRAC) plays a pivotal role in regulatory volume decrease (RVD). A variety of stimuli, signaling pathways and modulators have been reported to be involved in the activation and modulation of VRAC to some extent. Although VRAC's activation was extensively studied, most of the work in regard to the activation of VRAC was largely based on unspecific pharmacological inhibitors and performed by electrophysiological techniques without knowing the molecular nature of VRAC (Pedersen et al., 2016; Stauber, 2015; Strange et al., 2019). So far, the activation mechanism of VRAC in response to hypotonic swelling remained largely elusive. The recent discovery of VRAC's molecular identity and structures provides strong support to investigate the underlying activation and regulation mechanisms of VRAC activity.

3.2.1 FRET changes reflect C terminus movement during VRAC gating

Förster resonance energy transfer (FRET) describes a physical effect where energy can be transferred in a non-radiative way from a donor to an acceptor fluorophore with overlapping absorption and emission spectra respectively. As FRET is robustly dependent on the interfluorophore distance and the efficiency of energy transfer falls off with the 6th power of distance (Stryer and Haugland, 1967), it occurs only on the nanometer scale (typically in the range of 1-10 nm). For this reason, FRET between two fluorophores is usually used as a quantitative spectroscopic measure of protein-protein proximity (Duncan et al., 2004; Selvin, 2000). The application of FRET techniques was already previously used to explore ion channels in an attractive way (Bykova et al., 2006; König et al., 2019; Miranda et al., 2013; Zachariassen et al., 2016; Zheng and Zagotta, 2003).

Our lab introduced either CFP (cyan fluorescent protein) or YFP (yellow fluorescent protein) tags to the C-termini of LRRC8A or LEEC8E. The donor used in this thesis was Cerulean (equivalent to CFP) and the acceptor was Venus (equivalent to YFP) (Figure 15A). Cerulean and Venus are also referred to as CFP and YFP throughout. FRET occurs between the CFP donor and the YFP acceptor fused to LRRC8 (König et al., 2019). With this FRET optical sensor at hand, I first confirmed whether FRET changes could monitor the activation of VRAC in living cells. I utilized sensitized-

emission FRET (seFRET) and measured the corrected FRET (cFRET) in HeLa cells co-expressing LRRC8A-CFP and LRRC8E-YFP (A-CFP/E-YFP). As illustrated in Figure 15B, switching from isotonic (340 mOsm) to hypotonic (250 mOsm) bath solution caused a strong reduction in cFRET by roughly 16% within 70 seconds in HeLa cells. This reduction of cFRET was not due to changing the buffer, since no significant change was observed when the buffer was switched with isotonic (340 mOsm) or hypertonic solution (500 mOsm) (data not shown). In addition, cFRET decrease was reversible and repeatable. In all, cFRET changes indicate movement of C-termini of LRRC8 proteins in VRAC complex. Application of this FRET approach allowed us to track the movement of the C terminus in real-time during VRAC gating.

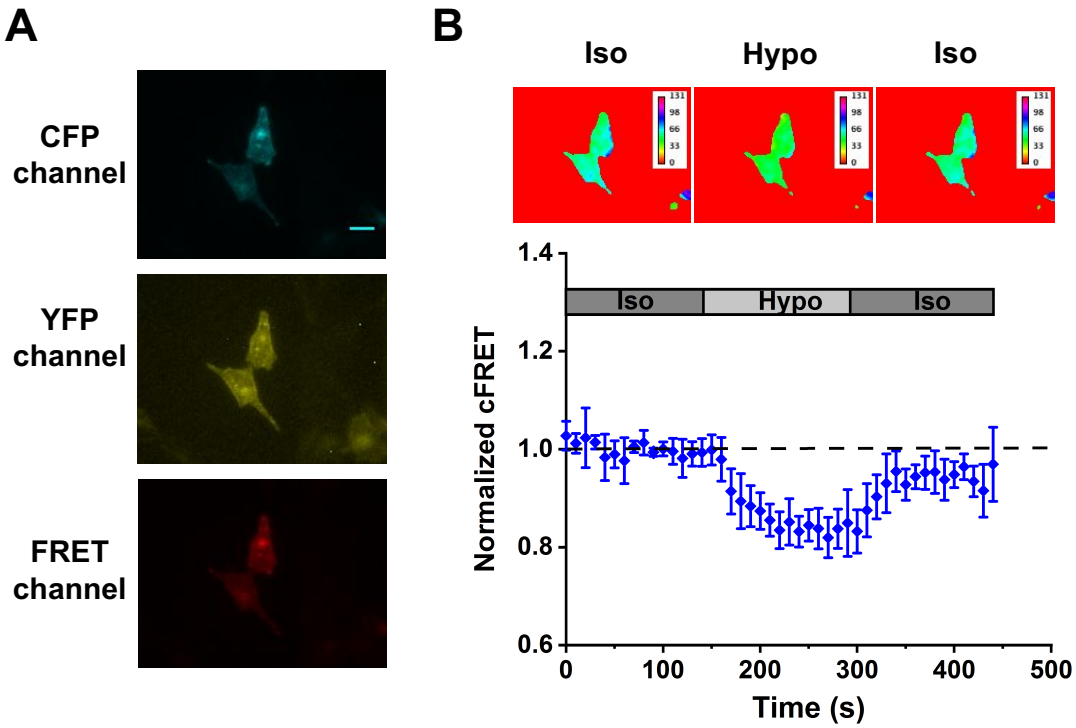

Figure 15. cFRET changes reflect activation of VRAC in response to hypotonic swelling
(**A**) CFP, YFP and sensitized emission (FRET) images were collected from HeLa cells expressing LRRC8A-CFP/LRRC8E-YFP. Scale bar, 20 µm. (**B**) Top panel: cFRET maps of HeLa cells expressing A-CFP/E-YFP during buffer switching from isotonic to hypotonic, then back to isotonic. Calibration bar right of cFRET map exhibits cFRET values and their respective color code in the look-up table (LUT). Bottom graph: cFRET normalized to isotonic conditions of the cell shown in top panel during buffer exchange experiments. Data represent the mean ± SD of 8 cells.

3.2.2 Effect of PKD pharmacological inhibition on swelling-induced VRAC activation

The protein kinase C (PKC) family has been linked to VRAC activation by pharmacological inhibition, mutation and siRNA depletion methods (Hermoso et al., 2004; Rudkouskaya et al., 2008). However, some inhibitor-based studies argued against the involvement of PKCs for VRAC activation in a variety of cell types (see section 1.3.2). PKCs have four conserved domains C1, C2, C3, and C4. C1 is the cysteine-rich motif that regulates binding to phorbol esters and diacylglycerol (DAG), which has been found in both the protein kinase C (PKC) family and protein kinase C mu (PKCμ, better known as PKD) family members. Recently, a study by the Stauber lab suggested that PKD rather than PKC is pertinent to the activation of VRAC (König et al., 2019). However, from all studies combined, the involvement of PKC or PKD in activating and regulating VRAC remains vague.

Therefore, in the next series of experiments, I aimed at to dissect whether PKDs or PKCs is indeed involved in the signaling underlying VRAC activation. To obtain further insights into this, I initially assessed whether pharmacological inhibition of PKDs affects VRAC activation using FRET measurements. Since PKD blocker CRT0066101 was applied and shown to inhibit hypotonicity-induced VRAC current and activation in a previous study (König et al., 2019), then I first tried to confirm the findings with PKD blocker CRT0066101. I observed that hypotonicity-induced decrease of cFRET was strongly diminished in HeLa cells expressing A-CFP/E-YFP after a 15 minutes pre-incubation with 5 μM CRT0066101 (Figure 16A), which is consistent with previous study (König et al., 2019).

To further determine the role of PKD in VRAC activation, I next evaluated the effect of CID2011756, an ATP competitive PKD inhibitor, on the activation of VRAC. Very similar to the impact of CRT0066101, I observed that the presence of 100 μM CID2011756 significantly inhibited the reduction of cFRET in response to osmotic swelling (Figure 16B). In addition, no increase was observed in cFRET value when the cells continuously exposed to 100 μM CID2011756-containing isotonic solution (data not shown), ruling out that the inhibitor itself can lead to an increase in cFRET value. Taken together, these results demonstrate that PKD probably plays a role in the swelling-induced VRAC activation.

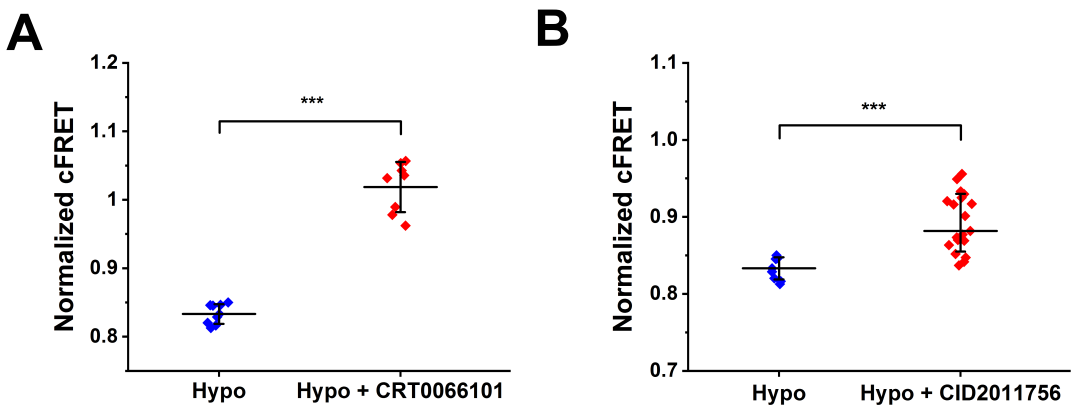

Figure 16. Effect of PKD inhibitors on hypotonicity-induced VRAC activation

(**A**) Quantification of normalized cFRET of HeLa cells expressing A-CFP/E-YFP in hypotonic buffer without (blue diamonds, n = 3, 8 cells) or with 5 µM CRT0066101 (red diamonds, n = 4, 8 cells). Cells were pre-incubated with 5 µM CRT0066101 in culture medium for 15 minutes. Data represent average cFRET of the last five time points per condition of individual cells, and mean of all cells ± SD. Statistics: ***p < 0.001 by Student's *t*-test. (**B**) Quantification of normalized cFRET of HeLa cells expressing A-CFP/E-YFP in hypotonic buffer without (blue diamonds, n = 3, 8 cells) or with 100 µM CID2011756 (red diamonds, n = 7, 19 cells). Cells were pre-incubated with 100 µM CID2011756 in culture medium for 20 minutes. Data represent average cFRET of the last five time points per condition of individual cells, and mean of all cells ± SD. ***p < 0.001 by Student's *t*-test.

Next, I tested whether PKC is involved in the activation of VRAC as well. I first tested the effect of the PKC inhibitor Chelerythrine Chloride (CC) on the swelling-induced activation of VRAC. Surprisingly, the presence of 10 µM CC led to a remarkable increase in cFRET value even under isotonic conditions (data not shown). Such an unexplained increase was also observed in my colleague study for PKC inhibitor Gö6983 (König et al., 2019). I noticed that even when applying 10 µM CC in isotonic solution, a dramatic raising of cFRET was obtained immediately not only in cells that expressed fluorescently tagged A-CFP/E-YFP, but apparently also in non-transfected HeLa cells that did not express A-CFP/E-YFP tagged VRAC. A possible explanation may be that the increase in cFRET value was induced by PKC inhibitor CC (and previously Gö6983) itself (or rather photophysical artifacts), instead of by its impairment VRAC's activation. Inspired by this finding, I asked whether the increase in cFRET caused by PKD inhibitor CRT0066101 (Figure 16A) was indeed due to the impaired activation of VRAC or the fluorescence of the inhibitor itself.

First of all, I monitored the cFRET changes in response to 5 µM CRT0066101-containing isotonic buffer. After pre-incubation with 5 µM CRT0066101 for 15 minutes, cFRET value was increased by 3% consecutively in isotonic buffer with 5 µM CRT0066101 (Figure 17A). When cells exposed to 5 µM CRT0066101-containing hypotonic solution led to a slightly decrease firstly and then an increase in cFRET in comparison to isotonic condition. Surprisingly, switching from hypotonic to isotonic solution resulted in a robust increase by roughly 20% in cFRET value (Figure 17B). I supposed that maybe the autofluorescence of CRT0066101 at a high concentration of 5 µM (beyond 1,000-fold of IC_{50} for all PKD isoforms) crosstalk between CFP, YFP or FRET channels during measurements resulting in a dramatic increase of cFRET value. As this was strikingly more pronounced after incubation in hypotonic buffer, these results indicated that CRT0066101 might enter the cells through VRAC and hypotonic swelling facilitates CRT0066101 influx.

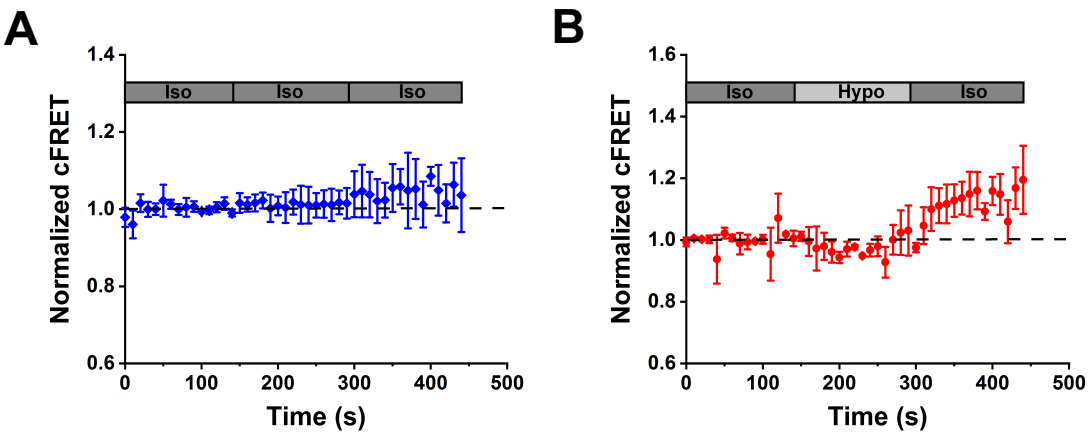

Figure 17. Activation of VRAC facilitates PKD inhibitor uptake

(**A**) Normalized cFRET values (blue diamonds) during buffer exchange experiment with A-CFP/E-YFP-expressing HeLa cells (all buffers with 5 µM CRT0066101). Data represent average cFRET of 8 cells ± SD. (**B**) cFRET values (red solid circles) normalized to isotonic conditions over time in different buffers (5 µM CRT0066101 in the presence of all buffers). Data represent mean ± SD cFRET of 8 individual cells.

Next, I explored whether the VRAC subunit composition determines the permeability to CRT0066101. I observed that the hypotonicity-induced uptake of CRT0066101 in cells expressing A-CFP/A-YFP homo-hexamer VRAC exhibited no significant difference compared with cells expressing A-CFP/E-YFP hetero-hexameric VRAC in HeLa cells (data not shown). Since LRRC8A homomers have been shown to

rather suppress VRAC channel activity, this finding questions an involvement of VRAC in the cellular uptake of these drugs.

CRT0066101 inhibits all PKD isoforms and IC_{50} values are 1, 2 and 2.5 nM for PKD1, PKD3 and PKD2, respectively (Harikumar et al., 2010). Following the hypothesis that the increase in cFRET value which induced by CRT0066101 is due to its own autofluorescence, I asked whether a lower concentration of CRT0066101 can prevent swelling-induced VRAC activation. Here, I examined the effect of 250 nM CRT0066101 (100-fold of IC_{50} for PKD2) on the hypotonicity-induced activation of VRAC. I observed that 250 nM CRT0066101 in hypotonic buffer did not significantly block swelling-induced cFRET decrease (Figure 18).

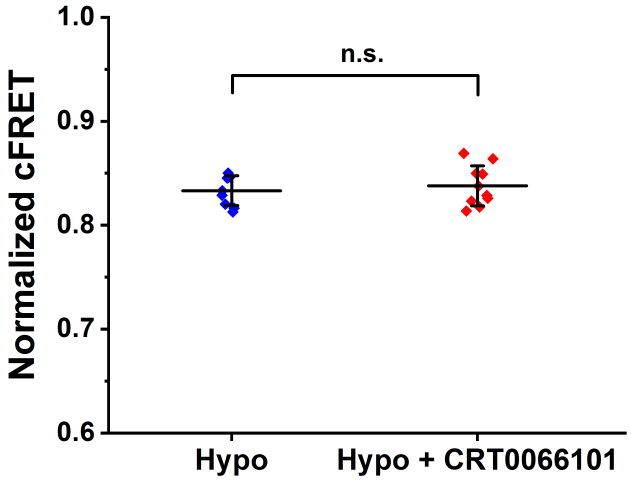

Figure 18. A lower concentration of PKD inhibitor CRT0066101 does not impair swelling-induced VRAC activation

cFRET was estimated for HeLa cells expressing VRAC containing A-CFP/E-YFP challenged with hypotonic buffer (blue diamonds, n = 3, 8 cells) or hypotonic buffer in the presence of 250 nM CRT0066101 (red diamonds, n = 4, 10 cells). Cells were pre-incubated with 250 nM CRT0066101 in cultured medium for 15 minutes. Data represent average cFRET of the last five time points per condition of individual cells and mean ± SD. Statistics: n.s., not significant, Student's *t*-test.

3.2.3 Downregulation of PKD1 or PKD2 inhibits VRAC activity

Pharmacological inhibitors are crucial tools for implicating signal transduction in specific cellular processes. However, CID2011756 and CRT0066101 have additional, usually unknown, intracellular targets. In order to further clarify the effect of PKD on the activation of VRAC, I carried out specific siRNA knockdown of PKD in HeLa cells expressing A-CFP/E-YFP heteromeric VRAC, decreased expression levels of PKD1 and PKD2 after 48h siRNA transfection were confirmed by Western blotting (Figure 19A). I observed that siRNA-mediated knockdown of PKD1 for 48 h significantly inhibited swelling-induced cFRET reduction (Figure 19B), pointing to the likely importance of PKD1 in the activation of VRAC. Very similar results were observed in siRNA-mediated knockdown of PKD2 (Figure 19B). These results demonstrate that PKD is required for hypotonic stress-induced activation of VRAC.

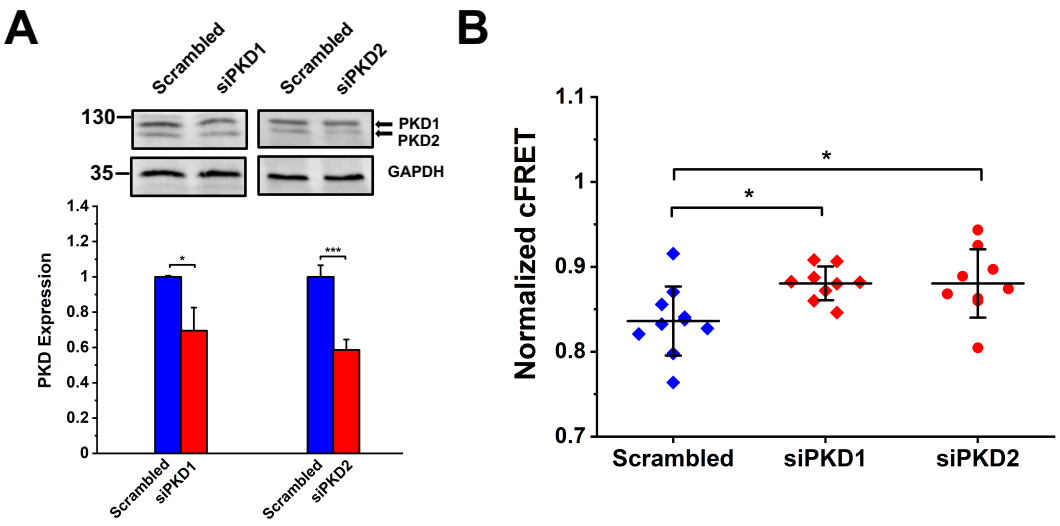

Figure 19. siRNA-mediated knockdown of PKD1/2 suppresses hypotonic-induced cFRET drop

(**A**) Expression levels of PKD1 and PKD2 significantly reduced after siRNA transfection for 48 h. Representative images of three independent experiments were shown. GAPDH used as loading control. Quantification of western blotting was determined by densitometry analysis and normalized to GAPDH. Data represent mean ± SD. Statistics: * $P < 0.05$, *** $P < 0.001$ vs. scrambled. Student's *t*-test. (**B**) cFRET was measured for HeLa cells expressing A-CFP/E-YFP challenged with hypotonic buffer in scrambled (blue diamonds, n = 5, 11 cells), siPKD1 (red diamonds, n = 3, 10 cells) and siPKD2 (red solid circles, n = 4, 9 cells). Data represent average cFRET of the last five time points per condition of individual cells and mean ± SD. Statistics: *$p < 0.05$, Student's *t*-test.

3.2.4 PMA induces VRAC activation and recruits C1 domain-containing proteins to the plasma membrane

Phospholipase C (PLC) activity has been proposed to play a role in $I_{Cl,swell}$ activation (see section 1.3.2). In erythrocytes, the intracellular level of diacylglycerol (DAG) is increased by hypotonic cell swelling (Musch and Goldstein, 1990). DAG is a product of PLC and able to activate the C1 domain-containing protein kinases PKC and PKD. Considering that the above results indicate that PKD may have an impact on the activation of VRAC and PKD is activated downstream of DAG, I next examined whether DAG is associated with the signaling events activating VRAC. Application of phorbol-12-myristate-13-acetate (PMA), an analog of DAG, led to a robust decrease (roughly 20%) of cFRET in HeLa cells expressing A-CFP/E-YFP under isotonic conditions (Figure 20), reconfirming that DAG might be participated in VRAC gating (König et al., 2019).

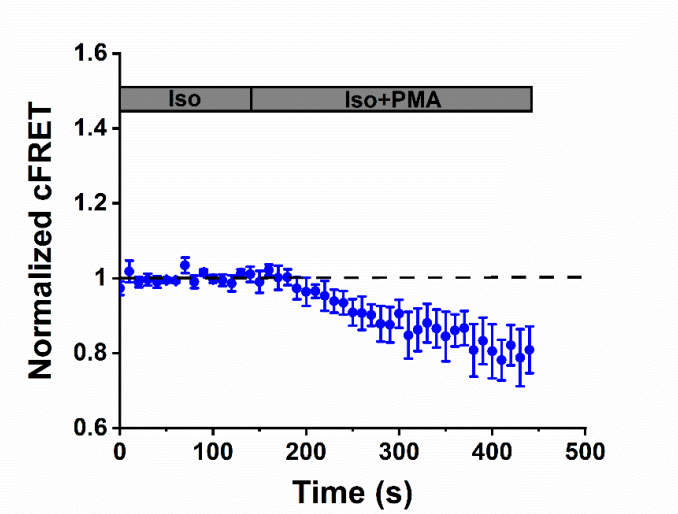

Figure 20. The DAG analog PMA induces VRAC activation
Time traces of HeLa cells expressing VRAC containing A-CFP/E-YFP treated with 1 µM PMA in isotonic solution. Data are mean ± SD of 8 individual cells.

A recent study showed that VRAC can be activated only when it is incorporated in the plasma membrane (König et al., 2019). Next, I tested whether PMA can recruit intracellular PKD to the cell membrane, where it could participate in the activation of VRAC. I monitored DAG dynamics using an effective genetically encoded biosensor PKCδ(C1)-GFP, which consists of the C1 domain of PKCδ fused to GFP (Schlam et al., 2013). Indeed, treatment with PMA for 15 minutes under isotonic condition led to a clear translocation of the DAG biosensor from the cytosol to the plasma membrane in HeLa cells expressing PKCδ(C1)-GFP (Figure 21). These

results demonstrate that PMA recruits PKDs onto the plasma membrane where it can activate PKD, which may via its phosphorylation consequently activate VRAC.

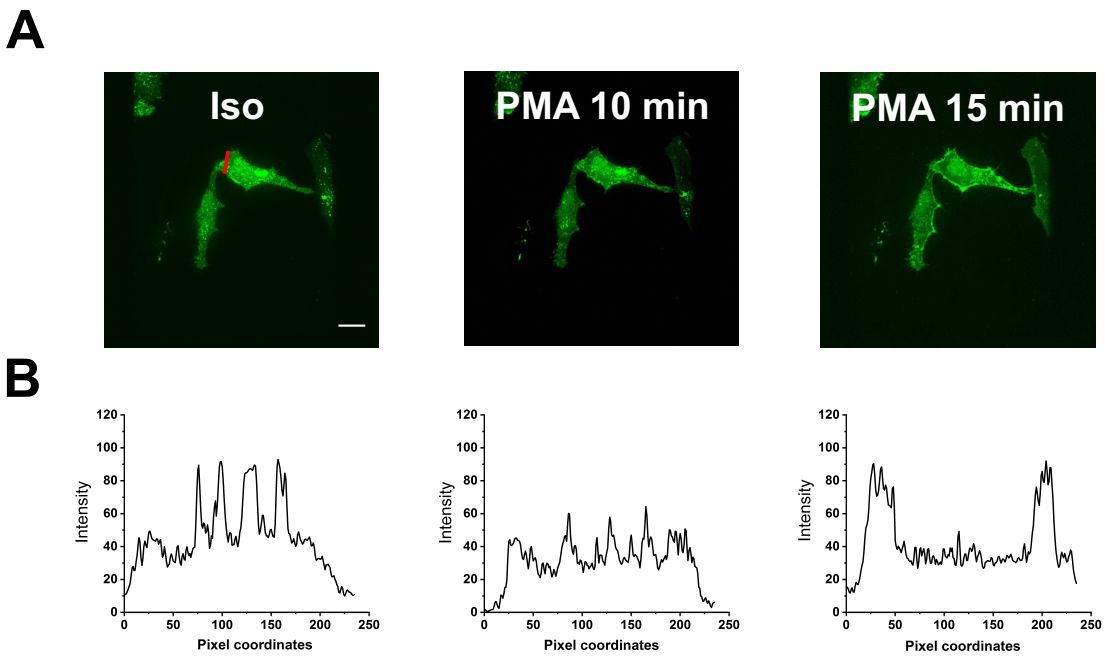

Figure 21. Application of PMA induces recruitment of DAG biosensors to the plasma membrane

Expression of the DAG biosensor PKCδ(C1)-GFP in HeLa cells. (**A**) Confocal images of HeLa cells after treatment with isotonic or isotonic buffer containing 1 μM PMA at indicated time points. (**B**) Intensity plot profiles of GFP fluorescence along with the red line as indicated in (**A**, Iso; plot of the pattern in the same position for PMA treatment) to reveal accumulation of DAG biosensor at the plasma membrane after PMA treatment for 10 and 15 min compared with the control Iso. Scale bar, 20 μm.

3.2.5 Hypotonic stress does not recruit DAG biosensors to the plasma membrane, possibly DAG is rapidly converted to PA

Next, I tested whether DAG generation and transport intracellular protein kinase C and D to the cell membrane can be induced by hypoosmotic stress. I observed that the DAG biosensors were not obviously recruited to the cell plasma membrane upon 50% hypotonicity solution for 10 or 15 minutes (Figure 22A). DAG acts as a second messenger signaling lipid, and is a product of the hydrolysis of the phospholipid phosphatidylinositol 4,5-bisphosphate (PIP_2) by phospholipase C (PLC). In some cells, DAG is rapidly phosphorylated to phosphatidic acid (PA) by diacylglycerol

kinase (DGK) (Florin-Christensen et al., 1992). This consumption could cover the transient production of DAG upon hypotonicity. Therefore, I next explored whether DAG production which induced by hypotonicity is rapidly converted to PA. To do so, I used an optimized PA probe (thereafter referred to as 2XPABD-GFP) (Schlam et al., 2013) to monitor PA generation and distribution in response to hypotonicity in HeLa cells. The results show that partially PA biosensors were translocated from cytosolic to the plasma membrane after treatment with hypotonic solution for 10 minutes (Figure 22B), pointing at PA generation at the cell plasma membrane.

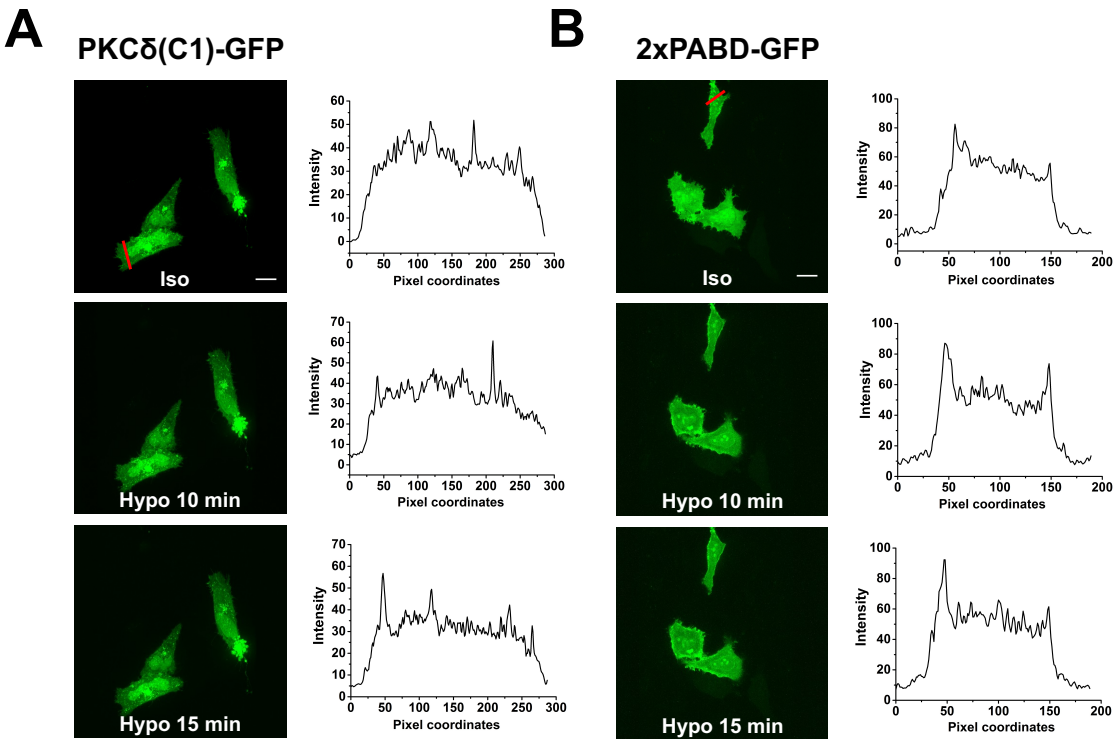

Figure 22. Effect of hypotonic cell swelling on DAG and PA translocation

(**A**) Hypotonicity did not apparently induce the translocation of DAG biosensors to the plasma membrane. Left panel: Confocal images of HeLa cells expressing DAG biosensor PKCδ(C1)-GFP after treatment with isotonic or 50% hypotonic solution at indicated time points. Right panel: Intensity plot profiles of GFP fluorescence along with the red line as indicated in (Left panel, Iso), plot of the pattern in the same position for hypotonicity treatment. Scale bar, 20 μm. (**B**) Hypotonic cell swelling induced PA formation at the plasma membrane. Left panel: Confocal images of HeLa cells expressed PA biosensor (2XPABD-GFP) after treatment with isotonic or 50% hypotonic solution at indicated time points. Right panel: Intensity plot profiles of GFP fluorescence along with the red line as indicated in (Left panel, Iso), plot of the pattern in the same position for hypotonicity treatment. Scale bar, 20 μm.

3.2.6 Phosphorylation of PKCs or PKDs in response to hypotonicity

In the above experiment, we observed that both pharmacological inhibition and siRNA-mediated knockdown of PKDs impaired hypotonicity-induced VRAC activation. Furthermore, hypotonic swelling induced the formation of PA at the plasma membrane, suggesting that DAG may activate PKD and is rapidly phosphorylated to PA. These results motivated me to examine whether PKDs phosphorylation is involved in swelling-induced VRAC activation, because phosphorylation is tightly associated with protein activity and is a pivotal point of protein function regulation. To determine the time-course of PKDs phosphorylation, HeLa and 3T3-L1 cells were harvested at several time points between 0-30 min after exposure to hypotonic buffer (170 mOsm, 50% osmolarity) and analyzed by Western blot. As a positive control, PMA treatment for 30 min led to dramatic phosphorylation of PKDs in HeLa and 3T3-L1 cells. However, hypotonicity did not induce phosphorylation of PKDs, or to some extent, it was only slightly increased in HeLa cells (after 10 and 20 minutes) (Figure 23).

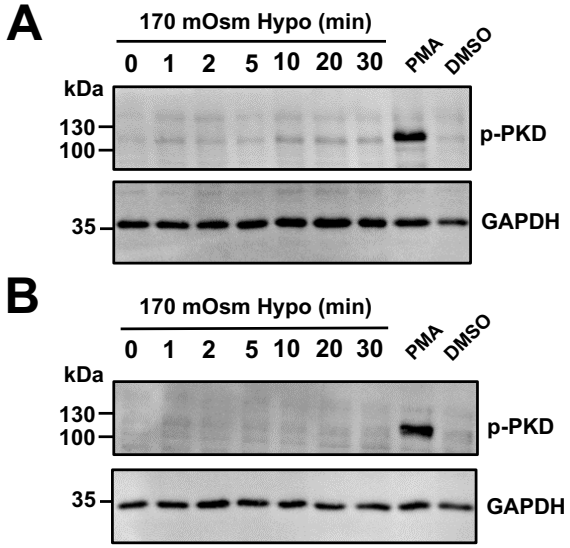

Figure 23. Effect of PMA and hypotonic on PKD phosphorylation

Representative western blot of whole cell lysates from HeLa (**A**) and 3T3-L1 (**B**) to analyze phosphorylated PKD levels. HeLa and 3T3-L1 cells were treated with PMA (200 nM in isotonic buffer for 30 min), DMSO (0.02% in isotonic buffer for 30 min) and hypotonic buffer (170 mOsm) for indicated time points.

Since PMA does not only induce the phosphorylation of PKDs (Stafford et al., 2003), but also PKCs (Robinson, 1992; Tahara et al., 2009), I cannot exclude the involvement of PKC in the activation of VRAC induced by hypotonicity. Therefore, I next aimed at manipulating PKCs to check for an effect on VRAC activation. I observed that 50% osmolarity or even lower 25% osmolarity (85 mOsm) hypotonic buffers did not lead to an increase in phosphorylation of PKCs in HeLa cells (Figure 24A) and very similar results were observed for 50% osmolarity solution in 3T3-L1 cells (Figure 24B). So I was not able to detect an activation of PKCs induced by hypotonic stress, which suggests their activation is dispensable for hypotonicity-induced VRAC activation.

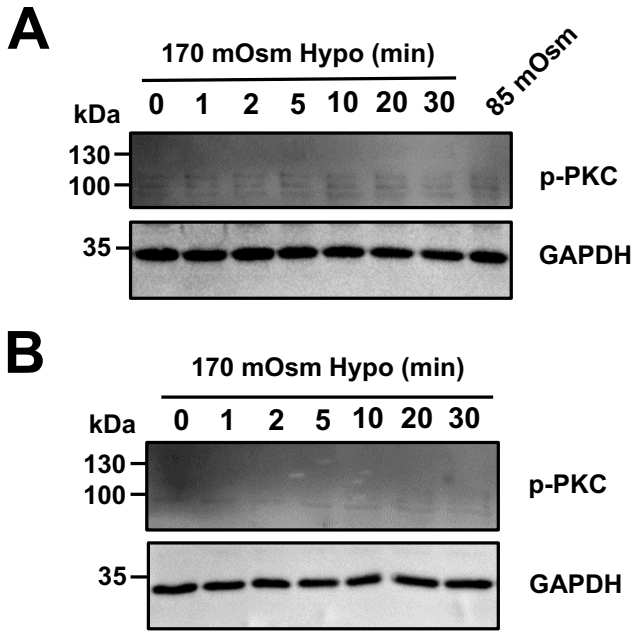

Figure 24. Hypotonic stress does not induce phosphorylation of PKCs

Representative western blot of whole cell lysates from HeLa and 3T3-L1 cells to analyze phosphorylated PKCs levels. (**A**) HeLa cells were treated with hypotonic buffer (170 mOsm, 50% osmolarity) for indicated time points or hypotonic buffer (85 mOsm, 25% osmolarity) for 5 min. (**B**) 3T3-L1 cells were treated with hypotonic buffer (170 mOsm, 50% osmolarity) for indicated time points.

Taken together, PKC and PKD phosphorylation seem to be non-essential for swelling-induced activation of VRAC in 3T3-L1 cells. However, the role of PKD for swelling-induced VRAC activation still needs further research.

4 DISCUSSION

4.1 LRRC8A/VRAC is dispensable for cell proliferation and migration

The volume-regulated anion channel (VRAC) is important constituent of the cellular to regulatory volume decrease (RVD) upon osmotic swelling (Jentsch, 2016), and ubiquitously expressed in vertebrate cells (Chen et al., 2019a; Jentsch, 2016; Pedersen et al., 2016). Since the osmolality of extracellular fluid is generally well controlled, most mammalian cell types hardly experience extracellular hypoosmolarity under normal conditions. VRAC activity is closely connected with the ability of cells to regulate their volume decrease. Cell proliferation is known to be correlated with cell volume change and largely inhibited by cell shrinkage (Dubois and Rouzaire-Dubois, 2004; Hoffmann et al., 2009). Cell migration mediates by many factors, such as the cytoskeleton, cell-matrix adhesion and cell volume regulation (Morishita et al., 2019). Due to its crucial role in RVD, VRAC is supposed to be involved in cell proliferation and migration (Hoffmann et al., 2009; Lang et al., 1998; Pedersen et al., 2016). Furthermore, Ion channels are frequently discussed as potential targets for cancer treatment owing to their roles concerning cell proliferation, malignant angiogenesis and migration (Bortner and Cidlowski, 2014). VRAC has been considered as a potential therapeutic target in the context of cancer as well.

Many studies have reported that an impairment of proliferation and/or migration of various cell lines in the presence of VRAC inhibitors (He et al., 2012; Klausen et al., 2007; Liang et al., 2014; Maertens et al., 2001; Mao et al., 2007; Nilius et al., 1997; Rouzaire-Dubois et al., 2000; Schlichter et al., 1996; Schumacher et al., 1995; Soroceanu et al., 1999; Voets et al., 1995; Wondergem et al., 2001; Wong et al., 2018). Nonetheless, the available VRAC blockers exhibit poor selectivity and often inhibit other anion channels as well (Decher et al., 2001; Friard et al., 2017; Okada et al., 2019). Even the most potent and best-in-class VRAC blocker, DCPIB, suffers from off-target activity toward several different channels and transporters such as potassium channels (Deng et al., 2016; Lv et al., 2019), and GLT-1 glutamate transporters (Bowens et al., 2013). In addition, the cumulative evidence for roles of VRAC in proliferation and migration was rather weak as a result of the unknown

molecular identity (Liu and Stauber, 2019). The identification of LRRC8 heteromers as an essential component of VRAC (Qiu et al., 2014; Voss et al., 2014) enabled exploring physiological functions of VRAC using molecular biological tools. Application by this approach, siRNA-mediated knockdown of the obligate VRAC subunit LRRC8A exhibited anti-proliferative effect of primary glioblastoma and of U251 GBM cells (Rubino et al., 2018), and in the colorectal cancer HCT116 cell line downregulation of LRRC8A was reported to limit cell motility in a wound healing assay (Zhang et al., 2018).

In my present thesis, using both pharmacological and molecular biological approaches, I could show that VRAC is dispensable for proliferation or migration in diverse cell lines including non-differentiated C2C12 myoblasts, colorectal cancer HCT116 cells, human embryonic kidney HEK293 cells and GBM cell lines U251 and U87. To obtain further insights into the impact of VRAC in cell proliferation and migration, several VRAC blockers were tested in order to eliminate the defect of each blocker. The application of VRAC blocker DCPIB (at higher concentrations than required to inhibit VRAC currents) in U251 and U87 GBM cell lines (Wong et al., 2018), and siRNA-mediated downregulation of LRRC8A in U251 cells (Rubino et al., 2018) was reported to impair cell viability and proliferation. In contrast, I did not observe such effect by either treatment in these cell lines. One possible explanation for the inconsistency of these data might be that I measured the increasing confluency of the proliferating cells while in the previous studies the cells' metabolic activity was measured in a 3-(4,5-dimethylthiazol-2-yl)-2,5-diphenyltetrazolium bromide (MTT) assay. Measuring the viable cells directly with a Coulter counter, the most efficient siRNA against LRRC8A showed much less reduction in cell proliferation compared to the MTT assay (Rubino et al., 2018). Unlike a study reported the reduction of migration of GBM cells with the presence of DCPIB (Wong et al., 2018), which I did not observe in my study, may be explained by their impaired proliferation also during the wound healing assay (Wong et al., 2018). The discrepancy between my results, on the one hand, disruption of LRRC8A or all LRRC8 members did not reduce HCT116 cell migration, on the one hand, and the previous report of reduced HCT116 movement upon LRRC8A knockdown (Zhang et al., 2018), is unlikely due to upregulation of compensatory mechanisms

in my case, because the migration speed was also unaltered upon acute pharmacological VRAC inactivation.

Other studies corroborate the notion that VRAC is non-essential for cell proliferation. The proliferation of HeLa cells was reported to be unaffected by siRNA-mediated knockdown of LRRC8A (Sirianant et al., 2016) and knockout of LRRC8A did not alter the cell morphology and proliferation rate in HAP-1 cells (Afzal et al., 2019).In HUVEC cells, the flavonoid Dh-morin inhibited VRAC currents but did not impair proliferation (Xue et al., 2018). Surprisingly, application of DCPIB even inhibited the anti-proliferative effect of cardiac glycosides that correlated with an increase in VRAC activity in HT-29 cells (Fujii et al., 2018). More recently, VRAC inhibitor DCPIB has been reported to suppress mitochondrial respiration and ATP production, and the same effects are observed in cells lacking the expression of the essential VRAC subunit, LRRC8A, they are likely independent of the function of VRAC (Afzal et al., 2019). Furthermore, my colleague Lingye Chen in the Stauber lab also found that siRNA-mediated LRRC8A knockdown did not affect the viability and proliferation of C2C12 myoblast cells in Cell Counting Kit-8 (CCK8) assay (Chen et al., 2019a).

The reduced proliferation and migration of U251 GBM cells were associated with a decreased PI3K/Akt/mTor signaling in the presence of 100 μM DCPIB for one or two days (Wong et al., 2018). In this thesis, I found that no differences in the basal phosphorylation state of Akt in U251 or U87 GBM cells upon application of 100 μM DCPIB for 24 or 48 hours. Neither did I observe diminished phosphorylation of the mTOR substrate ULK. Furthermore, siRNA-mediated knockdown of LRRC8A did not alter Akt signaling. This agree with the previously reported normal anti-CD3-mediated activation of Akt in thymocytes from LRRC8A-deficient mice (Kumar et al., 2014). LRRC8A deletion was reported to dampen insulin-stimulated phosphorylation of Akt2 in adipocytes, whereas no effect on Akt1 signaling was detected in response to LRRC8A knockout (Zhang et al., 2017), which is consistent with my findings for U251 and U87 glioblastoma cell lines.

To sum up, I could show that LRRC8/VRAC is not crucially involved in cell proliferation. Its inessentiality for cell migration in the wound healing assay does not exclude a role for VRAC in migration under particular conditions. In constricted

environments, directed osmotic water flux has been shown to drive cellular locomotion when actin polymerization was blocked (Stroka et al., 2014). The VRAC inhibitor NPPB was shown to impinge on this process of cell invasion (Ransom et al., 2001). Except for VRAC, other chloride channels may contribute, such as the calcium-activated chloride channel TMEM16A (Sauter et al., 2015). Further experiments are of necessity to elucidate the potentially cell type-specific roles of the different types of ion channels under more physiological conditions in cell migration and invasion.

4.2 Mechanisms of VRAC activation and regulation

While a lot of effort has been put into the investigation of cell volume regulation, the mechanisms underlying cell volume sensing and in the complex the signal transduction to plasma membrane effectors still largely uncharacterized (Hoffmann et al., 2009; Jentsch, 2016; Lang et al., 2006). Meanwhile, many studies attempted to reveal the regulation of VRAC, especially the mechanism underlying VRAC activation. However, it is of great importance that until the molecular identification of VRAC six years ago (Qiu et al., 2014; Voss et al., 2014), most previous studies illustrated the activation and regulation mechanisms of VRAC largely based on pharmacological and biophysical characteristics.

4.2.1 FRET approach in study the activity of VRAC channel

Patch-clamp electrophysiology has been considered as the “gold standard” for monitoring activity of ion channel and pharmacology. Still, there are some drawbacks in studying ion channels activity, such as its low throughput. VRAC has been extensively studied in the past few years, and most of the previous understanding of VRAC channels came from the frequently used whole cell configuration patch-clamp. This cell-attached configuration is obtained by breaking the plasma membrane patch within the pipette, which can affect the cellular signaling underlying the modulation of VRAC. As described in section 1.2.1, apart from Cl^-, VRAC conducts uncharged osmolytes, such as *myo*-inositol and taurine as well (Schober et al., 2017). In patch clamp experiments, these uncharged osmolytes cannot be recorded as currents.

Conformational dynamics displays a crucial role in the activation, deactivation, and open-close activities of ion channels in viable cells (Sasmal and Lu, 2014). Such conformational dynamics is usually inhomogeneous and hard to be profiled by patch-clamp directly. Compared with conventional analytical techniques, optical approaches offer great advantages. Förster resonance energy transfer (FRET) is a powerful phenomenon for monitoring interactions whereby a donor fluorophore transfers energy to a close acceptor. FRET measurements provide a higher throughput, spatio-temporal information, non-invasive and can fulfill longtime recording. FRET techniques have been used to study the conformational changes of chloride channels. For example, ClC-0 is the best-studied CLC chloride channel, which operates in two timescales: fast and slow gating (Chen, 2005; Miller, 2006). The molecular mechanism of slow gating was elusive until spectra FRET approach revealed large backbone movement in the C terminus (Bykova et al., 2006).

For dynamic live-cell FRET measurements, the sensitized-emission FRET (seFRET) technique is the most widely used approach (Zal and Gascoigne, 2004). Recently, the structures of LRRC8 were solved by cryo-EM (Deneka et al., 2018; Kasuya et al., 2018; Kefauver et al., 2018; Kern et al., 2019; Nakamura et al., 2020), providing the framework for understanding the activation and regulation mechanisms of VRAC channels. In these revealed structures, cytoplasmic leucine-rich domains (LRRDs) display a certain degree of flexibility, pointing a potential structural rearrangement of these regions during VRAC activation. In this thesis, by using seFRET technique I could show that cFRET changes reflect the C-termini movement of LRRC8 proteins in VRAC complexes during activation upon hypotonicity swelling. This is consistent with previous study clearly showing that the FRET changes indeed mirror the activation of VRAC (König et al., 2019).

4.2.2 PKD regulates the activation of VRAC

Ion channel activation and regulation that has been extensively studied, and protein phosphorylation appears to be a widespread mechanism (Levitan, 1994). Several chloride channels can be activated through directly phosphorylation. For instance, in order to activate cystic fibrosis transmembrane conductance regulator (CFTR) anion pore, the cytosolic regulatory (R) domain has to be phosphorylated by cAMP-dependent protein kinase (PKA) (Cohn et al., 1992; Tabcharani et al., 1991).

Additionally, both Na-K-Cl cotransporters (NKCCs) and K-Cl cotransporters (KCCs) are phosphorylated by SPAK (SPS1-related proline/alanine-rich kinase) and SPAK homolog OSR1 (oxidative stress-responsive 1 protein), which phosphorylate and activate Cl^--importing, Na^+-driven cation-Cl transporters (CCCs) or inhibit the Cl^--extruding, K^+-driven CCCs, resulting in cell volume regulation (de Los Heros et al., 2014; Rinehart et al., 2009; Thastrup et al., 2012).

As described in section 1.3.2, several studies reported that PKC or PKD were involved in VRAC activation and modulation (Hermoso et al., 2004; König et al., 2019; Rudkouskaya et al., 2008; Senju et al., 2015). By using the FRET-based approach, I found that not only pharmacological inhibition of PKD, but also gene-specific knockdown of PKD1 or PKD2 impaired hypotonicity-induced VRAC activation. The role of PKD for VRAC activation is further strengthened by the observation that VRAC can be activated by the DAG analog PMA under isotonic conditions in HeLa cells expressing VRAC containing A-CFP/E-YFP. These results suggest that PKD is implicated in swelling-induced activation of VRAC. A previous study reported that the application of hypo-osmotic solutions did not activate VRAC on endomembranes like ER and Golgi, and VRAC can be activated only when they traffic to the plasma membrane (König et al., 2019). PKD is a cytosolic serine-threonine kinase that binds DAG, which recruits PKD to the plasma membrane and activates PKDs and the phosphorylation of its substrates. Thus, I speculated that the application of PMA or hypotonicity solution may recruit PKDs to the cell surface and activated PKDs potentially directly phosphorylate plasma membrane localized-VRAC.

In addition to FRET measurements, further optical biosensors are powerful techniques to investigate cellular signaling, for their particularly high sensitivity, specification and small size (Dey and Goswami, 2011). In this present work, I used highly effective DAG and PA biosensors to monitor the signaling pathway underlying VRAC activation. My results showed that PMA strongly induced recruitment of PKDs to the plasma membrane. However, the effect of hypotonic solution on PKD translocation to the cell surface is difficult to monitor. A potential possibility for this phenomenon is that probably DAG was rapidly converted to PA by DAG-kinase (DGK), hence DAG biosensors did not detectably translocate to the cell membrane.

I subsequently evaluated the PA formation at the plasma membrane with hypotonic swelling treatment. In HeLa cells, I found that PA formation at the plasma membrane after treated with hypo-osmotic solution for 10 minutes. These results hinted that hypotonic swelling-induced VRAC activation possibly through DAG-PA signaling pathway. For further investigation, it will be valuable to examine whether hypotonicity induces recruitment of DAG biosensors to the plasma membrane when DGK is inhibited.

Since both PMA and hypotonic solution could induce the activation of VRAC, and PMA not only binds and activates PKDs but also PKCs. Although the cFRET increase induced by PKC inhibitor Chelerythrine Chloride (CC) is more likely attributed to the fluorescence of the inhibitor itself, I cannot exclude that PKC plays a role in VRAC activation. Thus, I investigated whether hypotonicity can trigger the phosphorylation of PKCs or PKDs and thereby activating VRAC. The present work demonstrated that hypotonicity slightly induced PKDs phosphorylation in HeLa cells after 10 minutes, but no increase was observed in 3T3-L1 cells. It is therefore possibly that hypotonicity induces PKD phosphorylation is cell-type specific. Although PKDs can be activated by hypotonic swelling, I should note that only a small amount of PKDs was activated. These results indicate that PKD may be partially involved in the activation of VRAC. In addition, PKD is not the only factor that activates VRAC current.

Recently, it has been reported that VRAC currents were completely absent by gene silencing of tweety homologue 1 and 2 (TTYH1 and TTYH2) in several cancer cells, leading to the unusual proposal that TTYH1 and TTYH2 may act as LRRC8A-independent VRAC (Bae et al., 2019). Furthermore, VRAC is unessential for swelling-activated anion currents in some cell types (Sirianant et al., 2016). Still, it is unknown if the phosphorylation of PKD is another upstream regulator or VRAC itself. It seems likely that the activation and regulation of VRAC are modulated by several different pathways.

PKCs were not activated upon hypotonic buffers in both HeLa and 3T3-L1 cells, as judged by their phosphorylation status checked in Western blot. Moreover, I could show that PMA stimulation resulted in membrane-translocation of PKCs in HeLa cells, but hypotonic stress did not. This is consistently with a previous study reported

that PMA induced membrane-translocation of PKCα, β and γ isoforms in rat cardiac myocytes, whereas hypotonicity did not (Sadoshima et al., 1996). In a word, DAG-dependent isoforms of PKC do not activate by hypotonic stress in cardiac myocytes (Sadoshima et al., 1996) and HeLa cells.

G-proteins can be brought into accordance with DAG mediated VRAC activation. Several studies implicated the involvement of G-proteins for VRAC activation (Estevez et al., 2001; Nilius et al., 1999; Voets et al., 1998). G-proteins were shown to be involved in organic osmolyte efflux upon hypotonic shock as well (Ruhfus et al., 1996). Some studies provided evidence that stimulation of purinergic G-protein-coupled receptors (P2YRs) leads to a limited isovolumic activation of VRAC in astrocytes (Akita et al., 2011; Darby et al., 2003; Mongin and Kimelberg, 2005; Takano et al., 2005). VRAC was also found to be activated by S1P, which can activate sphingosine-1-phosphate receptors (S1PRs), a family of plasma membrane GPCRs (Burow et al., 2015). Among the S1PR family members, S1PR2, 3 and 4 have been found to activate PLC (known as an upstream effector of DAG). S1PR1 was reported to be coupled to the subunit G_i that activates the tyrosine kinase Src, which can activate PLC (Zachos et al., 2013).

Taken together, I hypothesize that hypotonicity swelling leads to the stimulation of PLC by putative cell surface receptors like GPCRs and the subsequent generation of DAG. This would recruit and activate PKD before it is rapidly phosphorylated to PA by the DAG kinase. Activation of PKD would then alter the charge of LRRDs by phosphorylation on VRAC hexamers either directly or indirectly, which will lead to conformation rearrangements, and ultimately activates VRAC. I should stress that this hypothesis is just one possible signaling pathways underling VRAC activation, and this topic clearly requires further investigation.

4.2.3 Hypotonicity induces influx of PKD inhibitor via LRRC8/VRAC

LRRC8A, the only essential VRAC subunit, needs at least one of the other proteins (LRRC8B-E) encoded by the *LRRC8* gene family to form functional VRAC channels (Qiu et al., 2014; Voss et al., 2014). Over the past many years, several organic compounds have been proposed to be transported by VRAC (see section 1.2.3 and 1.2.4). Indeed, in this study I could show that a small fraction of PKD inhibitor

CRT0066101 (about 3% increase in cFRET value) entered the cells through passive diffusion across the plasma membrane under isotonic conditions. HeLa cells exposed to hypotonic solution in the presence of 5 μM CRT0066101 led to slightly decreasing firstly and then increasing in cFRET value compared with isotonic conditions. However, switching from hypotonic to isotonic solution resulted in a robust increase by ~20% in cFRET value.

One possible explanation is that hypotonicity induced VRAC activation (led to an initial decrease in cFRET value) thereby promoting the uptake of CRT0066101, resulting in an increasing in cFRET value. As for the drastic increase in cFRET after switching back to isotonic buffer, this can be understood as the swollen cells adjusted their volume decrease to counteract osmolarity change, which resulted in an increase in the concentration of CRT0066101 in the cells, and finally induced a strong increase in cFRET value. In short, it is therefore likely that heteromeric LRRC8/VRAC channels can transport CRT0066101 and hypotonic swelling strongly facilitates the uptake of CRT0066101 in the cells. Like taurine efflux (Voss et al., 2014), CRT0066101 uptake was vigorously stimulated by hypotonic swelling in HeLa cells expressing A-CFP/E-YFP. Interestingly, in this thesis I could show that LRRC8A homo-hexamers did not alter the uptake of CRT0066101, although LRRC8A expressed alone is not sufficient to form functional VRAC but rather suppresses endogenous VRAC currents (Qiu et al., 2014; Voss et al., 2014).

VRAC not only conducts halide ions, but also organic compounds like taurine, and glutamate (Hyzinski-García et al., 2014; Qiu et al., 2014; Ruhfus and Kinne, 1996; Schober et al., 2017; Voss et al., 2014; Yang et al., 2019; Zhou et al., 2020b). Recently, the platinum-containing drugs such as cisplatin and carboplatin have been revealed to accumulate in cancer cells via LRRC8A/D-containing heteromers (Planells-Cases et al., 2015; Sørensen et al., 2016). Together with blasticidin S (Lee et al., 2014) and CRT0066101, there is now a wide range of chemically diverse confirmed being value of VRAC substrates, implying a potential clinical value for targeting VRAC in a therapeutic context when the selectivity and specificity of VRAC pore for a specific pathological condition has been solved in the near future.

4.2.4 Conclusion & Outlook

With this work, I could show, by utilizing a FRET-based sensor, that both pharmacological inhibition and siRNA-mediated knockdown of PKDs impaired VRAC activation upon hypotonic swelling. The role of PKD for VRAC activation is further strengthened by the observation that the DAG analog PMA activates VRAC under isotonic conditions. I could also show an increase in PA amount at the plasma membrane in response to hypotonicity. These results corroborate the notion that VRAC activation upon hypotonic swelling involves DAG and PA signaling. Thus, further investigation should aim at the identification of plasma membrane-specific co-factors, such as GPCRs, that lead to VRAC activation. As the FRET approach applied in this study is subunit-specific, it will be interesting to label and test other LRRC8 members together with LRRC8A, such as in a LRRC8A-CFP/LRRC8D-YFP combination. Hence, I expect that other molecules will be identified as VRAC substrates through FRET approach. Investigating different subunit combinations with the FRET method will also allow for the study of cell type-specific regulatory mechanisms.

5 MATERIALS AND METHODS

5.1 Materials

5.1.1 Chemicals

All chemicals used in this thesis were purchased from Sigma-Aldrich, Roth or Merck, if not stated otherwise.

5.1.2 Drugs

Table 1 | Drugs

Chemical	Description	Supplier
CBX	VRAC inhibitor	Sigma-Aldrich
Chelerythrine Chloride	PKC inhibitor	Tocris
CID2011756	PKD inhibitor	Tocris
CRT0066101	PKD inhibitor	Tocris
DCPIB	Blocker of VRAC/$I_{Cl, swell}$	Tocris
Mitomycin C	DNA cross-linking antitumor agent	Taufkirchen
NPPB	calcium-sensitive chloride currents inhibitor	Tocris
PMA	analog of DAG	Tocris

5.1.3 Cell lines

Table 2 | Cell lines

Name	Description	RRID/Reference	Medium	Additional information
3T3-L1	mouse fibroblast	CVCL_0123	DMEM, 10%FBS, 1% P/S	Kindly provided P. Knaus, Freie Universität Berlin
C2C12	mouse skeletal muscle myoblast	CVCL_0188	DMEM, 10%FBS, 1% P/S	Kindly provided P. Knaus, Freie Universität Berlin
HCT116	Human colon cancer	CVCL_0291	McCoy's 5A, 10%FBS, 1% P/S	Obtained from Leibniz Forschungsinstitut DSMZ
LRRC8A KO (HCT116)	HCT116 cells with LRRC8A protein depleted	(Voss et al., 2014)	McCoy's 5A, 10%FBS, 1% P/S	kindly provided by T. J. Jentsch (FMP and MDC, Berlin, Germany)
LRRC8A~E KO (HCT116)	HCT116 cells with quintuple LRRC8 proteins depleted	(Voss et al., 2014)	McCoy's 5A, 10%FBS, 1% P/S	kindly provided by T. J. Jentsch (FMP and MDC, Berlin, Germany)
HEK293	human embryonic kidney	CVCL_0045	DMEM, 10%FBS, 1% P/S	Obtained from Leibniz Forschungsinstitut DSMZ
LRRC8A KO (HEK293)	HEK293 ells with LRRC8A protein depleted	(Lutter et al., 2017)	DMEM, 10%FBS, 1% P/S	kindly provided by T. J. Jentsch (FMP and MDC, Berlin, Germany)
LRRC8A~E KO (HEK293)	HEK293 cells with quintuple LRRC8 proteins depleted	(Lutter et al., 2017)	DMEM, 10%FBS, 1% P/S	kindly provided by T. J. Jentsch (FMP and MDC, Berlin, Germany)
HeLa	mammalian cervix carcinoma	CVCL_0030	DMEM, 10%FBS, 1% P/S	Obtained from Leibniz Forschungsinstitut DSMZ
U251	human glioblastoma	CVCL_0021	DMEM, 10%FBS, 1% P/S	Kindly provided U. Stein, MDC, Berlin, Germany
U87	human glioblastoma	CVCL_0022	DMEM, 10%FBS, 1% P/S	Kindly provided H. Kettenmann, MDC, Berlin, Germany

5.1.4 Antibodies

Table 3 | Primary antibodies

Antibody Name	No.*	Supplier	Dilution
Rabbit anti-Akt pan	4685	Cell Signaling	1:1000
Rabbit anti-phospho-Akt	4060	Cell Signaling	1:1000
Rabbit anti-ULK	8054	Cell Signaling	1:1000
Rabbit anti-phospho-ULK	14202	Cell Signaling	1:1000
Rabbit anti-phospho-PKC Pan	PA5-97368	Invitrogen	1:1000
Rabbit anti-PKD/PKCμ	ab131460	Abcam	1:1000
Rabbit anti-phospho-PKD/PKCμ	2054	Cell Signaling	1:1000
Rabbit anti-LRRC8A (1 μg/ml)	lab-generated	kindly provided by T. J. Jentsch (FMP and MDC, Berlin, Germany) (Voss et al., 2014)	1:1000
Rabbit anti-GAPDH	2118	Cell Signaling	1:1000

Table 4 | Secondary antibodies

Antibody name	Supplier	dilution
HRP goat-anti-rabbit	Jackson ImmunoResearch, Ely, UK	1:5000-1:10000

5.1.5 siRNAs

All siRNAs used were purchased from Thermo Fisher Scientific, Darmstadt, Germany. Their sequence is shown in table 5.

Table 5 | Used siRNAs and their sequence

siRNA	No.*	Sequence	Product Type
Scrambled siRNA	4390844	a non-targeting negative control siRNA	Silencer Select
siLRRC8A	s109501	sense: CCUUGUAAGUGGGUCACCATT	Silencer Select
siPKD1	s11119	sense: CGAAGUUUUUAAUUACUCATT	Silencer Select
siPKD2	103357	sense: GGUCAUUGACAAACUGCGCTT	Silencer

5.1.6 Plasmids

Table 6 | Plasmids

Plasmid Name	Number in internal database	Vector backbone	Description	Reference
2xPABD-GFP	107	pCDNA3.1	PA biosensor	(Bohdanowicz et al., 2013)
LRRC8A-Cerulean	105	pECFP-N1	CFP-tagged LRRC8A	(König et al., 2019)
LRRC8A-Venus	108	pEYFP-N1	YFP-tagged LRRC8A	(König et al., 2019)
LRRC8E-Venus	106	pEYFP-N1	YFP-tagged LRRC8E	(König et al., 2019)
PKCδ(C1)-GFP	109	pEGFP(C1)	DAG biosensor	(Schlam et al., 2013)

5.1.7 Cell culture medium components

Table 7 | Cell culture medium components

Name	Supplier	Product number
DMEM (supplemented with glucose, L-glutamine and $NaHCO_3$)	PAN-Biotech	P04-03550
McCoy's 5A medium	PAN-Biotech	P04-05500
Penicillin-Streptomycin, 10,000 U/ml Penicillin, 10 mg/ml Streptomycin	PAN-Biotech	P06-07100
FBS Premium	PAN-Biotech	P30-1506
Trypsin 0.25 % in PBS, w/o: Ca and Mg	PAN-Biotech	P10-021100
DPBS w/o: Ca and Mg	PAN-Biotech	P04-36500
Opti-MEM	Gibco	31985070
Fibronectin	Sigma-Aldrich	F1141
FuGENE 6	Promega	E2691

5.1.8 Imaging buffers

All imaging buffers were prepared with sterile filtered stock solutions. Isotonic imaging buffer (340 mOsm) contained (in mM): 150 NaCl, 6 KCl, 1 $MgCl_2$, 1.5 $CaCl_2$, 10 glucose,10 HEPES, pH 7.4 (adjusted with NaOH). For FRET experiments, hypotonic imaging buffer (250 mOsm) the concentration of NaCl was adjusted to 105 mM. Hypertonic imaging buffers (500 mOsm) were as isotonic buffer supplemented with 160 mM mannitol. For western blot assays, 50% hypotonic buffer (170 mOsm) and 25% hypotonic buffer (85 mOsm) contained 65 mM or 22.5 mM NaCl, respectively. For DAG and PA biosensors imaging experiments, an equal volume of ddH_2O was added to isotonic buffer (340 mOsm), resulting in a ~50% decrease in osmolarity.

5.2 Methods

5.2.1 Cell culture

Wild-type and LRRC8 knockout HCT116 cell lines (Voss et al., 2014), were maintained in McCoy's 5A Medium with 10% FBS at 37°C in the presence of antibiotics in a humidified atmosphere with 5% CO_2. Wild-type and LRRC8 knockout HEK293, HeLa, 3T3-L1, C2C12, U251 and U87 cell lines were maintained in Dulbecco's Modified Eagle Medium (DMEM) supplemented with 10% fetal bovine serum (FBS), 100 U/ml penicillin, and 100 µg/ml streptomycin in a 37°C, 5% CO_2 humidified chamber. U251 and U87 cells were authenticated using highly-polymorphic short tandem repeat loci (Microsynth, Balgach, Switzerland).

5.2.2 Bacterial transformation

For transformation, 1-5 µl of plasmids were transformed in chemically competent *E.coli* DH5α cells. Prior to application, *E.coli* aliquots were thawed on ice for 10 minutes. The plasmids were added to the bacteria and mixed gently by filcking the bottom of the tube. Competent cells and DNA mixtures were incubated for 30 minutes on ice and then incubation of the mixtures at 42 °C for 45 seconds. Following a two minutes incubation on ice. Then 600 µl of pre-warmed SOC media (no antibiotics) was added immediately, and the cells were allowed to recover at 37°C for 1 h before selected by either ampicillin or kanamycin containing LB-agar plates. Followling 200 µl of the transformation was plated onto a 10 cm LB agar plate containing the appropriate antibiotic and incubated at 37°C. The next day, an isolated colony was picked and incubated in LB medium overnight. DNA purication was performed using the NucleoSpin Plasmid QuickPure (Macherey-Nagel). Sequences were verified via Sanger sequencing (Microsynth- SeqLab,Göttingen, Germany).

5.2.3 Generation of C2C12 LRRC8A knockout cell lines

The C2C12 LRRC8A knockout cell lines were generated by Anja Kopp in the Stauber lab. For the disruption of LRRC8A in C2C12 cells using the CRISPR/Cas9 technology, the targeting sgRNA sequences (5'-

GCCCCGGAAGGAGTCGTTGCAGG-3') was cloned into the px459-V.2 vector and transfected into the wild-type C2C12 cells in a 6-well format. Two days post-transfecton, successfully transfected cells were selected by application of 10 µg/ml puromycin for 48 h prior to single clone expansion by dilution to statistically 0.5 cells per well in 96-well format. Monoclonal cell lines were tested for sequence alterations using target-site-specific PCR (primers: 5'-CATGTATGTCTCACTACACCTAACTTGTAG-3' and 5'-CCAGGAAGATGAGGGTGTGCA-3') on genomic DNA followed by Sanger-sequencing (Microsynth- SeqLab,Göttingen, Germany).

5.2.4 Transfection of mammalian cells

For transfection of siRNA, U251 and U87 cells were seeded in 6-well cell culture plates (1.5×10^5 cells per well) and HeLa cells were seeded at a density of 5×10^3 cells in 35mm glass-bottom dishes (MatTek). After 24 h, the cell culture medium was removed and cells were washed with the serum-free Opti-MEM, then transfected with siRNA against *LRRC8A* (*Lrrc8a* siRNA, ThermoFisher Scientific, Darmstadt, Germany, #s109501), *PKD1*(*PRKD1* siRNA, ThermoFisher Scientific, Darmstadt, Germany, #s11119) or *PKD2* (*PRKD2* siRNA, ThermoFisher Scientific, Darmstadt, Germany, #103357) at a concentration of 15 nM using Lipofectamine RNAiMAX transfecting agent (Invitrogen). A non-targeting, scrambled siRNA (Thermo Fisher Scientific, Darmstadt, Germany, 4390844) was used as negative control. For the proliferation assay, cells were further grown for 48 h before seeding into a 96-well plate. For the migration assay, cells were further grown for 30-42 h post-transfection (wounds were created 48 h post-transfection), then plated in a 96-well ImageLock™ tissue culture plate (Essen Bioscience). For FRET experiments, plasmids (LRRC8A-CFP, LRRC8E-YFP) were transfected 24 h after transfection of siRNA against *PKD1* or *PKD2*.

Transfection with plasmids (listed in table 6) was performed using FuGENE 6 according to the manufacturer's instructions. 3 µl FuGENE was added to 145 µl pre-warmed Opti-MEM and incubated for 5 minutes at room temperature. Subsequently, 1 µg DNA was added, for two plasmids (e.g. LRRC8A-CFP/LRRC8E-YFP) 500 ng of each were added. After addition of DNA, the mixture of DNA-FuGENE were vortexed for 10 seconds, following a 20 minutes incubation at room temperature.

Then, the transfection mixture were added to the cells. Cells were measured 24-48 hours after transfection with plasmids.

5.2.5 Drug treatment

All here described drugs are listed in table 1. For migration assay, cells were pretreated with 5 µg/ml Mitomycin C for 2 h prior to creating wounds using WoundMaker™ (Essen BioScience). The following drugs were applied at the respective concentration at time points indicated in Results: CBX (20, 25, 50, 100 µM; dissloved in H_2O at a conentration of 50 mM), DCPIB (20, 50, 100 µM; dissolved in DMSO at a concentration of 100 mM), NPPB (50 µM; dissolved in DMSO at a concentration of 100 mM), CID2011756 (50, 100 µM; dissolved in DMSO at a conentration of 50 mM), CRT0066101 (0.25, 5 µM; dissloved in H_2O at a concentration of 100 mM), Chelerythrine Chloride (10 µM; dissloved in H_2O at a concentration of 10 mM), PMA (0.5, 1 µM; dissloved in DMSO at a concentration of 100 mM). For the drugs dissloved in DMSO, equivalent DMSO was used as vehicle control.

5.2.6 Cell proliferation assays

For proliferation assays, 5,000 cells (1.0×10^4 cells in the case of HCT116) per well were seeded into a 96-well plate and placed the plate into the IncuCyte live-cell analysis system. Prior to scanning, allowed the plate to warm to 37°C for 30 minutes. Cell growth was monitored by using the IncuCyte system to capture phase contrast images every 2 hours during constant incubation at 37°C in a humidified atmosphere with 5% CO_2. Cell confluence was analyzed using the integrated confluence algorithm.

5.2.7 Cell migration assays

To assess cell migration, 2-8 × 10^4 cells (depending on cell type) per well were seeded into a 96-well ImageLock™ plate (Essen BioScience 4379) and incubated for 4-16 h at 37°C in a humidified atmosphere with 5% CO_2. Removed the medium and added 100 µl Mitomycin C-containing culture medium to each well. Mitomycin C was applied during the following steps, if not specified otherwise, to inhibit cell

proliferation so that this process would not distort my results on cell migration. After 2 h, precise and reproducible wounds were created in all wells of the 96-well ImageLock™ plate by using WoundMaker™ (Essen BioScience). Aspirated the medium and gently washed each well twice with culture medium to avoid dislodged cells settling and reattaching, then 100 µl of medium containing additional drugs (CBX, DCPIB, NPPB, or vehicle DMSO when appropriate) were added to each well. Migration was monitored by phase contrast imaging with an IncuCyte Zoom microscope, image acquisition every 2 h during constant incubation at 37°C in a humidified atmosphere with 5% CO_2. The IncuCyte Zoom image analysis software was used to detect cell edges automatically and generated an overlay mask, which was used to calculate the wound width. For the migration assay with HCT116, the 96-well ImageLock™ plates were coated with fibronectin prior to cell seeding according to the manufacturer's instructions.

5.2.8 Cell counting kit-8 (CCK8) cell proliferation assay

The cell viability was measured by using CCK-8 cell proliferation assay (Sigma-Aldrich). 100 µl of HEK293 cell suspension (5000 cells/well) were dispensed into a 96-well plate, with four duplicate wells in each group. Then placed the plate in a humidified incubator (at 37°C, 5% CO_2). Next, CCK-8 solution (10 µl) at a 1:10 dilution with FBS-free DMEM/F12 (100 µl) was added to each well and avoided to introduce bubbles to the wells, followed by a further 4 h incubation under 5% CO_2 at 37 °C. [2-(2-methoxy-4-nitrophenyl)-3-(4-nitrophenyl)-5-(2,4-disulfophenyl)-2H-tetrazolium, monosodium salt] (WST-8) was reduced by dehydrogenases in HEK293 cells to give an orange colored product (formazan), which was soluble in the culture medium. The amount of the formazan dye produced by dehydrogenases in HEK293 cells was directly proportional to the number of living cells and the absorbance was automatically measured at 450 nm with a microplate reader (Biochrom, Germany).

5.2.9 Western blotting

For western blotting, protein concentration were tested with a regular BCA assay (Pierce). Equivalent amounts of sample protein separated in 10% SDS-PAGE gel and transferred to nitrocellulose membrane (Macherey Nagel). After blocking with

5% BSA in TBS-T (20 mM Tris pH 7.6, 150 mM NaCl and 0.02% Tween-20), the membrane was immunoblotted with primary antibodies overnight at 4°C. On the next day, the membrane was washed three times for 5 min with TBS-T on a shaker and then incubated with goat-anti-rabbit secondary antibodies coupled to horseradish peroxidase. After 45-60 min, membrane was washed again three times for 5 min with TBS-T. Signals were detected by using an enhanced chemiluminescence reagent (HRP juice; PJK GmbH, Kleinblittersdorf, Germany) and a ChemiSmart5000 digital imaging system (Vilber-Lourmat, Collégien, France). Densitometrical quantification was performed with the Fiji software (Schindelin et al., 2012).

5.2.10 Expression constructs

Expression plasmids for human LRRC8A-CFP, LRRC8A-YFP, and LRRC8E-YFP were described previously (König et al., 2019). The DAG and PA biosensors were kindly provided by S. Grinstein , University of Toronto. The DAG biosensor consisted of an N-terminal GFP fused to the C1 domain of PKC in the pEGFP(C1) vector (Schlam et al., 2013). The plasmid encoding GFP-2PABD consisted of GFP fused to two PA-binding domains of the yeast protein Spo20p reported previously (Bohdanowicz et al., 2013; Du and Frohman, 2009). Cells were transfected with FuGENE 6 according to the manufacturer's instructions. For co-expression, equimolar ratios of constructs were co-transfected.

5.2.11 FRET measurements

For FRET experiments, images were collected on a high-speed setup of Leica Microsystems (Dmi6000B stage, 63x/1.4 oil objective, high-speed external Leica filter wheels with Leica FRET set filters (11522073), EL6000 light source, DFC360 FX camera, controlled by Las AF software platform). All experiments were conducted at room temperature.

Before imaging, all the cells were washed with isotionic buffer for three times. seFRET images were recoreded in donor, acceptor and FRET channels. Acquisition parameters were the same for all three channels (8x8 binning, gain 1, 100 ms exposure time, illumination intensity 2). Images were proccessed with Fiji

(Schindelin et al., 2012). cFRET maps processing were carried out with PixFRET plugin (Feige et al., 2005) (threshold to 1, Gaussian blur to 2) in accordance with the following equation (Jiang and Sorkin, 2002).

$$cFRET = \frac{I^{DA} - I^{DD} * \beta - I^{AA} * \gamma}{I^{AA}}$$

Where I^{DA}, I^{DD} and I^{AA} are the intensities of FRET, donor and acceptor channels, respectively. Caculation of correction factors (β = donor emission bleed, γ = cross excitation of acceptor by donor excitation) was described previously (König et al., 2019). cFRET maps were determined by hand-drawn regions of interest (ROIs). cFRET values of individual cells were normalized to their mean cFRET in isotonic solution.

5.2.12 Qualitative and quantitative microscopy

For monitoring the distribution of DAG and PA biosensors in the cells, images were recorded using a spinning disk confocal microscopy (CSU-W, Andor/Nikon). We used a 40x oil objective, and the images were recorded every 1 minute. The raw image files were stored as 16-bit in ".nd2" format at 337x337 µm (1024x1024 pixel) at an interval of 1 minute and a total of 21 images per series (total time per series: 20 minutes). The image processing was carried out with Fiji (Schindelin et al., 2012). All experiments were performed at room temperature.

5.2.13 Statistical analysis

Proliferation and migration was quantified with the IncuCyte Zoom image analysis software by measuring cell confluence and wound width over time, respectively. OriginPro 2017 software (OriginLab, Northampton, MA, USA) was used for statistical analyses. All data are presented as the mean values ± SD. For comparisons between two groups, p-values were determined using Student's *t*-test and are indicated according to convention: *p < 0.05, **p < 0.01 and ***p < 0.001.

6 REFERENCES

Abascal, F., and Zardoya, R. (2012). LRRC8 proteins share a common ancestor with pannexins, and may form hexameric channels involved in cell-cell communication. Bioessays *34*, 551-560.

Abbracchio, M.P., Burnstock, G., Boeynaems, J.M., Barnard, E.A., Boyer, J.L., Kennedy, C., Knight, G.E., Fumagalli, M., Gachet, C., Jacobson, K.A.*, et al.* (2006). International Union of Pharmacology LVIII: update on the P2Y G protein-coupled nucleotide receptors: from molecular mechanisms and pathophysiology to therapy. Pharmacol Rev *58*, 281-341.

Afzal, A., Figueroa, E.E., Kharade, S.V., Bittman, K., Matlock, B.K., Flaherty, D.K., and Denton, J.S. (2019). The LRRC8 volume-regulated anion channel inhibitor, DCPIB, inhibits mitochondrial respiration independently of the channel. Physiol Rep *7*, e14303.

Akita, T., Fedorovich, S.V., and Okada, Y. (2011). Ca^{2+} nanodomain-mediated component of swelling-induced volume-sensitive outwardly rectifying anion current triggered by autocrine action of ATP in mouse astrocytes. Cell Physiol Biochem *28*, 1181-1190.

Akita, T., and Okada, Y. (2014). Characteristics and roles of the volume-sensitive outwardly rectifying (VSOR) anion channel in the central nervous system. Neuroscience *275*, 211-231.

Arcangeli, A., and Becchetti, A. (2015). Novel perspectives in cancer therapy: Targeting ion channels. Drug Resist Updat *21*, 11-19.

Bae, Y., Kim, A., Cho, C.H., Kim, D., Jung, H.G., Kim, S.S., Yoo, J., Park, J.Y., and Hwang, E.M. (2019). TTYH1 and TTYH2 Serve as LRRC8A-Independent Volume-Regulated Anion Channels in Cancer Cells. Cells *8*.

Bao, J., Perez, C.J., Kim, J., Zhang, H., Murphy, C.J., Hamidi, T., Jaubert, J., Platt, C.D., Chou, J., Deng, M.*, et al.* (2018). Deficient LRRC8A-dependent volume-

regulated anion channel activity is associated with male infertility in mice. JCI Insight *3*.

Benfenati, V., Caprini, M., Nicchia, G.P., Rossi, A., Dovizio, M., Cervetto, C., Nobile, M., and Ferroni, S. (2009). Carbenoxolone inhibits volume-regulated anion conductance in cultured rat cortical astroglia. Channels (Austin) *3*, 323-336.

Best, L., and Brown, P.D. (2009). Studies of the mechanism of activation of the volume-regulated anion channel in rat pancreatic beta-cells. J Membr Biol *230*, 83-91.

Best, L., Brown, P.D., Sener, A., and Malaisse, W.J. (2010). Electrical activity in pancreatic islet cells: The VRAC hypothesis. Islets *2*, 59-64.

Bohdanowicz, M., Schlam, D., Hermansson, M., Rizzuti, D., Fairn, G.D., Ueyama, T., Somerharju, P., Du, G., and Grinstein, S. (2013). Phosphatidic acid is required for the constitutive ruffling and macropinocytosis of phagocytes. Mol Biol Cell *24*, 1700-1712, s1701-1707.

Bortner, C.D., and Cidlowski, J.A. (1998). A necessary role for cell shrinkage in apoptosis. Biochem Pharmacol *56*, 1549-1559.

Bortner, C.D., and Cidlowski, J.A. (2014). Ion channels and apoptosis in cancer. Philos Trans R Soc Lond B Biol Sci *369*, 20130104.

Bowens, N.H., Dohare, P., Kuo, Y.H., and Mongin, A.A. (2013). DCPIB, the proposed selective blocker of volume-regulated anion channels, inhibits several glutamate transport pathways in glial cells. Mol Pharmacol *83*, 22-32.

Bryan-Sisneros, A., Sabanov, V., Thoroed, S.M., and Doroshenko, P. (2000). Dual role of ATP in supporting volume-regulated chloride channels in mouse fibroblasts. Biochim Biophys Acta *1468*, 63-72.

Burow, P., Klapperstuck, M., and Markwardt, F. (2015). Activation of ATP secretion via volume-regulated anion channels by sphingosine-1-phosphate in RAW macrophages. Pflugers Arch *467*, 1215-1226.

Bykova, E.A., Zhang, X.D., Chen, T.Y., and Zheng, J. (2006). Large movement in the C terminus of CLC-0 chloride channel during slow gating. Nat Struct Mol Biol *13*, 1115-1119.

Cahalan, M.D., and Lewis, R.S. (1988). Role of potassium and chloride channels in volume regulation by T lymphocytes. Soc Gen Physiol Ser *43*, 281-301.

Cai, S., Zhang, T., Zhang, D., Qiu, G., and Liu, Y. (2015). Volume-sensitive chloride channels are involved in cisplatin treatment of osteosarcoma. Mol Med Rep *11*, 2465-2470.

Cannon, C.L., Basavappa, S., and Strange, K. (1998). Intracellular ionic strength regulates the volume sensitivity of a swelling-activated anion channel. Am J Physiol *275*, C416-422.

Caramia, M., Sforna, L., Franciolini, F., and Catacuzzeno, L. (2019). The Volume-Regulated Anion Channel in Glioblastoma. Cancers (Basel) *11*.

Catacuzzeno, L., Michelucci, A., Sforna, L., Aiello, F., Sciaccaluga, M., Fioretti, B., Castigli, E., and Franciolini, F. (2014). Identification of key signaling molecules involved in the activation of the swelling-activated chloride current in human glioblastoma cells. J Membr Biol *247*, 45-55.

Chen, L., Becker, T.M., Koch, U., and Stauber, T. (2019a). The LRRC8/VRAC anion channel facilitates myogenic differentiation of murine myoblasts by promoting membrane hyperpolarization. J Biol Chem *294*, 14279-14288.

Chen, L., König, B., Liu, T., Pervaiz, S., Razzaque, Y.S., and Stauber, T. (2019b). More than just a pressure relief valve: physiological roles of volume-regulated LRRC8 anion channels. Biol Chem *400*, 1481-1496.

Chen, T.Y. (2005). Structure and function of clc channels. Annu Rev Physiol *67*, 809-839.

Cohn, J.A., Nairn, A.C., Marino, C.R., Melhus, O., and Kole, J. (1992). Characterization of the cystic fibrosis transmembrane conductance regulator in a colonocyte cell line. Proc Natl Acad Sci U S A *89*, 2340-2344.

Cruse, G., Duffy, S.M., Brightling, C.E., and Bradding, P. (2006). Functional KCa3.1 K^+ channels are required for human lung mast cell migration. Thorax *61*, 880-885.

Darby, M., Kuzmiski, J.B., Panenka, W., Feighan, D., and MacVicar, B.A. (2003). ATP released from astrocytes during swelling activates chloride channels. J Neurophysiol *89*, 1870-1877.

de Los Heros, P., Alessi, D.R., Gourlay, R., Campbell, D.G., Deak, M., Macartney, T.J., Kahle, K.T., and Zhang, J. (2014). The WNK-regulated SPAK/OSR1 kinases directly phosphorylate and inhibit the K^+-Cl^- co-transporters. Biochem J *458*, 559-573.

Decher, N., Lang, H.J., Nilius, B., Brüggemann, A., Busch, A.E., and Steinmeyer, K. (2001). DCPIB is a novel selective blocker of $I_{Cl, swell}$ and prevents swelling-induced shortening of guinea-pig atrial action potential duration. Br J Pharmacol *134*, 1467-1479.

Deneka, D., Sawicka, M., Lam, A.K.M., Paulino, C., and Dutzler, R. (2018). Structure of a volume-regulated anion channel of the LRRC8 family. Nature *558*, 254-259.

Deng, W., Mahajan, R., Baumgarten, C.M., and Logothetis, D.E. (2016). The ICl,swell inhibitor DCPIB blocks Kir channels that possess weak affinity for PIP2. Pflugers Arch *468*, 817-824.

Dey, D., and Goswami, T. (2011). Optical biosensors: a revolution towards quantum nanoscale electronics device fabrication. J Biomed Biotechnol *2011*, 348218.

Dick, G.M., Bradley, K.K., Horowitz, B., Hume, J.R., and Sanders, K.M. (1998). Functional and molecular identification of a novel chloride conductance in canine colonic smooth muscle. Am J Physiol *275*, C940-950.

Djuzenova, C.S., Fiedler, V., Memmel, S., Katzer, A., Sisario, D., Brosch, P.K., Göhrung, A., Frister, S., Zimmermann, H., Flentje, M.*, et al.* (2019). Differential effects of the Akt inhibitor MK-2206 on migration and radiation sensitivity of glioblastoma cells. BMC Cancer *19*, 299.

Doroshenko, P. (1998). Pervanadate inhibits volume-sensitive chloride current in bovine chromaffin cells. Pflugers Arch *435*, 303-309.

Du, G., and Frohman, M.A. (2009). A lipid-signaled myosin phosphatase surge disperses cortical contractile force early in cell spreading. Mol Biol Cell *20*, 200-208.

Dubois, J.M., and Rouzaire-Dubois, B. (2004). The influence of cell volume changes on tumour cell proliferation. Eur Biophys J *33*, 227-232.

Duncan, R.R., Bergmann, A., Cousin, M.A., Apps, D.K., and Shipston, M.J. (2004). Multi-dimensional time-correlated single photon counting (TCSPC) fluorescence lifetime imaging microscopy (FLIM) to detect FRET in cells. J Microsc *215*, 1-12.

Eggermont, J., Trouet, D., Carton, I., and Nilius, B. (2001). Cellular function and control of volume-regulated anion channels. Cell Biochem Biophys *35*, 263-274.

Elorza-Vidal, X., Gaitán-Peñas, H., and Estévez, R. (2019). Chloride Channels in Astrocytes: Structure, Roles in Brain Homeostasis and Implications in Disease. Int J Mol Sci *20*, 1034.

Estevez, A.Y., Bond, T., and Strange, K. (2001). Regulation of I(Cl,swell) in neuroblastoma cells by G protein signaling pathways. Am J Physiol Cell Physiol *281*, C89-98.

Feige, J.N., Sage, D., Wahli, W., Desvergne, B., and Gelman, L. (2005). PixFRET, an ImageJ plug-in for FRET calculation that can accommodate variations in spectral bleed-throughs. Microsc Res Tech *68*, 51-58.

Feustel, P.J., Jin, Y., and Kimelberg, H.K. (2004). Volume-regulated anion channels are the predominant contributors to release of excitatory amino acids in the ischemic cortical penumbra. Stroke *35*, 1164-1168.

Fisher, S.K., Cheema, T.A., Foster, D.J., and Heacock, A.M. (2008). Volume-dependent osmolyte efflux from neural tissues: regulation by G-protein-coupled receptors. J Neurochem *106*, 1998-2014.

Fisher, S.K., Heacock, A.M., Keep, R.F., and Foster, D.J. (2010). Receptor regulation of osmolyte homeostasis in neural cells. J Physiol *588*, 3355-3364.

Florin-Christensen, J., Florin-Christensen, M., Delfino, J.M., Stegmann, T., and Rasmussen, H. (1992). Metabolic fate of plasma membrane diacylglycerols in NIH 3T3 fibroblasts. J Biol Chem *267*, 14783-14789.

Formaggio, F., Saracino, E., Mola, M.G., Rao, S.B., Amiry-Moghaddam, M., Muccini, M., Zamboni, R., Nicchia, G.P., Caprini, M., and Benfenati, V. (2019). LRRC8A is essential for swelling-activated chloride current and for regulatory volume decrease in astrocytes. FASEB J *33*, 101-113.

Franco, R., Panayiotidis, M.I., and de la Paz, L.D. (2008). Autocrine signaling involved in cell volume regulation: the role of released transmitters and plasma membrane receptors. J Cell Physiol *216*, 14-28.

Fraser, S.P., and Pardo, L.A. (2008). Ion channels: functional expression and therapeutic potential in cancer: Colloquium on Ion Channels and Cancer. EMBO reports *9*, 512-515.

Friard, J., Tauc, M., Cougnon, M., Compan, V., Duranton, C., and Rubera, I. (2017). Comparative effects of chloride channel inhibitors on LRRC8/VRAC-mediated chloride conductance. Front Pharmacol *8*, 328.

Fujii, M., Ohtsubo, M., Ogawa, T., Kamata, H., Hirata, H., and Yagisawa, H. (1999). Real-time visualization of PH domain-dependent translocation of phospholipase C-delta1 in renal epithelial cells (MDCK): response to hypo-osmotic stress. Biochem Biophys Res Commun *254*, 284-291.

Fujii, T., Shimizu, T., Yamamoto, S., Funayama, K., Fujita, K., Tabuchi, Y., Ikari, A., Takeshima, H., and Sakai, H. (2018). Crosstalk between Na^+, K^+-ATPase and a volume-regulated anion channel in membrane microdomains of human cancer cells. Biochimica et Biophysica Acta (BBA)-Molecular Basis of Disease *1864*, 3792-3804.

Fujii, T., Takahashi, Y., Takeshima, H., Saitoh, C., Shimizu, T., Takeguchi, N., and Sakai, H. (2015). Inhibition of gastric H^+,K^+-ATPase by 4-(2-butyl-6,7-dichloro-2-cyclopentylindan-1-on-5-yl)oxybutyric acid (DCPIB), an inhibitor of volume-regulated anion channel. Eur J Pharmacol *765*, 34-41.

Gaitán-Peñas, H., Gradogna, A., Laparra-Cuervo, L., Solsona, C., Fernández-Dueñas, V., Barrallo-Gimeno, A., Ciruela, F., Lakadamyali, M., Pusch, M., and Estévez, R. (2016). Investigation of LRRC8-Mediated Volume-Regulated Anion Currents in Xenopus Oocytes. Biophysical journal *111*, 1429-1443.

Gaitan-Penas, H., Gradogna, A., Laparra-Cuervo, L., Solsona, C., Fernandez-Duenas, V., Barrallo-Gimeno, A., Ciruela, F., Lakadamyali, M., Pusch, M., and Estevez, R. (2016). Investigation of LRRC8-Mediated Volume-Regulated Anion Currents in Xenopus Oocytes. Biophys J *111*, 1429-1443.

Ghosh, A., Khandelwal, N., Kumar, A., and Bera, A.K. (2018). Leucine-rich repeat-containing 8B protein is associated with the endoplasmic reticulum Ca^{2+} leak in HEK293 cells (doi: 10.1242/jcs.203646). J Cell Sci *131*.

Gradogna, A., Gaitán-Peñas, H., Boccaccio, A., Estévez, R., and Pusch, M. (2017). Cisplatin activates volume sensitive LRRC8 channel mediated currents in Xenopus oocytes. Channels (Austin) *11*, 254-260.

Grinstein, S., Clarke, C.A., Dupre, A., and Rothstein, A. (1982). Volume-induced increase of anion permeability in human lymphocytes. J Gen Physiol *80*, 801-823.

Haas, B.R., and Sontheimer, H. (2010). Inhibition of the Sodium-Potassium-Chloride Cotransporter Isoform-1 reduces glioma invasion. Cancer Res *70*, 5597-5606.

Habela, C.W., and Sontheimer, H. (2007). Cytoplasmic volume condensation is an integral part of mitosis. Cell cycle *6*, 1613-1620.

Harikumar, K.B., Kunnumakkara, A.B., Ochi, N., Tong, Z., Deorukhkar, A., Sung, B., Kelland, L., Jamieson, S., Sutherland, R., Raynham, T.*, et al.* (2010). A novel small-molecule inhibitor of protein kinase D blocks pancreatic cancer growth in vitro and in vivo. Mol Cancer Ther *9*, 1136-1146.

Harrigan, T.J., Abdullaev, I.F., Jourd'heuil, D., and Mongin, A.A. (2008). Activation of microglia with zymosan promotes excitatory amino acid release via volume-regulated anion channels: the role of NADPH oxidases. J Neurochem *106*, 2449-2462.

Hasegawa, Y., Shimizu, T., Takahashi, N., and Okada, Y. (2012). The apoptotic volume decrease is an upstream event of MAP kinase activation during Staurosporine-induced apoptosis in HeLa cells. Int J Mol Sci *13*, 9363-9379.

Hayashi, T., Nozaki, Y., Nishizuka, M., Ikawa, M., Osada, S., and Imagawa, M. (2011). Factor for adipocyte differentiation 158 gene disruption prevents the body weight gain and insulin resistance induced by a high-fat diet. Biol Pharm Bull *34*, 1257-1263.

Hazama, A., and Okada, Y. (1988). Ca^{2+} sensitivity of volume-regulatory K^+ and Cl^- channels in cultured human epithelial cells. J Physiol *402*, 687-702.

He, D., Luo, X., Wei, W., Xie, M., Wang, W., and Yu, Z. (2012). DCPIB, a specific inhibitor of volume-regulated anion channels (VRACs), inhibits astrocyte proliferation and cell cycle progression via G1/S arrest. J Mol Neurosci *46*, 249-257.

Hermoso, M., Olivero, P., Torres, R., Riveros, A., Quest, A.F., and Stutzin, A. (2004). Cell volume regulation in response to hypotonicity is impaired in HeLa cells expressing a protein kinase Calpha mutant lacking kinase activity. J Biol Chem *279*, 17681-17689.

Hoffmann, E.K. (1978). Regulation of cell volume by selective changes in the leak permeabilities of Ehrlich ascites tumor cells. Paper presented at: Alfred Benzon Symp.

Hoffmann, E.K., Lambert, I.H., and Pedersen, S.F. (2009). Physiology of cell volume regulation in vertebrates. Physiological reviews *89*, 193-277.

Hyzinski-García, M.C., Rudkouskaya, A., and Mongin, A.A. (2014). LRRC8A protein is indispensable for swelling-activated and ATP-induced release of excitatory amino acids in rat astrocytes. J Physiol *592*, 4855-4862.

Inoue, H., Ohtaki, H., Nakamachi, T., Shioda, S., and Okada, Y. (2007). Anion channel blockers attenuate delayed neuronal cell death induced by transient forebrain ischemia. J Neurosci Res *85*, 1427-1435.

Ise, T., Shimizu, T., Lee, E.L., Inoue, H., Kohno, K., and Okada, Y. (2005). Roles of volume-sensitive Cl^- channel in cisplatin-induced apoptosis in human epidermoid cancer cells. J Membr Biol *205*, 139-145.

Ishikawa, H., and Barber, G.N. (2008). STING is an endoplasmic reticulum adaptor that facilitates innate immune signalling. Nature *455*, 674-678.

Jackson, P.S., and Strange, K. (1993). Volume-sensitive anion channels mediate swelling-activated inositol and taurine efflux. Am J Physiol *265*, C1489-1500.

Jaeger, M., Carin, M., Medale, M., and Tryggvason, G. (1999). The osmotic migration of cells in a solute gradient. Biophys J *77*, 1257-1267.

Jentsch, T.J. (2016). VRACs and other ion channels and transporters in the regulation of cell volume and beyond. Nat Rev Mol Cell Biol *17*, 293.

Jentsch, T.J., Lutter, D., Planells-Cases, R., Ullrich, F., and Voss, F.K. (2016). VRAC: molecular identification as LRRC8 heteromers with differential functions. Pflugers Arch *468*, 385-393.

Jiang, X., and Sorkin, A. (2002). Coordinated traffic of Grb2 and Ras during epidermal growth factor receptor endocytosis visualized in living cells. Mol Biol Cell *13*, 1522-1535.

Kang, C., Xie, L., Gunasekar, S.K., Mishra, A., Zhang, Y., Pai, S., Gao, Y., Kumar, A., Norris, A.W., and Stephens, S.B. (2018). SWELL1 is a glucose sensor regulating β-cell excitability and systemic glycaemia. Nat Commun *9*, 367.

Kasuya, G., Nakane, T., Yokoyama, T., Jia, Y., Inoue, M., Watanabe, K., Nakamura, R., Nishizawa, T., Kusakizako, T., Tsutsumi, A.*, et al.* (2018). Cryo-EM structures of the human volume-regulated anion channel LRRC8. Nat Struct Mol Biol *25*, 797-804.

Kefauver, J.M., Saotome, K., Dubin, A.E., Pallesen, J., Cottrell, C.A., Cahalan, S.M., Qiu, Z., Hong, G., Crowley, C.S., Whitwam, T.*, et al.* (2018). Structure of the human volume regulated anion channel. eLife *7*.

Kern, D.M., Oh, S., Hite, R.K., and Brohawn, S.G. (2019). Cryo-EM structures of the DCPIB-inhibited volume-regulated anion channel LRRC8A in lipid nanodiscs. eLife *8*.

Kimelberg, H.K., Goderie, S.K., Higman, S., Pang, S., and Waniewski, R.A. (1990). Swelling-induced release of glutamate, aspartate, and taurine from astrocyte cultures. J Neurosci *10*, 1583-1591.

Kirk, K., Ellory, J.C., and Young, J.D. (1992). Transport of organic substrates via a volume-activated channel. J Biol Chem *267*, 23475-23478.

Kittl, M., Dobias, H., Beyreis, M., Kiesslich, T., Mayr, C., Gaisberger, M., Ritter, M., Kerschbaum, H.H., and Jakab, M. (2018). Glycine Induces Migration of Microglial BV-2 Cells via SNAT-Mediated Cell Swelling. Cellular Physiology and Biochemistry *50*, 1460-1473.

Klausen, T.K., Bergdahl, A., Hougaard, C., Christophersen, P., Pedersen, S.F., and Hoffmann, E.K. (2007). Cell cycle-dependent activity of the volume-and Ca^{2+}-activated anion currents in Ehrlich lettre ascites cells. Journal of cellular physiology *210*, 831-842.

Klausen, T.K., Preisler, S., Pedersen, S.F., and Hoffmann, E.K. (2010). Monovalent ions control proliferation of Ehrlich Lettre ascites cells. American Journal of Physiology-Cell Physiology *299*, C714-C725.

König, B., Hao, Y., Schwartz, S., Plested, A.J., and Stauber, T. (2019). A FRET sensor of C-terminal movement reveals VRAC activation by plasma membrane DAG signaling rather than ionic strength. eLife *8*.

König, B., and Stauber, T. (2019). Biophysics and structure-function relationships of LRRC8-formed volume-regulated anion channels (VRACs). Biophys J.

Kumagai, K., Toyoda, F., Staunton, C.A., Maeda, T., Okumura, N., Matsuura, H., Matsusue, Y., Imai, S., and Barrett-Jolley, R. (2016). Activation of a chondrocyte volume-sensitive Cl^- conductance prior to macroscopic cartilage lesion formation in the rabbit knee anterior cruciate ligament transection osteoarthritis model. Osteoarthritis Cartilage *24*, 1786-1794.

Kumar, L., Chou, J., Yee, C.S., Borzutzky, A., Vollmann, E.H., von Andrian, U.H., Park, S.-Y., Hollander, G., Manis, J.P., and Poliani, P.L. (2014). Leucine-rich repeat containing 8A (LRRC8A) is essential for T lymphocyte development and function. J Exp Med *211*, 929-942.

Kunzelmann, K. (2016). Ion channels in regulated cell death. Cell Mol Life Sci *73*, 2387-2403.

Lahey, L.J., Mardjuki, R.E., Wen, X., Hess, G.T., Ritchie, C., Carozza, J.A., Böhnert, V., Maduke, M., Bassik, M.C., and Li, L. (2020). LRRC8A:C/E Heteromeric Channels Are Ubiquitous Transporters of cGAMP. Mol Cell *80*, 578-591.e575.

Lai, T.W., Zhang, S., and Wang, Y.T. (2014). Excitotoxicity and stroke: identifying novel targets for neuroprotection. Prog Neurobiol *115*, 157-188.

Lalouette, A., Lablack, A., Guenet, J.L., Montagutelli, X., and Segretain, D. (1996). Male sterility caused by sperm cell-specific structural abnormalities in ebouriffé, a new mutation of the house mouse. Biol Reprod *55*, 355-363.

Lang, F., Busch, G.L., Ritter, M., Volkl, H., Waldegger, S., Gulbins, E., and Haussinger, D. (1998). Functional significance of cell volume regulatory mechanisms. Physiological reviews *78*, 247-306.

Lang, F., and Hoffmann, E.K. (2012). Role of ion transport in control of apoptotic cell death. Compr Physiol *2*, 2037-2061.

Lang, F., Shumilina, E., Ritter, M., Gulbins, E., Vereninov, A., and Huber, S.M. (2006). Ion channels and cell volume in regulation of cell proliferation and apoptotic cell death. Contrib Nephrol *152*, 142-160.

Lappano, R., and Maggiolini, M. (2011). G protein-coupled receptors: novel targets for drug discovery in cancer. Nat Rev Drug Discov *10*, 47-60.

Lee, C.C., Freinkman, E., Sabatini, D.M., and Ploegh, H.L. (2014). The protein synthesis inhibitor blasticidin s enters mammalian cells via leucine-rich repeat-containing protein 8D. J Biol Chem *289*, 17124-17131.

Lepple-Wienhues, A., Szabò, I., Laun, T., Kaba, N.K., Gulbins, E., and Lang, F. (1998). The tyrosine kinase p56lck mediates activation of swelling-induced chloride channels in lymphocytes. J Cell Biol *141*, 281-286.

Levitan, I.B. (1994). Modulation of ion channels by protein phosphorylation and dephosphorylation. Annu Rev Physiol *56*, 193-212.

Liang, W., Huang, L., Zhao, D., He, J.Z., Sharma, P., Liu, J., Gramolini, A.O., Ward, M.E., Cho, H.C., and Backx, P.H. (2014). Swelling-activated Cl^- currents and intracellular CLC-3 are involved in proliferation of human pulmonary artery smooth muscle cells. J Hypertens *32*, 318-330.

Liu, H.T., Akita, T., Shimizu, T., Sabirov, R.Z., and Okada, Y. (2009). Bradykinin-induced astrocyte-neuron signalling: glutamate release is mediated by ROS-activated volume-sensitive outwardly rectifying anion channels. J Physiol *587*, 2197-2209.

Liu, H.T., Tashmukhamedov, B.A., Inoue, H., Okada, Y., and Sabirov, R.Z. (2006). Roles of two types of anion channels in glutamate release from mouse astrocytes under ischemic or osmotic stress. Glia *54*, 343-357.

Liu, T., and Stauber, T. (2019). The Volume-Regulated Anion Channel LRRC8/VRAC Is Dispensable for Cell Proliferation and Migration. Int J Mol Sci *20*.

Louis, D.N., Ohgaki, H., Wiestler, O.D., Cavenee, W.K., Burger, P.C., Jouvet, A., Scheithauer, B.W., and Kleihues, P. (2007). The 2007 WHO classification of tumours of the central nervous system. Acta neuropathologica *114*, 97-109.

Lück, J.C., Puchkov, D., Ullrich, F., and Jentsch, T.J. (2018). LRRC8/VRAC anion channels are required for late stages of spermatid development in mice. J Biol Chem *293*, 11796-11808.

Lutter, D., Ullrich, F., Lueck, J.C., Kempa, S., and Jentsch, T.J. (2017). Selective transport of neurotransmitters and modulators by distinct volume-regulated LRRC8 anion channels. J Cell Sci *130*, 1122-1133.

Lv, J., Liang, Y., Zhang, S., Lan, Q., Xu, Z., Wu, X., Kang, L., Ren, J., Cao, Y., and Wu, T. (2019). DCPIB, an inhibitor of volume-regulated anion channels, distinctly modulates K2P channels. ACS Chem Neurosci.

Maeda, S., Nakagawa, S., Suga, M., Yamashita, E., Oshima, A., Fujiyoshi, Y., and Tsukihara, T. (2009). Structure of the connexin 26 gap junction channel at 3.5 A resolution. Nature *458*, 597-602.

Maertens, C., Droogmans, G., Chakraborty, P., and Nilius, B. (2001). Inhibition of volume-regulated anion channels in cultured endothelial cells by the anti-oestrogens clomiphene and nafoxidine. Br J Pharmacol *132*, 135-142.

Mao, J., Wang, L., Fan, A., Wang, J., Xu, B., Jacob, T., and Chen, L. (2007). Blockage of volume-activated chloride channels inhibits migration of nasopharyngeal carcinoma cells. Cell Physiol Biochem *19*, 249-258.

Mecca, C., Giambanco, I., Donato, R., and Arcuri, C. (2018). Targeting mTOR in Glioblastoma: Rationale and Preclinical/Clinical Evidence. Dis Markers *2018*.

Memmel, S., Sisario, D., Zöller, C., Fiedler, V., Katzer, A., Heiden, R., Becker, N., Eing, L., Ferreira, F.L.R., Zimmermann, H.*, et al.* (2017). Migration pattern, actin cytoskeleton organization and response to PI3K-, mTOR-, and Hsp90-inhibition of glioblastoma cells with different invasive capacities. Oncotarget *8*, 45298-45310.

Miley, H.E., Sheader, E.A., Brown, P.D., and Best, L. (1997). Glucose-induced swelling in rat pancreatic beta-cells. J Physiol *504 (Pt 1)*, 191-198.

Miller, C. (2006). ClC chloride channels viewed through a transporter lens. Nature *440*, 484-489.

Miranda, P., Contreras, J.E., Plested, A.J., Sigworth, F.J., Holmgren, M., and Giraldez, T. (2013). State-dependent FRET reports calcium- and voltage-dependent gating-ring motions in BK channels. Proc Natl Acad Sci U S A *110*, 5217-5222.

Mongin, A.A. (2016). Volume-regulated anion channel—a frenemy within the brain. Pflügers Arch *468*, 421-441.

Mongin, A.A., and Kimelberg, H.K. (2002). ATP potently modulates anion channel-mediated excitatory amino acid release from cultured astrocytes. Am J Physiol Cell Physiol *283*, C569-578.

Mongin, A.A., and Kimelberg, H.K. (2005). ATP regulates anion channel-mediated organic osmolyte release from cultured rat astrocytes via multiple Ca^{2+}-sensitive mechanisms. Am J Physiol Cell Physiol *288*, C204-213.

Moore, A.L., Roe, M.W., Melnick, R.F., and Lidofsky, S.D. (2002). Calcium mobilization evoked by hepatocellular swelling is linked to activation of phospholipase Cgamma. J Biol Chem *277*, 34030-34035.

Morishita, K., Watanabe, K., and Ichijo, H. (2019). Cell volume regulation in cancer cell migration driven by osmotic water flow. Cancer Sci *110*, 2337-2347.

Musch, M.W., and Goldstein, L. (1990). Hypotonicity stimulates phosphatidylcholine hydrolysis and generates diacylglycerol in erythrocytes. J Biol Chem *265*, 13055-13059.

Nakamura, R., Numata, T., Kasuya, G., Yokoyama, T., Nishizawa, T., Kusakizako, T., Kato, T., Hagino, T., Dohmae, N., Inoue, M.*, et al.* (2020). Cryo-EM structure of the volume-regulated anion channel LRRC8D isoform identifies features important for substrate permeation. Commun Biol *3*, 240.

Nilius, B., and Droogmans, G. (2003). Amazing chloride channels: an overview. Acta Physiol Scand *177*, 119-147.

Nilius, B., Eggermont, J., Voets, T., Buyse, G., Manolopoulos, V., Droogmans, G., and biology, m. (1997). Properties of volume-regulated anion channels in mammalian cells. Prog Biophys Mol Biol *68*, 69-119.

Nilius, B., Voets, T., Prenen, J., Barth, H., Aktories, K., Kaibuchi, K., Droogmans, G., and Eggermont, J. (1999). Role of Rho and Rho kinase in the activation of volume-regulated anion channels in bovine endothelial cells. J Physiol *516 (Pt 1)*, 67-74.

Okada, Y. (1997). Volume expansion-sensing outward-rectifier Cl^- channel: fresh start to the molecular identity and volume sensor. American Journal of Physiology-Cell Physiology *273*, C755-C789.

Okada, Y., Okada, T., Sato-Numata, K., Islam, M.R., Ando-Akatsuka, Y., Numata, T., Kubo, M., Shimizu, T., Kurbannazarova, R.S., and Marunaka, Y. (2019). Cell Volume-Activated and Volume-Correlated Anion Channels in Mammalian Cells: Their Biophysical, Molecular, and Pharmacological Properties. Pharmacol Rev *71*, 49-88.

Okada, Y., Sato, K., and Numata, T. (2009). Pathophysiology and puzzles of the volume-sensitive outwardly rectifying anion channel. J Physiol *587*, 2141-2149.

Okada, Y., Shimizu, T., Maeno, E., Tanabe, S., Wang, X., and Takahashi, N. (2006). Volume-sensitive chloride channels involved in apoptotic volume decrease and cell death. J Membr Biol *209*, 21-29.

Orlov, S.N., Platonova, A.A., Hamet, P., and Grygorczyk, R. (2013). Cell volume and monovalent ion transporters: their role in cell death machinery triggering and progression. Am J Physiol Cell Physiol *305*, C361-372.

Oshima, A., Tani, K., and Fujiyoshi, Y. (2016). Atomic structure of the innexin-6 gap junction channel determined by cryo-EM. Nat Commun *7*, 13681.

Pedersen, S.F., Beisner, K.H., Hougaard, C., Willumsen, B.M., Lambert, I.H., and Hoffmann, E.K. (2002). Rho family GTP binding proteins are involved in the regulatory volume decrease process in NIH3T3 mouse fibroblasts. J Physiol *541*, 779-796.

Pedersen, S.F., Kapus, A., and Hoffmann, E.K. (2011). Osmosensory mechanisms in cellular and systemic volume regulation. J Am Soc Nephrol *22*, 1587-1597.

Pedersen, S.F., Klausen, T.K., and Nilius, B. (2015). The identification of a volume-regulated anion channel: an amazing Odyssey. Acta Physiol (Oxf) *213*, 868-881.

Pedersen, S.F., Okada, Y., and Nilius, B. (2016). Biophysics and physiology of the volume-regulated anion channel (VRAC)/volume-sensitive outwardly rectifying anion channel (VSOR). Pflügers Arch *468*, 371-383.

Pervaiz, S., Kopp, A., von Kleist, L., and Stauber, T. (2019). Absolute Protein Amounts and Relative Abundance of Volume-regulated Anion Channel (VRAC) LRRC8 Subunits in Cells and Tissues Revealed by Quantitative Immunoblotting. Int J Mol Sci *20*.

Planells-Cases, R., Lutter, D., Guyader, C., Gerhards, N.M., Ullrich, F., Elger, D.A., Kucukosmanoglu, A., Xu, G., Voss, F.K., Reincke, S.M.*, et al.* (2015). Subunit composition of VRAC channels determines substrate specificity and cellular resistance to Pt-based anti-cancer drugs. EMBO J *34*, 2993-3008.

Platt, C.D., Chou, J., Houlihan, P., Badran, Y.R., Kumar, L., Bainter, W., Poliani, P.L., Perez, C.J., Dent, S.Y., and Clapham, D.E. (2017). Leucine-rich repeat containing 8A (LRRC8A)–dependent volume-regulated anion channel activity is dispensable for T-cell development and function. Journal of Allergy Clinical Immunology
140, 1651-1659. e1651.

Poulsen, K.A., Andersen, E.C., Hansen, C.F., Klausen, T.K., Hougaard, C., Lambert, I.H., and Hoffmann, E.K. (2010). Deregulation of apoptotic volume decrease and ionic movements in multidrug-resistant tumor cells: role of chloride channels. Am J Physiol Cell Physiol *298*, C14-25.

Preusser, M., De Ribaupierre, S., Wöhrer, A., Erridge, S.C., Hegi, M., Weller, M., and Stupp, R. (2011). Current concepts and management of glioblastoma. Ann Neurol *70*, 9-21.

Prevarskaya, N., Skryma, R., and Shuba, Y. (2018). Ion channels in cancer: are cancer hallmarks oncochannelopathies? Physiological reviews *98*, 559-621.

Qiu, Z., Dubin, A.E., Mathur, J., Tu, B., Reddy, K., Miraglia, L.J., Reinhardt, J., Orth, A.P., and Patapoutian, A. (2014). SWELL1, a plasma membrane protein, is an essential component of volume-regulated anion channel. Cell *157*, 447-458.

Ransom, C.B., O'Neal, J.T., and Sontheimer, H. (2001). Volume-activated chloride currents contribute to the resting conductance and invasive migration of human glioma cells. J Neurosci *21*, 7674-7683.

Reid, B., Song, B., McCaig, C.D., and Zhao, M. (2005). Wound healing in rat cornea: the role of electric currents. FASEB J *19*, 379-386.

Rinehart, J., Maksimova, Y.D., Tanis, J.E., Stone, K.L., Hodson, C.A., Zhang, J., Risinger, M., Pan, W., Wu, D., Colangelo, C.M.*, et al.* (2009). Sites of regulated phosphorylation that control K-Cl cotransporter activity. Cell *138*, 525-536.

Robinson, P.J. (1992). Differential stimulation of protein kinase C activity by phorbol ester or calcium/phosphatidylserine in vitro and in intact synaptosomes. J Biol Chem *267*, 21637-21644.

Rouzaire-Dubois, B., Milandri, J.-B., Bostel, S., and Dubois, J.-M. (2000). Control of cell proliferation by cell volume alterations in rat C6 glioma cells. Pflügers Arch *440*, 881-888.

Roy, G. (1995). Amino acid current through anion channels in cultured human glial cells. J Membr Biol *147*, 35-44.

Rubino, S., Bach, M.D., Schober, A.L., Lambert, I.H., and Mongin, A.A. (2018). Downregulation of leucine-rich repeat-containing 8A limits proliferation and increases sensitivity of glioblastoma to temozolomide and carmustine. Front Oncol *8*.

Rudkouskaya, A., Chernoguz, A., Haskew-Layton, R.E., and Mongin, A.A. (2008). Two conventional protein kinase C isoforms, alpha and beta I, are involved in the ATP-induced activation of volume-regulated anion channel and glutamate release in cultured astrocytes. J Neurochem *105*, 2260-2270.

Ruhfus, B., and Kinne, R.K. (1996). Hypotonicity-activated efflux of taurine and myo-inositol in rat inner medullary collecting duct cells: evidence for a major common pathway. Kidney Blood Press Res *19*, 317-324.

Ruhfus, B., Tinel, H., and Kinne, R.K. (1996). Role of G-proteins in the regulation of organic osmolyte efflux from isolated rat renal inner medullary collecting duct cells. Pflugers Arch *433*, 35-41.

Ruwhof, C., van Wamel, J.T., Noordzij, L.A., Aydin, S., Harper, J.C., and van der Laarse, A. (2001). Mechanical stress stimulates phospholipase C activity and intracellular calcium ion levels in neonatal rat cardiomyocytes. Cell Calcium *29*, 73-83.

Sabirov, R.Z., Prenen, J., Tomita, T., Droogmans, G., and Nilius, B. (2000). Reduction of ionic strength activates single volume-regulated anion channels (VRAC) in endothelial cells. Pflugers Arch *439*, 315-320.

Sadoshima, J., Qiu, Z., Morgan, J.P., and Izumo, S. (1996). Tyrosine kinase activation is an immediate and essential step in hypotonic cell swelling-induced ERK activation and c-fos gene expression in cardiac myocytes. EMBO J *15*, 5535-5546.

Sasmal, D.K., and Lu, H.P. (2014). Single-molecule patch-clamp FRET microscopy studies of NMDA receptor ion channel dynamics in living cells: revealing the multiple conformational states associated with a channel at its electrical off state. J Am Chem Soc *136*, 12998-13005.

Sauter, D.R.P., Novak, I., Pedersen, S.F., Larsen, E.H., and Hoffmann, E.K. (2015). ANO1 (TMEM16A) in pancreatic ductal adenocarcinoma (PDAC). Pflügers Arch *467*, 1495-1508.

Sawada, A., Takihara, Y., Kim, J.Y., Matsuda-Hashii, Y., Tokimasa, S., Fujisaki, H., Kubota, K., Endo, H., Onodera, T., Ohta, H.*, et al.* (2003). A congenital mutation of the novel gene LRRC8 causes agammaglobulinemia in humans. J Clin Invest *112*, 1707-1713.

Schilling, T., Stock, C., Schwab, A., and Eder, C. (2004). Functional importance of Ca^{2+}-activated K^+ channels for lysophosphatidic acid-induced microglial migration. Eur J Neurosci *19*, 1469-1474.

Schindelin, J., Arganda-Carreras, I., Frise, E., Kaynig, V., Longair, M., Pietzsch, T., Preibisch, S., Rueden, C., Saalfeld, S., and Schmid, B. (2012). Fiji: an open-source platform for biological-image analysis. Nat Methods *9*, 676.

Schlam, D., Bohdanowicz, M., Chatgilialoglu, A., Steinberg, B.E., Ueyama, T., Du, G., Grinstein, S., and Fairn, G.D. (2013). Diacylglycerol kinases terminate diacylglycerol signaling during the respiratory burst leading to heterogeneous phagosomal NADPH oxidase activation. J Biol Chem *288*, 23090-23104.

Schlichter, L., Sakellaropoulos, G., Ballyk, B., Pennefather, P., and Phipps, D. (1996). Properties of K^+ and Cl^- channels and their involvement in proliferation of rat microglial cells. Glia *17*, 225-236.

Schneider, L., Klausen, T.K., Stock, C., Mally, S., Christensen, S.T., Pedersen, S.F., Hoffmann, E.K., and Schwab, A. (2008). H-ras transformation sensitizes volume-activated anion channels and increases migratory activity of NIH3T3 fibroblasts. Pflugers Arch *455*, 1055-1062.

Schober, A.L., Wilson, C.S., and Mongin, A.A. (2017). Molecular composition and heterogeneity of the LRRC8-containing swelling-activated osmolyte channels in primary rat astrocytes. J Physiol *595*, 6939-6951.

Schumacher, P., Sakellaropoulos, G., Phipps, D., and Schlichter, L. (1995). Small-conductance chloride channels in human peripheral T lymphocytes. J Membr Biol *145*, 217-232.

Schwab, A., Fabian, A., Hanley, P.J., and Stock, C. (2012). Role of ion channels and transporters in cell migration. Physiological reviews *92*, 1865-1913.

Schwab, A., Gabriel, K., Finsterwalder, F., Folprecht, G., Greger, R., Kramer, A., and Oberleithner, H. (1995). Polarized ion transport during migration of transformed Madin-Darby canine kidney cells. Pflügers Arch *430*, 802-807.

Sciaccaluga, M., Fioretti, B., Catacuzzeno, L., Pagani, F., Bertollini, C., Rosito, M., Catalano, M., D'Alessandro, G., Santoro, A., Cantore, G.*, et al.* (2010). CXCL12-induced glioblastoma cell migration requires intermediate conductance Ca^{2+}-activated K^+ channel activity. Am J Physiol Cell Physiol *299*, C175-184.

Selvin, P.R. (2000). The renaissance of fluorescence resonance energy transfer. Nat Struct Biol *7*, 730-734.

Senju, Y., Rosenbaum, E., Shah, C., Hamada-Nakahara, S., Itoh, Y., Yamamoto, K., Hanawa-Suetsugu, K., Daumke, O., and Suetsugu, S. (2015). Phosphorylation of PACSIN2 by protein kinase C triggers the removal of caveolae from the plasma membrane. J Cell Sci *128*, 2766-2780.

Sforna, L., Cenciarini, M., Belia, S., Michelucci, A., Pessia, M., Franciolini, F., and Catacuzzeno, L. (2017). Hypoxia Modulates the Swelling-Activated Cl Current in Human Glioblastoma Cells: Role in Volume Regulation and Cell Survival. J Cell Physiol *232*, 91-100.

Shen, M.R., Droogmans, G., Eggermont, J., Voets, T., Ellory, J.C., and Nilius, B. (2000). Differential expression of volume-regulated anion channels during cell cycle progression of human cervical cancer cells. J Physiol *529*, 385-394.

Shimizu, T., Numata, T., and Okada, Y. (2004). A role of reactive oxygen species in apoptotic activation of volume-sensitive Cl(-) channel. Proc Natl Acad Sci U S A *101*, 6770-6773.

Shimizu, T., Ohtake, H., Fujii, T., Tabuchi, Y., and Sakai, H. (2015). Volume-sensitive outwardly rectifying Cl(-) channels contribute to butyrate-triggered apoptosis of murine colonic epithelial MCE301 cells. J Physiol Sci *65*, 151-157.

Sirianant, L., Wanitchakool, P., Ousingsawat, J., Benedetto, R., Zormpa, A., Cabrita, I., Schreiber, R., and Kunzelmann, K. (2016). Non-essential contribution of LRRC8A to volume regulation. Pflügers Arch *468*, 805-816.

Sørensen, B.H., Dam, C.S., Stürup, S., and Lambert, I.H. (2016). Dual role of LRRC8A-containing transporters on cisplatin resistance in human ovarian cancer cells. J Inorg Biochem *160*, 287-295.

Soroceanu, L., Manning, T.J., and Sontheimer, H. (1999). Modulation of glioma cell migration and invasion using Cl^- and K^+ ion channel blockers. J Neurosci *19*, 5942-5954.

Sorota, S. (1995). Tyrosine protein kinase inhibitors prevent activation of cardiac swelling-induced chloride current. Pflugers Arch *431*, 178-185.

Stafford, M.J., Watson, S.P., and Pears, C.J. (2003). PKD: a new protein kinase C-dependent pathway in platelets. Blood *101*, 1392-1399.

Stauber, T. (2015). The volume-regulated anion channel is formed by LRRC8 heteromers–molecular identification and roles in membrane transport and physiology. Biol Chem *396*, 975-990.

Strange, K., Emma, F., and Jackson, P.S. (1996). Cellular and molecular physiology of volume-sensitive anion channels. Am J Physiol *270*, C711-730.

Strange, K., Yamada, T., and Denton, J.S. (2019). A 30-year journey from volume-regulated anion currents to molecular structure of the LRRC8 channel. J Gen Physiol *151*, 100-117.

Stroka, K.M., Jiang, H., Chen, S.-H., Tong, Z., Wirtz, D., Sun, S.X., and Konstantopoulos, K. (2014). Water permeation drives tumor cell migration in confined microenvironments. Cell *157*, 611-623.

Stryer, L., and Haugland, R.P. (1967). Energy transfer: a spectroscopic ruler. Proc Natl Acad Sci U S A *58*, 719-726.

Stuhlmann, T., Planells-Cases, R., and Jentsch, T.J. (2018). LRRC8/VRAC anion channels enhance β-cell glucose sensing and insulin secretion. Nat Commun *9*, 1974.

Sun, L., Wu, J., Du, F., Chen, X., and Chen, Z.J. (2013). Cyclic GMP-AMP synthase is a cytosolic DNA sensor that activates the type I interferon pathway. Science *339*, 786-791.

Sun, W., Li, Y., Chen, L., Chen, H., You, F., Zhou, X., Zhou, Y., Zhai, Z., Chen, D., and Jiang, Z. (2009). ERIS, an endoplasmic reticulum IFN stimulator, activates innate immune signaling through dimerization. Proc Natl Acad Sci U S A *106*, 8653-8658.

Syeda, R., Qiu, Z., Dubin, A.E., Murthy, S.E., Florendo, M.N., Mason, D.E., Mathur, J., Cahalan, S.M., Peters, E.C., and Montal, M. (2016). LRRC8 proteins form volume-regulated anion channels that sense ionic strength. Cell *164*, 499-511.

Tabcharani, J.A., Chang, X.B., Riordan, J.R., and Hanrahan, J.W. (1991). Phosphorylation-regulated Cl^- channel in CHO cells stably expressing the cystic fibrosis gene. Nature *352*, 628-631.

Tahara, E., Kadara, H., Lacroix, L., Lotan, D., and Lotan, R. (2009). Activation of protein kinase C by phorbol 12-myristate 13-acetate suppresses the growth of lung cancer cells through KLF6 induction. Cancer Biol Ther *8*, 801-807.

Takano, T., Kang, J., Jaiswal, J.K., Simon, S.M., Lin, J.H., Yu, Y., Li, Y., Yang, J., Dienel, G., Zielke, H.R.*, et al.* (2005). Receptor-mediated glutamate release from volume sensitive channels in astrocytes. Proc Natl Acad Sci U S A *102*, 16466-16471.

Thastrup, J.O., Rafiqi, F.H., Vitari, A.C., Pozo-Guisado, E., Deak, M., Mehellou, Y., and Alessi, D.R. (2012). SPAK/OSR1 regulate NKCC1 and WNK activity: analysis of WNK isoform interactions and activation by T-loop trans-autophosphorylation. Biochem J *441*, 325-337.

Thoroed, S.M., Bryan-Sisneros, A., and Doroshenko, P. (1999). Protein phosphotyrosine phosphatase inhibitors suppress regulatory volume decrease and the volume-sensitive Cl^- conductance in mouse fibroblasts. Pflugers Arch *438*, 133-140.

Tilly, B.C., van den Berghe, N., Tertoolen, L.G., Edixhoven, M.J., and de Jonge, H.R. (1993). Protein tyrosine phosphorylation is involved in osmoregulation of ionic conductances. J Biol Chem *268*, 19919-19922.

Tominaga, K., Kondo, C., Kagata, T., Hishida, T., Nishizuka, M., and Imagawa, M. (2004). The novel gene fad158, having a transmembrane domain and leucine-rich repeat, stimulates adipocyte differentiation. J Biol Chem *279*, 34840-34848.

Ullrich, F., Reincke, S.M., Voss, F.K., Stauber, T., and Jentsch, T.J. (2016). Inactivation and Anion Selectivity of Volume-regulated Anion Channels (VRACs)

Depend on C-terminal Residues of the First Extracellular Loop. J Biol Chem *291*, 17040-17048.

Vakili, A., Hosseinzadeh, S.A., and Khorasani, M.Z. (2009). Peripheral administration of carbenoxolone reduces ischemic reperfusion injury in transient model of cerebral ischemia. J Stroke Cerebrovasc Dis *18*, 81-85.

Voets, T., Droogmans, G., Raskin, G., Eggermont, J., and Nilius, B. (1999). Reduced intracellular ionic strength as the initial trigger for activation of endothelial volume-regulated anion channels. Proc Natl Acad Sci U S A *96*, 5298-5303.

Voets, T., Manolopoulos, V., Eggermont, J., Ellory, C., Droogmans, G., and Nilius, B. (1998). Regulation of a swelling-activated chloride current in bovine endothelium by protein tyrosine phosphorylation and G proteins. J Physiol *506 (Pt 2)*, 341-352.

Voets, T., Szücs, G., Droogmans, G., and Nilius, B. (1995). Blockers of volume-activated Cl^- currents inhibit endothelial cell proliferation. Pflügers Arch *431*, 132-134.

von Weikersthal, S.F., Barrand, M.A., and Hladky, S.B. (1999). Functional and molecular characterization of a volume-sensitive chloride current in rat brain endothelial cells. J Physiol *516 (Pt 1)*, 75-84.

Voss, F.K., Ullrich, F., Münch, J., Lazarow, K., Lutter, D., Mah, N., Andrade-Navarro, M.A., von Kries, J.P., Stauber, T., and Jentsch, T.J. (2014). Identification of LRRC8 heteromers as an essential component of the volume-regulated anion channel VRAC. Science *344*, 634-638.

Wehner, F. (2006). Cell volume-regulated cation channels. Contrib Nephrol *152*, 25-53.

Wondergem, R., Gong, W., Monen, S.H., Dooley, S.N., Gonce, J.L., Conner, T.D., Houser, M., Ecay, T.W., and Ferslew, K.E. (2001). Blocking swelling-activated chloride current inhibits mouse liver cell proliferation. J Physiol *532*, 661-672.

Wong, R., Chen, W., Zhong, X., Rutka, J.T., Feng, Z.P., and Sun, H.S. (2018). Swelling-induced chloride current in glioblastoma proliferation, migration, and invasion. Journal of cellular physiology *233*, 363-370.

Xia, Y., Liu, Y., Xia, T., Li, X., Huo, C., Jia, X., Wang, L., Xu, R., Wang, N., Zhang, M.*, et al.* (2016). Activation of volume-sensitive Cl^- channel mediates autophagy-related cell death in myocardial ischaemia/reperfusion injury. Oncotarget *7*, 39345-39362.

Xue, Y., Li, H., Zhang, Y., Han, X., Zhang, G., Li, W., Zhang, H., Lin, Y., Chen, P., and Sun, X. (2018). Natural and synthetic flavonoids, novel blockers of the volume-regulated anion channels, inhibit endothelial cell proliferation. Pflügers Arch *470*, 1473-1483.

Yamada, T., and Strange, K. (2018). Intracellular and extracellular loops of LRRC8 are essential for volume-regulated anion channel function. J Gen Physiol *150*, 1003-1015.

Yamada, T., Wondergem, R., Morrison, R., Yin, V.P., and Strange, K. (2016). Leucine-rich repeat containing protein LRRC8A is essential for swelling-activated Cl^- currents and embryonic development in zebrafish. Physiol Rep *4*.

Yang, J., del Carmen Vitery, M., Chen, J., Osei-Owusu, J., Chu, J., and Qiu, Z. (2019). Glutamate-Releasing SWELL1 Channel in Astrocytes Modulates Synaptic Transmission and Promotes Brain Damage in Stroke. Neuron.

Zachariassen, L.G., Katchan, L., Jensen, A.G., Pickering, D.S., Plested, A.J., and Kristensen, A.S. (2016). Structural rearrangement of the intracellular domains during AMPA receptor activation. Proc Natl Acad Sci U S A *113*, E3950-3959.

Zachos, N.C., Lee, L.J., Kovbasnjuk, O., Li, X., and Donowitz, M. (2013). PLC-γ directly binds activated c-Src, which is necessary for carbachol-mediated inhibition of NHE3 activity in Caco-2/BBe cells. Am J Physiol Cell Physiol *305*, C266-275.

Zal, T., and Gascoigne, N.R. (2004). Photobleaching-corrected FRET efficiency imaging of live cells. Biophys J *86*, 3923-3939.

Zhang, H., Deng, Z., Zhang, D., Li, H., Zhang, L., Niu, J., Zuo, W., Fu, R., Fan, L., and Ye, J. (2018). High expression of leucinerich repeatcontaining 8A is indicative of a worse outcome of colon cancer patients by enhancing cancer cell growth and metastasis. Oncol Rep *40*, 1275-1286.

Zhang, J., and Lieberman, M. (1996). Chloride conductance is activated by membrane distention of cultured chick heart cells. Cardiovasc Res *32*, 168-179.

Zhang, Y., Xie, L., Gunasekar, S.K., Tong, D., Mishra, A., Gibson, W.J., Wang, C., Fidler, T., Marthaler, B., Klingelhutz, A.*, et al.* (2017). SWELL1 is a regulator of adipocyte size, insulin signalling and glucose homeostasis. Nat Cell Biol *19*, 504-517.

Zheng, J., and Zagotta, W.N. (2003). Patch-clamp fluorometry recording of conformational rearrangements of ion channels. Sci STKE *2003*, Pl7.

Zholos, A., Beck, B., Sydorenko, V., Lemonnier, L., Bordat, P., Prevarskaya, N., and Skryma, R. (2005). Ca^{2+}- and volume-sensitive chloride currents are differentially regulated by agonists and store-operated Ca^{2+} entry. J Gen Physiol *125*, 197-211.

Zhong, B., Yang, Y., Li, S., Wang, Y.Y., Li, Y., Diao, F., Lei, C., He, X., Zhang, L., Tien, P.*, et al.* (2008). The adaptor protein MITA links virus-sensing receptors to IRF3 transcription factor activation. Immunity *29*, 538-550.

Zhou, C., Chen, X., Planells-Cases, R., Chu, J., Wang, L., Cao, L., Li, Z., López-Cayuqueo, K.I., Xie, Y., Ye, S.*, et al.* (2020a). Transfer of cGAMP into Bystander Cells via LRRC8 Volume-Regulated Anion Channels Augments STING-Mediated Interferon Responses and Anti-viral Immunity. Immunity *52*, 767-781.e766.

Zhou, J.J., Luo, Y., Chen, S.R., Shao, J.Y., Sah, R., and Pan, H.L. (2020b). LRRC8A-dependent volume-regulated anion channels contribute to ischemia-induced brain injury and glutamatergic input to hippocampal neurons. Exp Neurol *332*, 113391.

7 PUBLICATIONS

Liu T and Stauber T (2019) The Volume-Regulated Anion Channel LRRC8/VRAC Is Dispensable for Cell Proliferation and Migration. *Int J Mol Sci*, 20: E2663. https://doi.org/10.3390/ijms20112663

Chen L, König B, **Liu T**, Pervaiz S, Razzaque YS and Stauber T (2019) More than just a pressure relief valve: physiological roles of volume-regulated LRRC8 anion channels. *Biol Chem*. 400:1481-1496. https://doi.org/10.1515/hsz-2019-0189